Analyses and quantification of modelling uncertainties in streamflow simulations with applications to two catchments: the small lowland Kielstau basin in Germany and the mesoscale mountainous XitaoXi basin in China

Dissertation

zur Erlangung des Doktorgrades
der Mathematisch-Naturwissenschaftlichen Fakultät
der Christian-Albrechts-Universität zu Kiel
vorgelegt von

MSc. **Xiaoyong Zhang**

Institute for Natural Resource Conservation
Department of Hydrology and Water Resources Management
Kiel University, Kiel, Germany

2012

Referentin: Professor Dr. Nicola Fohrer

Koreferentin: Professor Dr. Natascha Oppelt

Tag der mündlichen Prüfung: 02 March 2012

Zum Druck genehmigt: Kiel, 02 March 2012

gez. Professor Dr. Lutz Kipp Dekan

Summary

Models are the primary way to predict the values of various system performance indicators in hydrologic researches. The usefulness of any model depends in part on the accuracy and reliability of its output. This PhD thesis presents the development of a methodological framework to analyse the impacts of three sources of modelling uncertainty (namely model structure error, parameter estimation and input data resolution) on streamflow simulation and to quantify the associated modelling uncertainties. The case study includes two catchments: the small lowland Kielstau catchment (51.5 km²) in Northern Germany and the mesoscale mountainous XitaoXi basin (2271 km²) in Southern China. The river discharge simulation is completed through the KIDS model (**Ki**elstau **D**ischarge **S**imulation model, Hörmann et al. 2007; Zhang et al. 2007) using PCRaster modelling language (Van Deursen 1995; Wesseling et al. 1996). The main criterion of model output performance is the Nash-Sutcliffe efficiency (Nash & Sutcliffe 1970). The structural uncertainty is assessed by developing a set of model ensembles with increasing model complexity. The modelling uncertainty induced by parameter estimation is investigated through Monte Carlo based sampling strategy in the framework of SUFI-2 analysis routine (Sequential Uncertainty Fitting, ver. 2, Abbaspour et al. 2004). The uncertainty of changing input data resolutions is analysed by aggregating grid cells. For each of them, a method has been developed to quantify the inherent modelling uncertainties with two statistical measures: *R* factor and *P* factor (Abbaspour et al. 2004; Schuol & Abbaspour 2006). Considering the two different catchments of Kielstau and XitaoXi, investigating the effects of model structure on model performance helps to identify the most appropriate model adapted to local hydrological features. Also, result comparisons for the parameter estimation and resolution impacts are conducted between the two basins. It is shown that the uncertainties induced by the different model structures tested in this study are much higher than the ones induced by parameter calibration and input data resolutions using a fixed hydrological model structure. However, modelling uncertainties from different sources are not independent of each other, they can interact in various ways and it is hard to calculate them separately. All the uncertainties obtained here refer to the overall modelling uncertainty while focusing on one aspect of influencing sources. It indicates that model output and modelling efficiency highly depend on tradition and empirical assumptions concerning the choice of model structures, parameter estimation, and the selection of appropriate resolution level. This study may provide a methodology to investigate these issues in the study basins.

Zusammenfassung

Modelle sind die wichtigsten Werkzeuge zur Vorhersage des Verhaltens von verschiedenen Systemindikatoren in der hydrologischen Forschung. Die Anwendbarheit der Modelle hängt zum Teil von der Genauigkeit und Zuverlässigkeit der Ergebnisse ab. Diese Dissertation stellt einen methodischen Rahmen vor, um die Auswirkungen von drei verschiedenen Quellen von Unsicherheit in der Modellierung von Abfluss zu analysieren und zu quantifizieren: Fehler in der Modellstruktur, der Parameterschätzung und räumlichen und zeitlichen Auflösung von Eingabedaten. Die Studie wurde für zwei Einzugsgebiete durchgeführt: das kleine Tiefland-Einzugsgebiet der Kielstau (51,5 km²) in Nord-Deutschland und das mesoskalige, bergige XitaoXi Einzugsgebiet (2271 km²) in Südchina. Die Abflusssimulation wurde mit dem die KIDS Modell durchgeführt (**Ki**elstau **D**ischarge **S**imulationsmodell, Hörmann et al. 2007; Zhang et al. 2007), das in der PCRaster Modellierungssprache (Van Deursen 1995; Wesseling et al. 1996) implementiert ist. Das wichtigste Kriterium zur Beurteilung der Modellierungsgüte ist der Nash-Sutcliffe Koeffizient (Nash & Sutcliffe 1970). Die strukturelle Unsicherheit wurde durch die Entwicklung einer Reihe von Modell-Ensembles mit zunehmender Komplexität erfasst. Die durch Parameterschätzung induzierte Unsicherheit wird durch eine Monte-Carlo-basierte Sampling Strategie im Rahmen der SUFI-2 Analyse Methode (Sequential Uncertainty Fitting, Ver. 2, Abbaspour et al. 2004) ermittelt. Die von unterschiedlichen Auflösungen verursachte Unsicherheit wurde schließlich durch Aggregation der Gitterzellen analysiert. Für alle Simulationen wurde die Unsicherheit der Modellierung mit zwei statistischen Kennzahlen quantifiziert, dem *R* Faktor und dem *P* Faktor (Abbaspour et al. 2004; Schuol & Abbaspour 2006). Diese Betrachtungsweise hilft schließlich, für die zwei unterschiedlichen Einzugsgebiete der Kielstau und des XitaoXi, das am besten geeignete, an die lokalen hydrologischen Merkmale angepasste Modell zu finden. Außerdem wurden die unterschiedlichen Auswirkungen der Parameterschätzung und der Auflösung auf die beiden Einzugsgebiete analysiert. Insgesamt waren die Unsicherheiten durch die unterschiedlichen Modellstrukturen wesenteich höher als die durch Parameter-Kalibrierung und Auflösung der Eingabedaten. Allerdings sind die Modellierungsunsicherheiten aus unterschiedlichen Quellen nicht unabhängig voneinander, sondern interagieren auf verschiedene Weise, so dass es schwierig ist, sie unabhängig zu berechnen. Alle hier betrachteten Unsicherheiten beziehen sich jeweils auf einen einzigen Aspekt der gesamten Modellierung. Es zeigte sich, dass Modellergebnis und -effizienz stark abhängen von der Herangehensweise und den empirischen Annahmen bei der Auswahl der Modellstruktur, der

Parameterschätzung und der Auswahl der geeigneten Auflösung. Die Ergebnisse und die in dieser Studie genutzten Methoden können helfen, die verschiedenen Quellen von Unsicherheiten bei der Modellierung zu quantifizieren.

Acknowledgement

My first thanks go to Professor Nicola Fohrer who proposed me to join her research group and followed my work on the PhD-thesis. I very much appreciated the liberty she gave me to develop my ideas, the excellent and motivating working atmosphere during my whole PhD study, and the mother-like understandings and cares when I am in the hard time of both doing research and taking care of my baby boy. A special thank goes to Dr. Georg Hörmann, who gave me a lot of essential hints about the runoff modelling in the Kielstau basin, from whom I learnt a lot and who followed closely my research. I greatly appreciated our scientific discussions and his remarks on all my manuscripts he reviewed. The work on the case study of XitaoXi catchment would not have been possible without the help of Professor Gao Junfeng from the Nanjing Institute of Geography and Limnology, Chinese Academy Sciences (NIGLAS), whom I would like to thank for his invaluable comments, and his explanations about PCRaster modelling in XitaoXi. Thanks also to Dr. Xiaoli Jin from NIGLAS who passed on to me her experience in the area of hydrological processes for the XitaoXi watershed. And I wish to thank Dr. Willem Van Deursen, Cees Wesseling, Derek Karssenberg, for the technical support of PCRaster modelling language. I would also like to thank my colleague Oliver Schmitz who made the automatic parameter calibration possible for the KIDS model and who has always been available to help in any computer related problems; Jens Kiesel who helped me with the update of Kielstau data; Guangju Zhao with whom I had a lot of discussions and had shared experiences on PCRaster modelling; and many other colleagues who have made the work much more enjoyable. A special thank goes to the Kiel University for the major financial support of this program. I finally would like to thank my family, especially my husband and my parents, who always stood by my side and encouraged me in all my decisions, who shared not only the pleasing but also the difficult moments. Without their support and convictions, I would never have been able to get through all this. Xie Xie!

Content

List of Figures

List of Tables

Chapter 1

Introduction

Abstract

The present PhD thesis is composed of five papers either published or accepted to publication. This introductory section, the detailed description of the case studies and the overall conclusions, completes them. The present section introduces first the general research context. The fundamental scientific questions in the area of hydrological modelling uncertainty research are briefly presented before discussing the applications for river runoff simulations in the Kielstau and XitaoXi catchments, on which this thesis is focused. This overview of the research context is followed by the scientific questions that motivated this PhD research and an introduction to the methodological framework developed to answer them. Finally, the content of the different papers composing this thesis is set out with a special emphasis on how they integrate into the methodological framework and how they contribute to answer the main underlying scientific questions.

1.1 Research context - Uncertainty in hydrological modelling

In hydrological modelling, all model output values are subject to imprecision. It can be caused by many sources in the modelling system including: imperfect simplifications inherent in the model structure, uncertainty due to the values of the model parameters, and data measurement errors (Refsgaard & Storm 1996; Lindenschmidt et al. 2007). The end result is imprecision and uncertainty associated with model output. In recent years, increasing attention has been paid to accurately predict the model reliability when applying the models to watershed conditions. Many studies (Beven 1989; Beven & Binley 1992; Gupta et al. 1998; Beven 2000, 2006; Beven & Freer 2001; Van Griensven et al. 2008) have recommended that a realistic estimate of prediction uncertainty should be incorporated into model application owing to the limitation of generating the currency of hydrological models. If the simulation results are used in management or planning decisions, the estimation of the precision and the exactitude of the obtained results is fundamental for the decision maker to judge his confidence in the results (Liu & Gupta 2007; Zhang et al. 2009).

This thesis gives a special emphasis to the hydrological modelling uncertainties induced by three different sources: model structure errors, parameter calibrations and input data resolutions. Their quantification is currently one of the key issues in hydrological research (e.g. Beven & Freer 2001; Vrugt et al. 2003; Gattke & Schumann 2007; Geza et al. 2009).

Uncertainty in model output can result from errors in the model structure compared to the real system. We refer to this source of modelling uncertainty as the model structural uncertainty. A model is a simplified representation of a natural phenomenon and is therefore imperfect. Even if the input and output data were exact, the model would not be able to match the observed output perfectly. Structural uncertainty can significantly influence the overall modelling prediction. However, such uncertainties are difficult to assess explicitly or to separate from other uncertainties during the calibration process. Studies for assessing the impact of model structure on modelling uncertainty are quite limited, or in many cases, analyses are mixed with other sensitivity or uncertainty analysis (e.g. Uhlenbrook et al. 1999; Butts et al. 2004, Son & Sivapalan 2007; Ewen et al. 2006; Schuol & Abbaspour 2006; Lindenschmidt et al. 2007). Furthermore, increasing model complexity in order to more closely represent the complexity of the real system may not only add to the cost of data collection, but may also introduce even more parameters, and thus even more potential sources of error in model output. It is not an easy task to judge the appropriate level of model

complexity and to estimate the resulting levels of uncertainty associated with various assumptions regarding model structure and solution methods.

The second source of uncertainty is perhaps the most extensively studied in hydrological literature. The type of errors induced by the parameters depends on how they are estimated. Physical parameters are assumed to represent a measurable property of the studied system. But some parameters in many hydrological models are purely conceptual or the necessary system characteristics have not been or cannot be observed. These parameters have to be calibrated, i.e. the best parameter values are estimated so that the model output matches as closely as possible the observed data. This best parameter set – if it exists – is difficult to find and several different parameter sets can yield equally good results for the model calibration (Beven & Binley 1992; Gupta et al. 1998). In the past, the determination of the best or the most probable parameter set has been subject to intense research (Duan et al. 1992; Yapo et al. 1998; Madsen 2003) whereas current research concentrates on the estimation of the entire probability distribution of the parameters (Kuczera & Parent 1998; Vrugt et al. 2003).

Another possible source of uncertainty results from the selection of input data resolution. It is a great challenge to select a proper grid resolution as the grid size selection generally leads to predictive uncertainty and also directly determines the amount of work required (Haverkamp et al. 2005; Shrestha et al. 2006). It is generally accepted that higher resolution increases the accuracy of the simulation, but it demands a massive amount of data and modelling work (Vazquez et al. 2002). Many researches tried to compromise between increasing spatial resolution and data handling requirements, and some focuses on the effects of input data on model parameters, hydrologic response, model sensitivity and uncertainty (see Franchini et al. 1996; Horritt & Bates 2001; Ciarapica & Todini 2002; Liang et al. 2004; Bogena et al. 2005; Haverkamp et al. 2005; Bormann 2008). We consider it is an important step in modelling process to select an appropriate input data resolution. Knowledge of the effect of forcing input scale is important for both hydrological and meteorological studies. Ability to choose an adequate input resolution at the preliminary investigation stage will result in an appropriate modelling framework, with fewer problems later and higher simulation accuracy.

This study intends to exam these three aspects with a simple discharge simulation model KIDS in two case studies: the small lowland Kielstau catchment (51.5 km²) in Germany and the mesoscale mountainous XitaoXi basin (2271 km²) in China.

1.2 Fundamental questions of this PhD research

In the context of hydrological model applications, the identification and quantification of the modelling uncertainties is essential to assess whether the modelling system is a reliable tool to facilitate the decision-making process or for further analysis.

Most studies on modelling uncertainty aimed at reducing the prediction uncertainty by additional research and data collection and analysis. Accordingly, most studies suffer from an important drawback: they only focus on uncertainty assessment from one source, while neglecting the fact that modelling uncertainties from different sources are not independent of each other – they can interact in various ways. The present PhD thesis faces this major challenge in the field of modelling uncertainty research: to investigate the modelling uncertainty from different kinds of sources with application both in low land watershed and in mountainous river basin.

The research concentrated on the quantification of the modelling uncertainty associated with the streamflow simulation for the river basin system. The results of the two study basins are compared to show the method feasibility in different hydrological systems. Ultimately, the developed methodology should give the answer to the following main question: Can the discharge simulation model reproduce the observed data with an acceptable degree of accuracy? If yes, how reliable are these simulations? Referring to the modelling uncertainty itself, could we evaluate and quantify the simulation uncertainty associated with different sources? How do the uncertainties propagate to modelling output? And when faced with uncertain outcomes from various sources, which one contributes the most to the overall uncertainty?

1.3 Methodological framework

We used PCRaster (Van Deursen 1995; Wesseling et al. 1996) to construct the Kielstau Discharge Simulation (KIDS) models for the streamflow simulations in the two study basins: a small lowland catchment (51.5 km²) in Northern Germany, and XitaoXi - a mesoscale mountainous basin (2271 km²) in the south of China. Figure 1.1 presents a schematic process to set up the KIDS model. Basic input forcing data for the KIDS model included a digital elevation model (DEM) and meteorological data. Other geospatial inputs like soils and land cover are important input parameters to KIDS but optional. It provides a flexible platform to create different model structures. The basic model structure is implemented with one lumped soil layer and one groundwater aquifer. The river discharge is composed of overland flow, interflow and base flow from groundwater. Flow direction is then determined based on DEM, and channel flow is modeled with fully dynamic runoff routing using kinematic wave

function. With the support of interactive raster GIS environment in PCRaster, the KIDS model allows immediate pre- or post-modelling visualization of spatio-temporal data. This is utilized in this study for continuous discharge simulation over long periods.

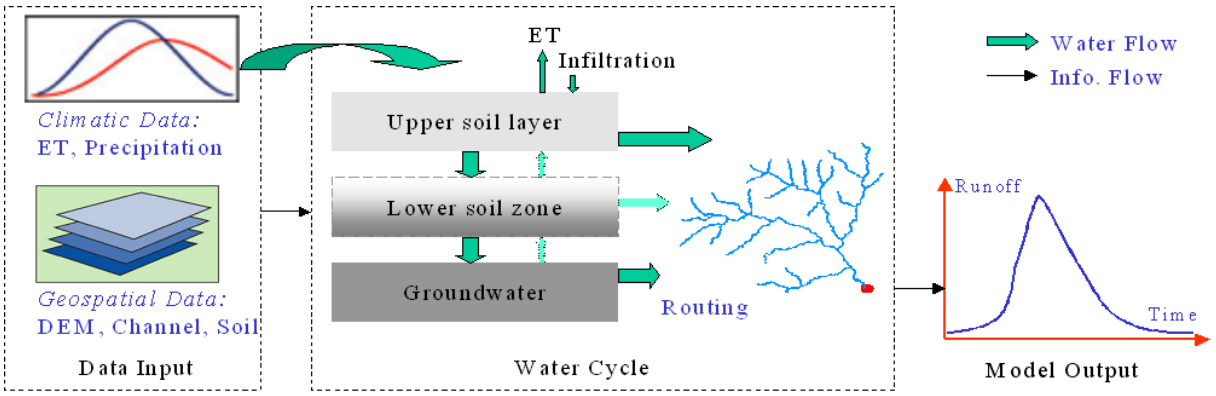

Figure 1.1 Flowchart of the set-up process for the KIDS model.

The main objective of the present research is to quantify the modelling uncertainties associated with the different sources, and thus three major analysis steps are set up as shown in Figure 1.2. The first step is to assess structural uncertainty by investigating effects of different model structures on modelling outcomes, and to identify an appropriate model that reproduces the most relevant hydrologic processes in this modelling frame. With the given model structure, the second step focuses on the parameter calibration procedure and, in particular, the assessment of model prediction uncertainty through Monte Carlo simulations of the model output. The final part deals with the impact of different grid resolutions of spatial input data on modeled river runoff by upscaling grid sizes. This objective considerably influenced the design choices during the modelling and analysis steps on the local scale. For each of them, the inherent sources of modelling uncertainty are quantified through two statistical measures referred as P-factor and R-factor (Abbaspour et al. 2004; Schuol & Abbaspour 2006).

The relative contribution of the different sources to the overall uncertainty is judged by comparing the obtained results of simulated hydrograph bands and uncertainty indicators for the calibration and validation period. It can show how significant of these uncertainty impacts on the overall model simulation.

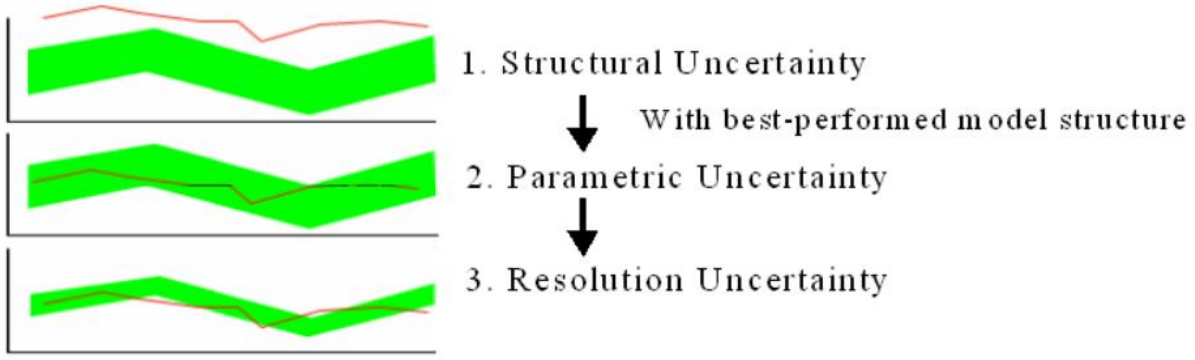

Figure 1.2 Outline of the uncertainty analysis steps (figure is revised referring to Abbaspour et al. 2004).

1.4 Outline of the thesis

During my PhD study on this thesis topic, the obtained results have been submitted to publication in international journals with rigorous peer reviewing and presented at a number of conferences. The resulting final document is therefore a collection of papers (published or accepted for publication) completed by the present introductory chapter (Chapter 1), the main case studies for uncertainty assessment (Chapter 2-6) and the general conclusions (Chapter 7). Each of the papers corresponds to a chapter of this final manuscript but forms an independent unit that can be understood without the context of the entire manuscript. The main features of the study basins and of the hydrological model are shortly presented in each chapter as far as they are necessary for the understanding of the corresponding paper. The content of the chapters composing this thesis is briefly outlined below.

Chapter 2 gives a preliminary investigation of the effects of different model structures on model performance represented by the Nash Sutcliffe Index (NS). It highlights that the model structure is a considerable source of uncertainty in model simulation.

Chapter 3 presents a hydrologic comparison between the two catchments under study for further research in modelling uncertainty issues using KIDS model.

Chapter 4 addresses the quantification of the simulation uncertainty arising from model structure error, and examines the uncertainty behavior further by using a peak-flow low-flow split testing.

Chapter 5 introduces a methodology SUFI-2 (Sequential Uncertainty Fitting, ver. 2, Abbaspour et al. 2004) for parameter calibration and uncertainty estimation, and to quantify the uncertainty induced by the parameter estimation.

Chapter 6 discusses the impacts and estimates the uncertainty of changing spatial input data resolutions on streamflow simulations in two basins.

Chapter 7 contains a summary of the main results, the overall conclusions and an overview over the questions that remain unanswered or that have been raised through this research.

References

Abbaspour, K.C., Johnson, C.A., & van Genuchten, M.T. 2004 Estimating uncertain flow and transport parameters using a sequential uncertainty fitting procedure, *Vadose Zone J.* 3, 1340–1352.

Beven, K.J. 1989 Changing ideas in hydrology, the case of physically based models. *J. Hydrol.* 105, 157-172.

Beven, K.J., 2000 Rainfall–Runoff Modelling: The Primer. John Wiley & Sons Press, New York.

Beven, K.J., 2006 A manifesto for the enquiringly thesis. *J. Hydrol.* 320, 18–36.

Beven, K.J. & Binley, A. 1992 The future of distributed models – model calibration and uncertainty prediction. *Hydrol. Process.* 6 (3), 279–298.

Beven, K.J. & Freer, J. 2001 Equifinality, data assimilation, and uncertainty estimation in mechanistic modelling of complex environmental systems. *J. Hydrol.* 249, 11–29.

Bogena, H., Kunkel, R., Montzka, C. & Wendland, F. 2005 Uncertainties in the simulation of groundwater recharge at different scales. *Adv. Geosci.* 5, 25–30.

Bormann, H. 2008 Sensitivity of a soil-vegetation-atmosphere-transfer scheme to input data resolution and data classification. *J. Hydrol.* 351, 154–169.

Butts, M.B., Payne, J.T., Kristensen, M. & Madsen, H. 2004 An evaluation of the impact of model structure on hydrological modelling uncertainty for streamflow simulation. *J. Hydrol.* 298, 242–266.

Ciarapica, L. & Todini, E. 2002 TOPKAPI: a model for the representation of the ainfall-runoff process at different scales. *Hydrol. Process.* 16, 207–229.

Duan, Q., Sorooshian, S. & Gupta, V. 1992 Effective and efficient global optimization for conceptual rainfall–runoff models. *Water Resour. Res.* 28 (4), 1015–1031.

Ewen, J., O'Donnell, G., Burton, A. & O'Connell, E. 2006 Errors and uncertainty in physically-based rainfall-runoff modelling of catchment change effects. *J. Hydrol.* 330 (3-4), 641-650.

Franchini, M., Wendling, J., Obled, Ch. & Todini, E. 1996 Physical interpretation and sensitivity analysis of the TOPMODEL. *J. Hydrol.* 175, 293–338.

Gattke, C. & Schumann, A. 2007 Comparison of different approaches to quantify the reliability of hydrological simulations. *Adv. Geosci.* 11, 15–20,

Geza, M., Poeter, E.P., McCray, J.E. 2009 Quantifying predictive uncertainty for a mountain-watershed model. *J. Hydrol.* 376, 170–181.

Gupta, H.V., Sorooshian, S. & Yapo, P.O. 1998 Toward improved calibration of hydrologic models: multiple and noncommensurate measures of information. *Water Resour. Res.* 34 (4), 751–763.

Haverkamp, S., Fohrer, N. & Frede, H.G. 2005 Assessment of the effect of land use patterns on hydrologic landscape functions - a comprehensive GIS-based tool to minimize model uncertainty resulting from spatial aggregation. *Hydrol. Process.* 19, 715–727.

Horritt, M.S. & Bates, P.D. 2001 Effects of spatial resolution on a raster based model of flood flow. *J. Hydrol.* 253, 239–249.

Kuczera, G. & Parent, E. 1998 Monte Carlo assessment of parameter uncertainty in conceptual catchment models: the Metropolis algorithm. *J. Hydrol.* 211, 69–85.

Liang, X., Guo, J. & Leung, L.R. 2004 Assessment of the effects of spatial resolutions on daily water flux simulations. *J. Hydrol.* 298, 287–310.

Lindenschmidt, K.E., Fleischbein, K. & Baborowski, M. 2007 Structural uncertainty in a river water quality modelling system. *Ecolog. Model.*, 204, 289–300.

Liu, Y. & Gupta, V. 2007 Uncertainty in hydrologic modelling: toward an integrated data assimilation framework. *Water Resour. Res.* 43 (7), 1-18.

Madsen, H. 2003 Parameter estimation in distributed hydrological catchment modelling using automatic calibration with multiple objectives. *Adv. Water Resour.* 26, 205–216.

Montanari, A. & Brath, A. 2004 A stochastic approach for assessing the uncertainty of rainfall-runoff simulations. *Water Resour. Res.* 40 (1), W01106, 1-11.

Refsgaard, J.C. & Storm, B. 1996 Construction, calibration and validation of hydrological models. In: M.B. Abbott and J.C. Refsgaard (Editors), *Distributed hydrological modelling*. Kluwer Academic Press, Dordrecht, Netherlands, 41-54.

Schuol, J. & Abbaspour, K.C. 2006 Calibration and uncertainty issues of a hydrological model (SWAT) applied to West Africa. *Adv. Geosci.* 9, 137–143.

Shresthaa, R., Tachikawab, Y. & Takara, K. 2006 Input data resolution analysis for distributed hydrological modelling. *J. Hydrol.* 319, 36–50.

Son, K. & Sivapalan, M. 2007 Improving model structure and reducing parameter uncertainty in conceptual water balance models through the use of auxiliary data. *Water Resour. Res.* 43 (1) 1-18.

Uhlenbrook, S., Seibert, J., Leibundgut, C. & Rodhe, A. 1999 Prediction uncertainty of conceptual rainfall-runoff models caused by problems to identify model parameters and structure. *Hydrol. Sci. J.* 44 (5), 279-299.

Van Deursen, W.P.A. 1995 Geographical Information Systems and Dynamic Models: development and application of a prototype spatial modelling language. *Netherlands Geographic Studies*, Issue 190, 195p.

Van Griensven, A., Meixner, T., Srinivasan, R. & Grunwals, S. 2008 Fit-for-purpose analysis of uncertainty using split-sampling evaluations. *Hydrol. Sci. J.* 53 (5), 1090–1103.

Vazquez, R.F., Feyen, L., Feyen, J. & Refsgaard, J.C. 2002 Effect of grid size on effective parameters and model performance of the MIKE-SHE code. *Hydrol. Process.* 16, 355–372.

Vrugt, J.A., Gupta, H.V., Bouten, W. & Sorooshian, S. 2003 A shuffled complex evolution Metropolis algorithm for optimization and uncertainty assessment of hydrologic models. *Water Resour. Res.* 39 (8), 1201-1213.

Wesseling, C.G., Karssenberg, D.J., Burrough, P.A. & Van Deursen, W.P.A. 1996 Integrated dynamic environmental models in GIS: The development of a Dynamic Modelling language. *Transactions in GIS*, 1 (1), 40–48.

Yapo, P.O., Gupta, H.V. & Sorooshian, S. 1998 Multi-objective global optimization for hydrological models. *J. Hydrol.* 204, 83–97.

Zhang, X., Srinivasan, R. & Bosch, D. 2009 Calibration and uncertainty analysis of the SWAT model using Genetic Algorithms and Bayesian Model Averaging. *J. Hydrol.* 374, 307–317.

Chapter 2

An investigation of the effects of model structure on model performance to reduce discharge simulation uncertainty in two catchments

X.Y. Zhang, G. Hörmann, and N. Fohrer
Advances in Geosciences, 18, 31–35, 2008

Abstract

This paper investigates the variations of model performance caused by different model structures in both flow processes and model complexity level. Two case studies indicate that model efficiency is strongly dependent on model structure. The resulting substantial variation in both the model efficiency and the hydrographs from different model structures is used to estimate the structural uncertainty. The results help to select the most appropriate model adapted to local situations, which reveal great conformity with the actual hydrological patterns in both study basins.

Keywords: model structure; model efficiency; simulation uncertainty; Kielstau; XitaoXi

2.1 Introduction

Uncertainty analysis is a valuable tool to test a model concept and to enhance confidence in streamflow simulation with hydrologic models. Model uncertainties generally stem from a variety of sources, like input data, formalization of model structure and parameter estimation, where it can affect the model predictions (Gupta et al. 2005). The system structure of hydrologic models is understood to be the algorithms and equations used to describe the natural flow systems that are themselves imperfectly known; the model uncertainty due to different structures can thus be of great significance in model predictions. However, compared to the abundance of literature on parameter and input data uncertainty, the topic of model structure and the associated uncertainty analysis has received relatively little attention in research. Only a few attempts are found in the literature to address this problem separately (Georgakakos et al. 2004; Lindenschmidt et al. 2007). This imbalance is partly due to the difficulty in assessing structural uncertainty or to separate it from other uncertainties during the calibration process (Beven & Binley 1992). This study investigates the structural uncertainty by examining the performance of models at various complexity levels programmed with the dynamic modelling language PCRaster (Wesseling et al. 1996). It was applied to two study basins – Kielstau in Germany and XitaoXi in China – which differ greatly in both geologic and hydrologic features. As all models are an approximation of the real world, the model structure should embody the essential hydrologic processes in the study region. The aims of this study are i) to identify the impact of variation in model structure on discharge simulation; ii) to reduce model uncertainty by selecting the most appropriate and efficient model structure for each catchment; and iii) to examine if the selected model can capture the observed different features in the catchment.

2.2 Study area

Two different catchments – Kielstau and XitaoXi – are selected for this study, in order to find the best model structure for any given basins. Kielstau is a lowland watershed in Northern Germany, with an area of 51.49 km². The maximum altitude difference within this area is 50 meters. Land use in Kielstau is predominantly agricultural (55.8%) and grass (26.1%). The main soil types are Cambisol and Luvisol, with dominating soil texture of sandy loam. XitaoXi, a 2271 km² sized mountainous basin located in the semitropical zone in Southern China, is a sub-basin of the Taihu Lake. In the XitaoXi region, 63.4% of land use is forest and grass, 20% paddy rice land. Probably owing to the near surface ground water and a large fraction of wetland area in the Kielstau region, the hydrology of the Kielstau area is

characterized by a special seasonal distribution of runoff/precipitation relation (Figure 2.1 left). The monthly discharge values are not always in positive correlation with corresponding rainfall volumes. On the contrary, the distribution of river runoff in the XitaoXi catchment is mainly controlled by rainfall, which is quite common in mountainous regions (Figure 2.1 right). All analyses in the following sections will be done in parallel for the two catchments.

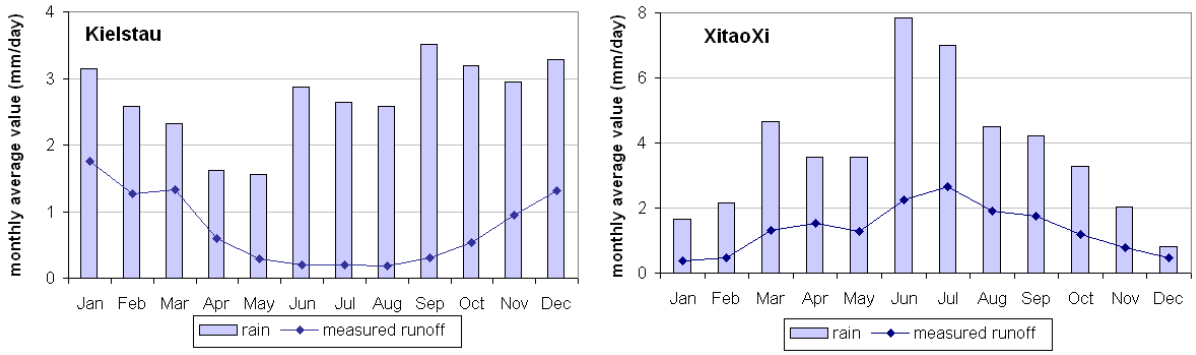

Figure 2.1 Monthly rain and discharge mean value, based on data from 1990 to 1999 (for Kielstau), and from 1979 to 1988 (for XitaoXi).

2.3 KIDS model and its derivatives

The basic KIDS model concept was developed in Hörmann et al. 2007 for discharge simulation in the Kielstau catchment using PCRaster modelling language. It is simply structured as one-way hydrological flux without feedback. As indicated in Figure 2.2, it is implemented with one lumped soil layer and one groundwater aquifer. The model is driven by meteorological input data like precipitation and evapotranspiration. The simulated hydrological fluxes include interception, infiltration, overland flow, and subsurface flow. River discharge is calculated with the kinematic wave function. More details about the KIDS model can be found in Hörmann et al. (2007) and Zhang et al. (2007).

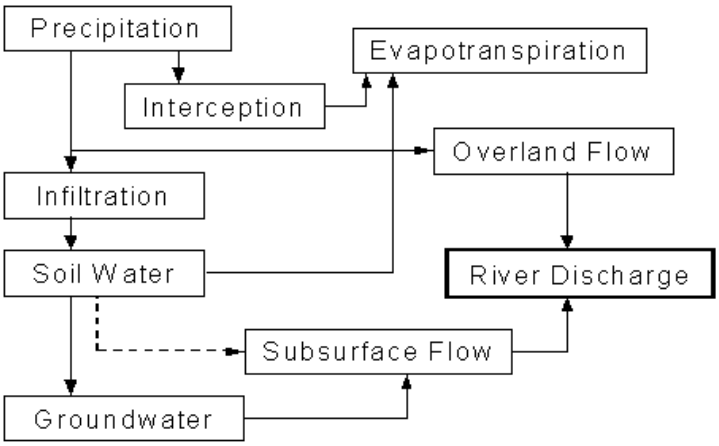

Figure 2.2 Illustrations of the basic KIDS model structure 'M'.

We take the simple KIDS model concept as the basic model structure (abbreviated as 'M') for both study basins. With this basic structure, other inputs like soils and land cover can be added as extended sub-modules to generate similar models. All derivative models form the KIDS model ensembles.

The model structures are developed with the following components: First, sub-modules are derived representing an extended process to be added to the basic model. We developed seven sub-modules for both Kielstau basin (H, S, L, T, G, D, W) and XitaoXi basin (P, E, X, G, L, T, R). A short description of all modules is summarized in Table 2.1. Secondly, the basic model 'M' is combined with one or more modules from the first step to form a new model. All models are named with the characters of the sub-modules. The number of coupled modules indicates the model complexity. Finally, with the establishment of the models with different structures, the Nash-Sutcliffe (NS) index is used as model efficiency criterion to determine the most appropriate model structure for validation.

Table 2.1 Short descriptions of all sub-modules in this study.

Basin	ID	Module description
Kielstau	H	Evapotranspiration (ET) calculated with Haude method (DVWK 1996)
	S	Upper soil layer integrated with spatial distribution of 'Soil Water Content' referring to Sponagel et al. (2005)
	L	Subsurface water flow from soil layer to river runoff
	T	Spatial distributed ET adjusted with land use coefficients referring to Penman Monteith method (Allen et al. 1998)
	G	Outflow threshold of groundwater flow to river discharge
	D	Subsurface drainage
	W	Additional wetland fraction (12%) in the soil zone, which has unlimited water support for evaporation as its actual ET equals the potential ET
XitaoXi	P	Lumped precipitation distribution and subbasin distributed ET
	E	Lumped ET distribution and subbasin distributed precipitation
	X	'Xinanjiang' runoff-producing process (Zhao & Liu 1995) applied to the land use area of 'forest and grass'
	G	Outflow threshold of groundwater flow to river discharge
	L	Subsurface water flow from soil layer to river runoff
	T	Spatial distributed ET adjusted with land use coefficients referring to Gao (2006)
	R	Integration of two reservoirs in the upstream area referring to Jin & Gao (2006)

As the focus of this study is to evaluate the performance of different structures, all parameter values in the basic model 'M' were kept unchanged for any model structure combinations. Owing to the different catchment scale and data availability, the model 'M' in Kielstau basin is set up with a completely lumped distribution of precipitation and evaporation (calculated with Penman-Monteith method); while in XitaoXi catchment we used sub-basin distributed rainfall and evaporation (measured with the Chinese pan standard method).

2.4 Results and discussion

2.4.1 Model structural uncertainty for calibration periods

All created models were used to simulate river runoff for the calibration period from 1990 to 1994 for the Kielstau and from 1979 to 1983 for the XitaoXi. The resulting NS values are presented in Figure 2.3 together with the corresponding model code and model complexity level. It was beyond the scope of this paper to list the complete set of model structure combinations. However, the models selected here are plausible alternatives for discharge simulation incorporating the main processes occurring in the basin. Not surprisingly, there is a high variation in model performances caused by the different model structures. This variation can be used as an estimate of structural uncertainty of the selected models. In both catchments, the NS value has a general tendency to increase with the model complexity level. The simpler models, like those coupled with only one module, perform relatively poor as compared with the more complex models.

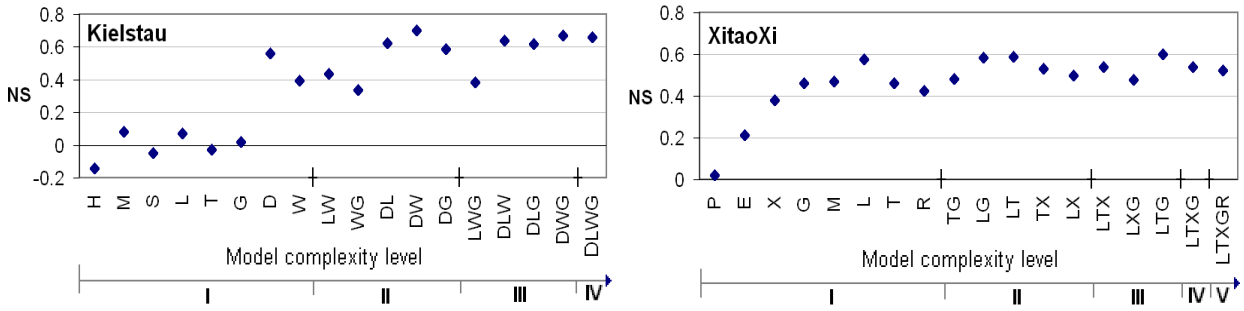

Figure 2.3 The model efficiency (Nash-Sutcliffe index) of all model structures in relation with its complexity level for the Kielstau and the XitaoXi basin.

For the Kielstau lowland basin the influence of drainage ('D') and wetland fraction ('W') improves model efficiency significantly. This is observed in the performance of its combination model as well: model 'DW' outperforms all the selected models. Due to the low altitude variance, the lateral flow is not distinct in the Kielstau area. Instead, the wetland plays

a more important role. For the mountainous XitaoXi basin, the most complex model 'LTXGR' did not perform much better than simple models. It indicates that we could reduce the model complexity. Among all the tested models, the best performance is achieved by model 'LTG', which is coupled with lateral flow process and groundwater outflow threshold, using spatial distribution of evaporation adjusted with land use coefficients. This indicates to a certain extent that the lateral flow is one of the dominating processes, and the influence from the groundwater is very limited.

Noted that different model structures can bring great variation in model efficiency, we plotted the simulated river discharges of all tested model structures along with the observations in Figure 2.4. The gray areas of ensemble model simulations represent the structural uncertainty intervals around the observed discharge values. It shows that the simulations embrace the observed data most of time. The variation produced by different model structures for Kielstau catchment is observed to be wider than that for XitaoXi catchment. To some extent this dispersion of ensemble flows indicates the magnitude of structural uncertainty.

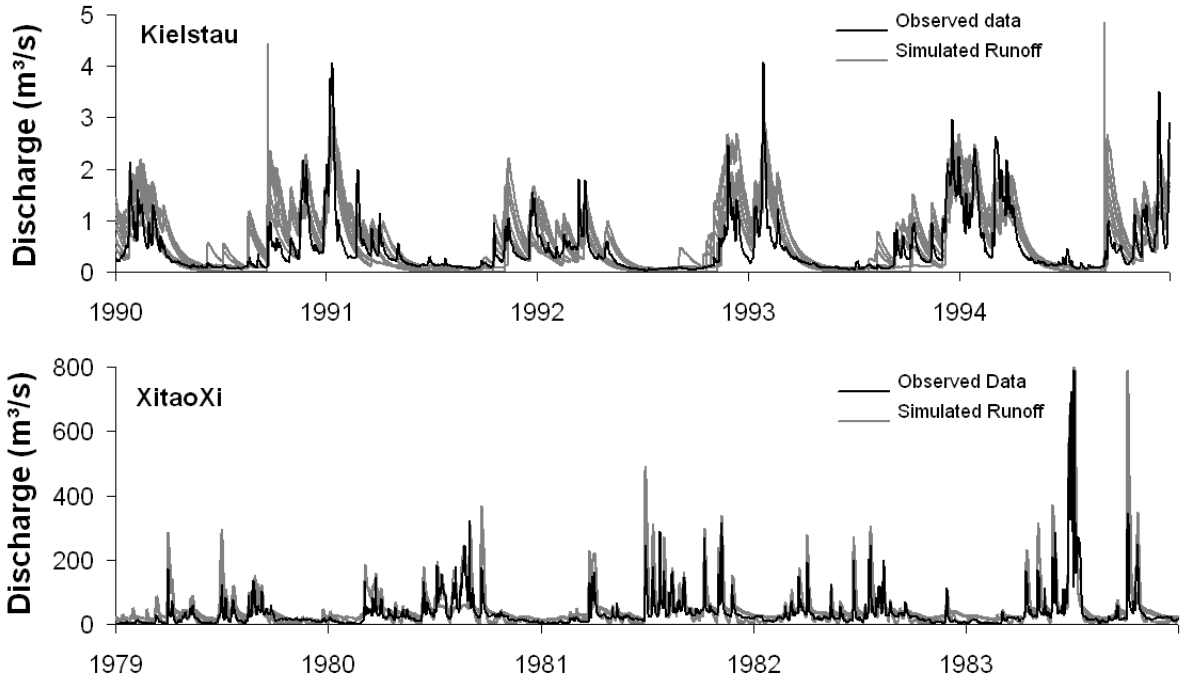

Figure 2.4 Simulation results of different model structures for two study basins, with the shaded area showing the uncertainty intervals along with the measured discharge.

2.4.2 Selecting the best performing model

This result of uncertainty analysis is used to determine the most appropriate model structure for each basin. Model 'DW' and model 'LTG' are thus taken for model validation. As can be seen from the plots of observed and simulated hydrographs in Figure 2.5, both selected

models can reproduce the measured discharge reasonably well. The NS value for model 'DW' of the Kielstau basin is 0.73, and for model 'LTG' of the XitaoXi basin it is 0.6. From the validation result, the discharge simulations can represent the observations in an acceptable range both in hydrographs and in measure of Nash-Sutcliffe coefficient. It ensured that the selected models could be considered to better capture better the hydrological mechanisms in the catchment than other tested models. Moreover, it can help to identify peculiarities of the hydrological processes in the study area.

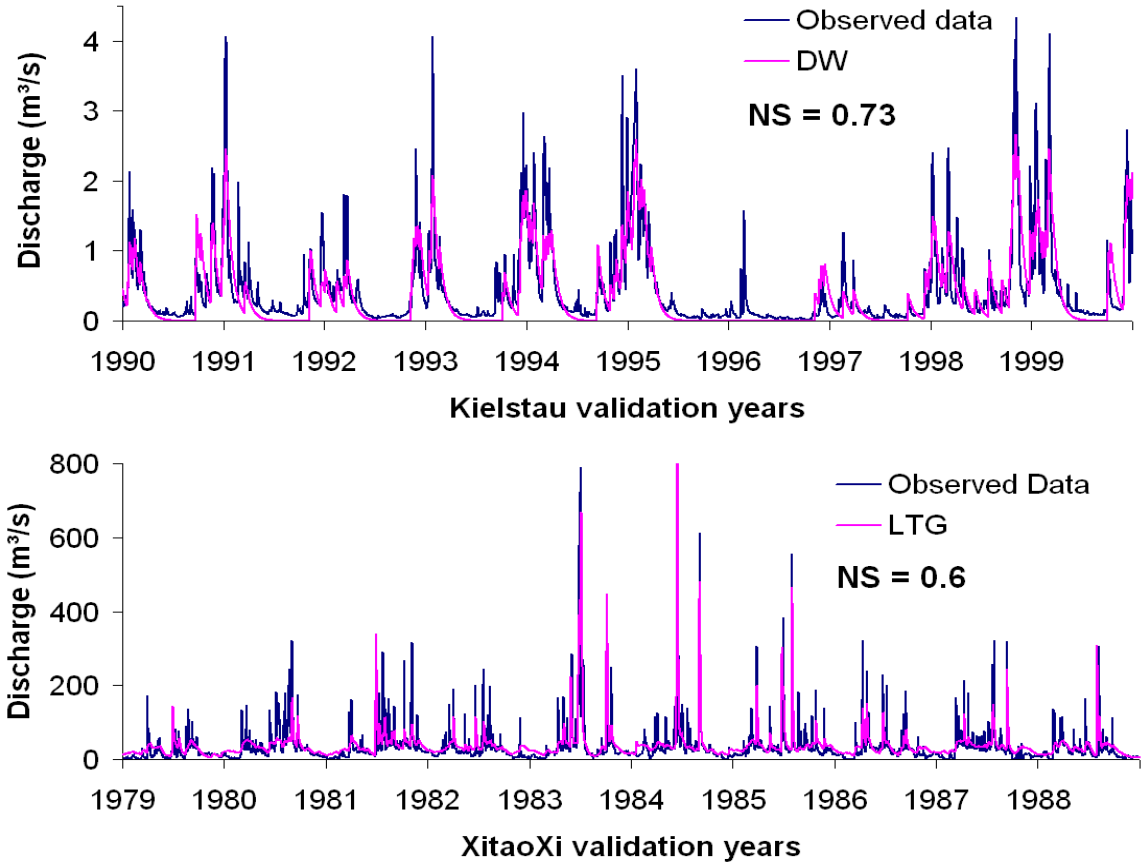

Figure 2.5 Validated simulations of best-performing model structure compared to observed river discharge data.

2.5 Conclusions

Two case studies are conducted in this paper to investigate the effects of different model structures. The results show that model efficiency represented by the NS index is strongly dependent on model structure. The variation in model performances is taken as an estimation of structural uncertainty. Both case studies demonstrate that there is a trade-off between model complexity and simulation ability. The most complex model, which is a combination of all available process modules, does not produce the best simulation. The most appropriate

model structure for each catchment is determined from the uncertainty analysis. The validated simulation with the best-performing model reaches a NS value of 0.73 for the Kielstau and 0.6 for the XitaoXi. The final outcome of this study is that for reducing model simulation uncertainty, it is important to explore different model structures and to adapt the models to the local situation. A further exploration of this uncertainty from model structure will be conducted with multi-criteria methods as an extended research in the near future.

Edited by: F. Portmann, K. Berkhoff, and M. Hunger
Reviewed by: two anonymous referees and the editors

References

Allen, R.G., Pereira, L.S., Raes, D. & Smith, M. 1998 Crop evapotranspiration - Guidelines for computing crop water requirements - FAO Irrigation and drainage paper 56. FAO Rome, M-56, ISBN 92-5-104219-5.

Beven, K. & Binley, A. 1992 The Future Of Distributed Models - Model Calibration And Uncertainty Prediction. *Hydrol. Process.* 6 (3), 279-298.

DVWK - Deutscher Verband für Wasserwirtschaft und Kulturbau e.V. 1996 Ermittlung der Verdunstung von Land- und Wasserflächen. DVWK-Merkblätter zur Wasserwirtschaft, Heft 238, Bonn, 135p.

Gao, J., Lu, G., Zhao, G. & Li, J. 2006 Watershed data model: a case study of Xitiaoxi sub-waterhed, Taihu Basin. *Journal of Lake Sciences*, 18 (3), 312-318.

Georgakakos, K.P., Seo, D.-J., Gupta, H., Schaake, J. & Butts, M.B. 2004 Characterising streamflow simulation uncertainty through multimodel ensembles. *J. Hydrol.* 298 (1–4), 222–241.

Gupta, H.V., Beven, K.J. & Wagener, T. 2005 Model calibration and uncertainty estimation. In: Encyclopedia of hydrologic sciences (ed. by M. Anderson), Wiley, Chichester.

Hörmann, G., Zhang, X.Y. & Fohrer, N. 2007 Comparison of a simple and a spatially distributed hydrologic model for the simulation of a lowland catchment in Northern Germany. *Ecolog. Model.* 209 (1), 21-28.

Jin, X.& Gao, J. 2006 Modeling of Human Activities Impacts to Hydrological Process - Based on Distributed Hydrological model. Master thesis, Nanjing Institute of Geography & Limnology, Chinese Academy of Sciences.

Lindenschmidt, K.E., Fleischbein, K. & Baborowski, M. 2007 Structural uncertainty in a river water quality modelling system. *Ecolog. Model.* 204, 289–300.

Sponagel. H., Grottenthaler, W. & Hartmann, K.J. 2005 Bodenkundliche Kartieranleitung. 5. verbesserte und erweiterte Auflage, Hannover, 438p.

Wesseling, C.G., Karssenberg, D.J., Burrough, P.A. & Van Deursen, W.P.A. 1996 Integrated dynamic environmental models in GIS: The development of a Dynamic Modelling language. *Transactions in GIS*, 1 (1) 40-48.

Zhang, X.Y., Hörmann, G. & Fohrer, N. 2007 The Effects of Different Model Complexity on the Quality of Discharge Simulation for a Lowland Catchment in Northern Germany. Heft 20.07 ‘Einfluss von Bewirtschaftung und Klima auf Wasser- und Stoffhaushalt von Gewässern’, Band 2, *Forum für Hydrologie und Wasserbewirtschaftung*, 111-114.

Zhao, R. & Liu, X. 1995 The Xinanjiang Model. In: Singh, V. (Ed.), Computer models of watershed hydrology. Water Resources publications, Littleton, Colorado, 215-232.

Chapter 3

Hydrologic comparison between a lowland catchment (Kielstau, Germany) and a mountainous catchment (XitaoXi, China) using KIDS model in PCRaster

X.Y. Zhang, G. Hörmann, and N. Fohrer
Advances in Geosciences, 21, 125–130, 2009

Abstract

The KIDS model (Kielstau Discharge Simulation model) is a simple rainfall-runoff model developed originally for the Kielstau catchment. To extend its range of application we applied it to a completely different catchment, the XitaoXi catchment in China. Kielstau is a small (51 km²) lowland basin in Northern Germany, with large proportion of wetland area. And XitaoXi is a mesoscale (2271 km²) mountainous basin in the south of China. Both catchments differ greatly in size, topography, landuse, soil properties, and weather conditions. We compared two catchments in these features and stress on the analysis how the specific catchment characteristics could guide the adaptation of KIDS model and the parameter estimation for

streamflow simulation. The Nash and Sutcliffe coefficient was 0.73 for Kielstau and 0.65 for XitaoXi. The results suggest that the application of KIDS model may require adjustments according to the specific physical background of the study basin.

3.1 Introduction

Recent years have seen a rapid development of various hydrologic models. With the ever-growing technology in remote sensing, data telemetry and computing, model development is striving how best to represent the heterogeneous characteristics of a watershed. Much of the growth in sophistication of hydrological modelling is attributable to the digital revolution of distributed models and the availability of geospatial data through the last hundred years (Vieux 2004). However, as modelling and data power has increased there has been a concurrent debate in its disadvantage, e.g. the cost and time required in the collection of massive hydrological data. It is also argued that it can lead to more model uncertainty from the integration of more input data and the increasing number of model parameters, where it can affect the model prediction (Gupta et al. 2005). In some cases, simple model development like lumped models is sufficient in its own right (Silberstein 2006; Li et al. 2009). They are still used for various applications, including the study of hydrological processes (Bingeman et al. 2007), estimation of runoff and catchment water balance (Xu 1999), and assessment of land use and climate change impacts on runoff (Akhtar et al. 2008). Because lumped models have relatively few parameters, they can easily be regionalised to predict runoff. The modelling result is not therefore strongly depending on how sophisticated the model is. Another question concerning model application is whether a model is unique for each environmental problem. Even for a perfect model system, the unique properties of a location lead to a very important identifiability problem to decide the ‘optimal’ model structure and parameter sets (Beven 2001). As a result, computer models are needed that can easily be adapted to the problem under study. The KIDS model used in this study is such a flexible model, which is a simple rainfall-runoff conceptual model with the potential to be adjusted from lumped to distributed ones. It is programmed in the dynamic modelling language PCRaster (Wesseling et al. 1996). It was developed for the streamflow simulation in the Kielstau catchment, which is a very flat region with large area of wetlands (Zhang et al. 2007). The model structure was adjusted with integration of wetland representation for a better simulation result. To extend the range of the KIDS model application we applied it to a completely different catchment, the mesoscale mountainous XitaoXi watershed in southern China. The goal of this study was to determine the applicability of KIDS model for modelling

streamflow by comparing these two different watersheds in the hydrologic characteristics and modelling results. Specific objectives of this study were to: (1) analyse the unique features of the two catchments based on the available data, (2) compare the simulation results of the basic and adapted KIDS models, and (3) check the link between parameter estimation and hydrologic characteristics of the selected study basin.

3.2 Methods

The analysis framework includes three steps. First it is worth stressing the watershed and hydrometeorological characteristics for both large and small watersheds, by accounting for differences in topography, vegetation, soil properties, weather conditions and other important hydrologic features. With these considerations the KIDS model is then adapted to both locations for river discharge simulation. In addition, the problems of parameter estimation of the hydrology model for both catchments are discussed with focuses on the parameter sensitivity and its link to the unique catchment characteristics.

3.2.1 Site description

The study was carried out in the Kielstau and XitaoXi watersheds. Geographic location, catchment scale and the digital elevation map for both river basins are shown in Figure 3.1. The Kielstau catchment is located in the region of Schleswig-Holstein, Northern Germany, and covers an area of about 50 km². The catchment has a rather flat relief, with maximum elevation difference of 55m. Soils are mainly consisting of Gleysol, Podsol and Luvisol, among which Gleysol belongs to the major wetland soil types (Sponagel 2005). Most of the land in this catchment is used for agriculture (87%), forest and urban landuse share the remaining area. Average annual precipitation is around 860mm, and evaporation around 400mm (Schmidtke 1999). A large fraction of wetland area and the near-surface groundwater level are observed in this region (Trepel 2004), but there is no accurate mapping data for it. The interaction between surface water and groundwater is active, especially in the riparian wetland area for this region (Springer 2006).

The second study watershed XitaoXi is a 2271 km^2 sized mountainous basin located in the semitropical zone in Southern China. It is a sub-basin of the Taihu Lake. In the XitaoXi region, 63.4% of land use is agriculture-used drought area and commercial forest, 20% paddy rice land. Average rainfall within the watershed is 1466mm annually, and average evaporation from water surface ranges from 800mm to 900mm annually. The spatio-temporal variations in precipitation distribution and evaporation value are statistically significant (Gao 2006). The

dominant soil types are red soil and rocky soil. Since these soils tend to have limited water storage capacity, the highest fraction of the river discharge comes from surface runoff and interflow.

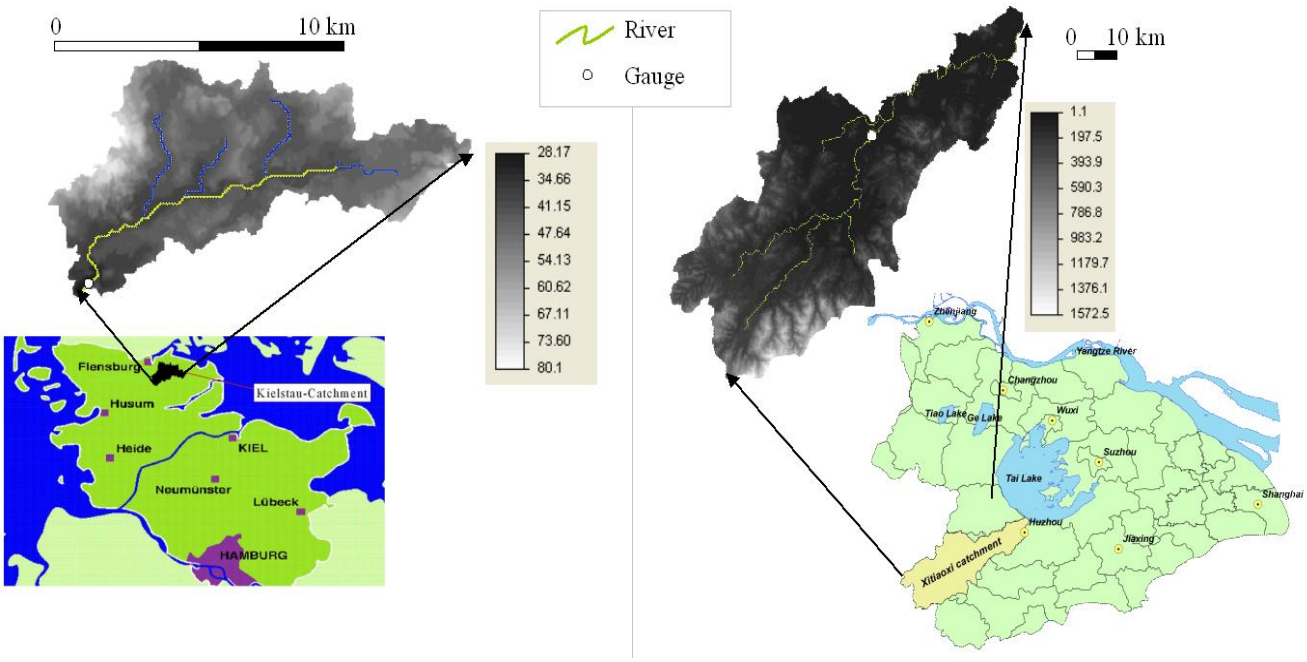

Figure 3.1 Geographic location and DEM for the Kielstau (left) and the XitaoXi basin (right).

3.2.2 Data collection

Basic spatial data for the KIDS model included a digital elevation model (DEM) and meteorological data. Other inputs like soils and land cover are important input parameters to KIDS but optional, as it can be added as extended submodels to the basic model structure. Based on long-term climatic data (1983-1999) from some nearby weather stations, there was no considerable spatial variation around the Kielstau region (Zhang 2006). The climatic data for Kielstau catchment was taken from the data set of the Flenburg station, 9km north from Kielstau basin (German Weather Service, Deutscher Wetterdienst, DWD). The DEM was provided by Landesvermessungsamt Kiel, and the LANU - Landesamt für Natur und Umwelt - has provided river discharge values from 1990 to 1999 (at the official Soltfeld gauge station). Other spatial data like land use, soil maps are from the BGR (Bundesamt für Geowissenschaften und Rohstoffe). Owing to the data limitation and the flat area, the model in Kielstau basin is set up with a completely lumped distribution of precipitation and evaporation (calculated with Penman-Monteith method).

In XitaoXi catchment, precipitation data are available from seven stations within the watershed area, and evaporation data are from two among the seven stations. Considering the

spatial and temporal variation of the climate in this mesoscale mountainous area, we used sub-basin distributed rainfall and evaporation (measured with the Chinese pan standard method). The discharge data set from the Hengtangcun gauge station is available from 1978 to 1987. All data including soil and land use were provided by the Administrative Bureau of TaiHu Basin.

3.2.3 The KIDS model and model adjustments

The basic KIDS model is driven by meteorological input data and simulates river discharge in given river basins as a dynamic function of spatial information. It is composed of one lumped soil layer and one groundwater aquifer, where the flow from soil to groundwater is calculated according to Glugla (1969). Sub-surface flow is modelled as 1D bucket flow and the groundwater layer as a linear storage. There are five important parameters contained in the basic module: 'Intercp_max' (maximum interception amount of vegetation cover); 'Inf_factor' (water infiltration rate of upper soil layer); 'SWC' (maximum soil water capacity); 'soil_gw_flux' (water seepage rate from soil zone to groundwater aquifer); 'gw_factor' (groundwater discharge rate to the river baseflow). Runoff is calculated on each grid cell:

Runoff =P-ETa-I-ΔS-ΔGW

Where P is precipitation and ETa is actual evapotranspiration;

I is interception, I = *f* ('Intercp_max');

ΔS is storage change of soil water, ΔS = *f* ('SWC' ,'Inf_factor', 'soil_gw_flux');

ΔGW is storage change of groundwater, ΔGW = *f* ('gw_factor').

Flow direction is then determined based on DEM, and channel flow is modelled with fully dynamic runoff routing using kinematic wave function. For more details see Hörmann et al. (2007) and Zhang et al. (2007).

In our previous study on model structure uncertainty (Zhang et. al. 2008), we cited the method to build up the KIDS model ensembles in order to find out the 'optimal' model structure for a specific location. Based on the result, we take the basic KIDS model and the optimized model structure for both basins to compare model simulation. For the Kielstau basin it is model 'DW' with consideration of the influence of agricultural drainage and wetland fraction. The agricultural drainage is introduced as the water amount extracted from the available soil water decided with the new parameter 'drainage_factor'. Wetland fraction (12%) is modelled based on the soil map as additional water storage layer in the soil zone, which has unlimited water support for evaporation as its actual ET equals the potential ET. The modified model for the

XitaoXi basin is 'LTG', which is coupled with lateral flow process and groundwater outflow threshold, using spatial distribution of potential evaporation adjusted with landuse coefficients. As the behavior of rainwater tends to be more affected by lateral flow on slope area, another parameter 'lateral_factor' is added to the XitaoXi model to generate lateral flow. The water amount recharged from groundwater to river base flow is here restrained by a groundwater outflow threshold, which represents limited influence on river discharge. Spatial distributed ETp adjusted with landuse coefficients referring to Gao et al. (2006), especially for drought area and paddy rice land of season changes. The adjusted KIDS models with submodels added accordingly are expected to produce better simulations as presented further in the next section.

3.3 Results and discussion

3.3.1 Hydrometeorological comparison

As mentioned above, the two catchments in this study differ greatly in catchment scale, topography, soil properties, landuse and weather conditions. The analysis of long-term mean monthly precipitation shows a very distinct seasonal pattern in the XitaoXi basin, with 75% of rain falling between April and October (Monsoon). The average daily runoff of the XitaoXi river (35.09 m^3/s) is much higher than that of the Kielstau stream (0.45 m^3/s). The difference is significant as well when considering the different discharge area of the selected gauge stations for both basins. The runoff rate per unit area is 8.82 l/s/km² for Kielstau, and 23.02 l/s/km² for XitaoXi. The two watersheds also differ in streamflow response to summer rains. Runoff efficiency based on the ratio of monthly stream flow to monthly precipitation (Wu & Johnston 2008) is plotted in Figure 3.2 for the two watersheds. Runoff efficiencies ranged from 0.08 to 0.58 in Kielstau basin and 0.22 to 0.58 for the XitaoXi catchment. The larger variations in runoff efficiency of the Kielstau basin might be caused by high evapotranspiration in the wetland area of the watershed and its capacity to impound surface runoff or to deter the streamflow events. The Kielstau and XitaoXi watersheds have quite different hydrologic regimes, thereby providing diverse data sets to test the adapted KIDS model used in this study.

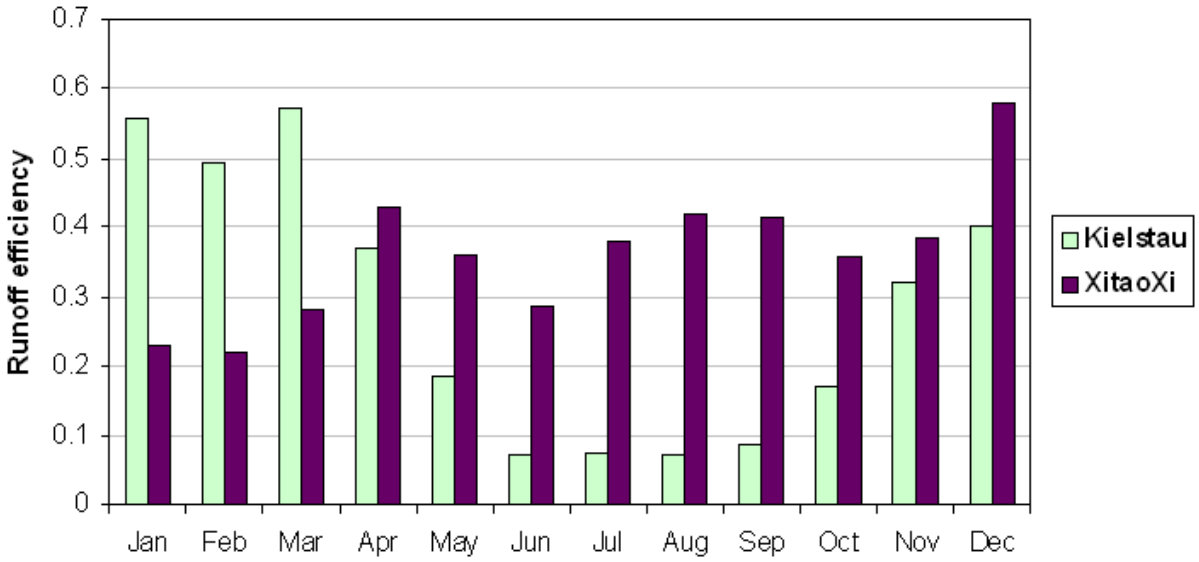

Figure 3.2 Seasonal patterns of long-term monthly runoff efficiency (monthly streamflow to monthly precipitation) in the 10-year data periods: 1990-1999 in Kielstau and 1979-1988 in XitaoXi.

3.3.2 Model simulation comparison

Runoff simulations were carried for the calibration period from 1990 to 1994 for the Kielstau and from 1979 to 1983 for the XitaoXi with the basic KIDS model and its optimal model version respectively. The resulting NS values (Nash and Sutcliffe, 1970) are listed in Table 3.1. The first results of the simulation using the default basic KIDS model yielded a low model efficiency of 0.08 for Kielstau and 0.2 for XitaoXi. With the adjusted model structure, the model efficiency improves significantly to an NS value of 0.73 for the validation period for model 'DW' of the Kielstau basin and to 0.65 for model 'LTG' of the XitaoXi basin. The result demonstrates that the selected submodels describe the hydrology of the catchment fairly well.

Table 3.1 Nash and Sutcliffe coefficient NS for 5 year period model calibration and a 10 year period validation in the two watersheds.

	Kielstau		XitaoXi	
	Periods	NS	Periods	NS
Default	1990 to1994	0.08	1979 to1983	0.21
Calibration	1990 to1994	0.70	1979 to1983	0.61
Validation	1990 to1999	0.73	1979 to1988	0.65

For the lowland Kielstau basin, the lateral flow may not be distinct due to the low altitude variance. Instead, the drainage ('D') reflects anthropogenic influence to some extent, with the evidence of large proportion of agriculture use in the local region and drainage pipes and

ditches commonly seen in the field. Moreover, the wetland ('W') plays an important role in the local water cycle. It can increase the capacity of a watershed to impound surface runoff and to enhance evapotranspiration dramatically especially in summer and autumn seasons. The model performance shows that the influence of drainage and wetland fraction makes a great difference in model efficiency. For the mountainous XitaoXi basin, lateral flow ('L') is required as one of the dominating processes in sloping area. Spatial distribution of evaporation ('T') is adjusted with empirical coefficients applied to various land use types. This is an alternative to the very limited evaporation data from only two weather stations within the large-scale catchment. Groundwater outflow threshold ('G') is a simply set value to reduce water discharge to base flow. It indicates that the influence from the groundwater is limited. From the model performance assessment, the 'LTG' model structure may better capture the hydrological mechanisms in the XitaoXi basin.

3.3.3 Parameter Calibration

In the adapted model versions, six parameters need to be determined by calibration using daily discharge observations. As introduced before, five parameters are same for both study basins and one different: 'drainage_factor' for Kielstau and 'lateral_factor' for XitaoXi. Most of the parameters were adjusted on a trial-and-error basis, modifying parameter values within reasonable limits and selecting final values with maximum model efficiency.

The result of the parameter estimation is displayed in Figure 3.3. The flat response surface of parameters 'intercp_max' and 'soil_gw_flux' indicates low parameter sensitivity for both catchments. The optimum value of 'swc' is much higher for the Kielstau than for the XitaoXi, which corresponds to large water storage capacity of the loamy soils in Kielstau. The sharp curves of the parameters 'gw_factor' and 'drainage/lateral_factor' for the Kielstau model suggest the influence of groundwater and drainage is important for streamflow simulation, but they are negligible for the XitaoXi catchment. Parameter identification problems will become easier to solve with more detailed information about the catchments that may be helpful to understand the uniqueness of location and its hydrological processes.

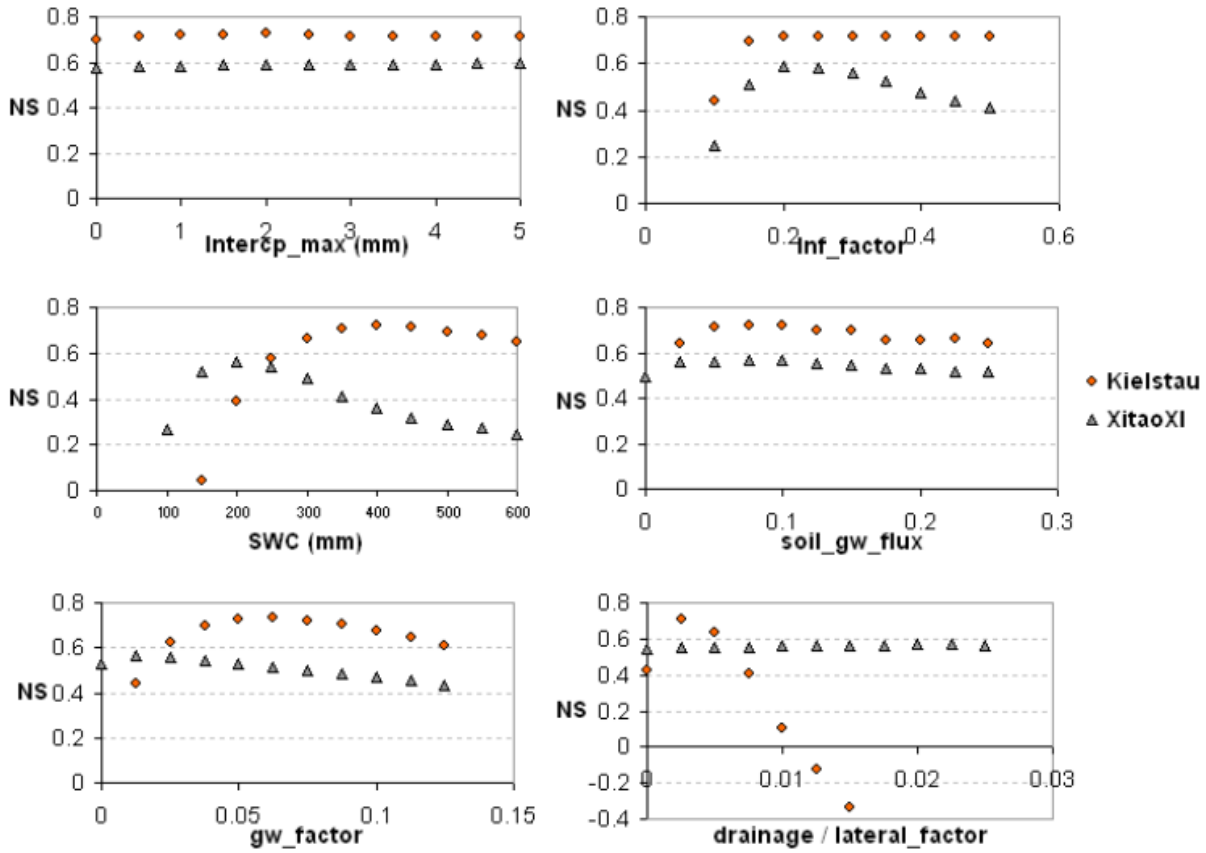

Figure 3.3 Nash-Sutcliffe model efficiency with different, variable parameters in Kielstau and XitaoXi Watershed.

3.4 Conclusions

Performance of KIDS model simulation was carried out for a small flat and a large mountainous watershed in different climates. The differences between the two hydrogeological regions are significant in many ways like catchment scale, topography, geology, landuse, soil properties, and weather conditions. For the purpose of river runoff simulation, we analysed the unique features based on observations and existing data base, discussed the possible model adjustments that can improve simulations, and compared the results in model efficiency and parameter estimations. Overall, the simulation provided satisfactory agreement between observed and simulated discharge. The validated simulation reaches a NS value of 0.73 for Kielstau and 0.65 for XitaoXi. It proved the general applicability and flexibility of KIDS basic model and submodel ensembles with for specific features of study area. For the Kielstau catchment, lumped model is adequate for this small region and better model performance can be achieved when considering the influence of wetland. Based on the long-term climatic data, it exhibited substantially different flow trends in the Kielstau than in the XitaoXi catchment, with lower runoff efficiency during summer months. It suggests an important storage function of wetland and groundwater, and

representative of the wetland components was necessary as added submodel. In the XitaoXi watershed we observed a significant impact of adjusted evapotranspiration for various landuse types and limited effects from groundwater. Owing to the larger catchment scale and distinct heterogeneity in topographic characteristics, more accurate geospatial data and distributed modelling are crucial for more accurate and reliable hydrologic predictions. The parameter calibrations in both case studies demonstrate the strong link between parameter estimation and the observed catchment features. This study stressed that, for simulating the hydrological behavior of a watershed, we should consider the unique features of the place much more explicitly (Beven 2000), and adapt the models to the local situation.

Edited by: B. Schmalz, K. Bieger, and N. Fohrer
Reviewed by: H. Bormann and one anonymous referee

References

Akhtar, M., Ahmad, N. & Booij, M. J. 2008 The impact of climate change on the water resources of Hindukush–Karakorum–Himalaya region under different glacier coverage scenarios. *J. Hydrol.* 355 (1-4), 148-163.

Bingeman, A. Kouwen, N. & Soulis, E.D. 2006 Validation of the Hydrological Processes in a Hydrological Model. *J. Hydrol. Eng.* 11 (5), 451-463

Beven, K. 2000 Uniqueness of place and the representation of hydrological processes, *Hydrol. Earth Syst. Sci.* 4, 203-213.

Beven, K. 2001 How far can we go in distributed hydrological modelling? *Hydrol. Earth Syst. Sci.* 5 (1), 1-12.

Gao, J., Lu, G., Zhao, G. & Li, J. 2006 Watershed data model: a case study of Xitiaoxi sub-waterhed, Taihu Basin. *Journal of Lake Sciences*, 18 (3), 312-318.

Glugla, G. 1969 Berechnungsverfahren zur Ermittlung des aktuellen Wassergehalts und Gravitationswasserabflusses im Boden. *Albrecht-Thaer-Archiv*, 13 (4), 371-376.

Gupta, H.V., Beven, K.J. & Wagener, T. 2005 Model calibration and uncertainty estimation. In: Encyclopedia of hydrologic sciences (ed. by M. Anderson), Wiley, Chichester.

Hörmann, G., Zhang, X.Y. & Fohrer, N. 2007 Comparison of a simple and a spatially distributed hydrologic model for the simulation of a lowland catchment in Northern Germany. *Ecolog. Model.* 209 (1), 21-28.

Li, H., Zhang, Y. & Chiew, F.H.S. 2009 Predicting runoff in ungauged catchments by using Xinanjiang model with MODIS leaf area index. *J. Hydrol.* 370 (1-4), 155-162.

Nash, J.E. & Sutcliffe, J.V. 1970 River flow forecasting through conceptual models. Part I: A discussion on principles. *J. Hydrol.* 10, 282-290.

Schmidtke, K.D. 1999 Land im Wind, Wetter und Klima in Schleswig-Holstein. Wachholtz Verlag, 119p.

Silberstein R.P. 2006 Hydrological models are so good, do we still need data? *Environ. Modell. Softw.* 21, 1340-1352.

Sponagel. H., Grottenthaler, W. & Hartmann, K.J. 2005 Bodenkundliche Kartieranleitung. 5. verbesserte und erweiterte Auflage, Hannover, 438p.

Springer, P. 2006 Analyse der Interaktion zwischen Oberflächenwasser und Grundwasser am Beispiel einer Flussniederung im Norddeutschen Tiefland. Diplomarbeit im Fach Geographie, der Christian-Albrechts-Universität zu Kiel. 191p.

Trepel, M. 2004 Development and application of a GISbased peatland inventory for SchleswigHolstein (Germany). In: Päivänen, J. (ed.) Proceedings of the 12th International Peat Congress Wise Use of Peatlands, 2, 931-936.

Vieux. B.E. 2004 Distributed Hydrologic Modeling Using GIS. Second edition, Kluwer Academic Publishers, Norwell, Massachusetts, Water Science Technology Series, Vol. 48. ISBN 1-4020-2459-2, 289p.

Wesseling, C.G., Karssenberg, D.J., Burrough, P.A. & Van Deursen, W.P.A. 1996 Integrated dynamic environmental models in GIS: The development of a Dynamic Modelling language. *Transactions in GIS*, 1 (1) 40-48.

Wu, K. & Johnston, C.A. 2008 Hydrologic comparison between a forested and a wetland/lake dominated watershed using SWAT. *Hydrol. Process.* 22, 1431–1442.

Xu, C.Y. 1999 Estimation of parameters of a conceptual water balance model for ungauged catchments. *Water Resour. Manag.* 13 (5), 353–368.

Zhang, X.Y. 2006 Test and application of hydrological models with a spatial modelling language (PCRaster) for the discharge simulation of a wetland dominated catchment in Northern Germany. Master Thesis. Christian-Albrechts-University of Kiel. 100p.

Zhang, X.Y., Hörmann, G. & Fohrer, N. 2007 The Effects of Different Model Complexity on the Quality of Discharge Simulation for a Lowland Catchment in Northern Germany. Heft 20.07 ‘Einfluss von Bewirtschaftung und Klima auf Wasser- und Stoffhaushalt von Gewässern’, Band 2, *Forum für Hydrologie und Wasserbewirtschaftung*, 111-114.

Zhang, X.Y., Hörmann, G. & Fohrer, N. 2008 An investigation of the effects of model structure on model performance to reduce discharge simulation uncertainty in two catchments. *Adv. Geosci.* 18, 31–35.

Chapter 4

Structural uncertainty assessment in a discharge simulation model

X.Y. Zhang, G. Hörmann, J.F. Gao and N. Fohrer
Hydrological Sciences Journal, 56 (5), 854–869, 2011

Abstract

A major goal in hydrological modelling is to identify and quantify different sources of uncertainty in the modelling process. This paper analyses the structural uncertainty in a streamflow modelling system by investigating a set of models with increasing model structure complexity. The models are applied to two basins: Kielstau in Germany and XitaoXi in China. The results show that the model structure is an important factor affecting model performance. For the Kielstau basin, influences from drainage and wetland are critical for the local runoff generation, while for the XitaoXi basin accurate distributions of precipitation and evapotranspiration are two of the determining factors for the success of the river flow simulations. The derived model uncertainty bounds exhibit appropriate coverage of observations. Both case studies indicate that simulation uncertainty for the low-flow period

contributes more to the overall uncertainty than that for peak-flow period, although the main hydrological features in these two basins differ greatly.

Keywords: hydrological modelling; perceptual model; model structural uncertainty; Kielstau, Germany; XitaoXi, China; PCRaster

4.1 Introduction

Hydrological models are always simplifications of the reality, and are therefore all subject to varying degrees of uncertainty. It is commonly accepted that the model uncertainty stems from a variety of sources where it can affect the model predictions (Melching 1995; Gupta et al. 2005). For example, many data sets needed as model inputs are defined through measurement in the field or laboratory, which introduces measurement errors and generates "data-driven uncertainty" (Brown & Heuvelink 2005). Then the estimation of parameters and formalization of model structure may lead to "explanatory uncertainty" (Brown & Heuvelink 2005) in model predictions. Some model parameters are inherently uncertain when they refer to real, measurable quantities such as soil hydrological conductivity, while some are empirical quantities applied to models and must therefore be estimated using measurements of the system inputs and outputs. Rather, we are uncertain about the errors in our understanding of the real system represented in the model structure. The natural flow systems that are themselves imperfectly known and understood have to be translated in the hydrological models. This is particularly important because models are more frequently used but observations are still limited.

In recent years, uncertainty of hydrological models has been investigated extensively, in particular the uncertainty induced by model inputs and parameter values (e.g. Rogers et al. 1985; Clausnitzer et al. 1998; Haan et al. 1998; Hanson et al. 1999; Beven & Freer 2001; Christiaens & Feyen 2002; Carpenter & Georgakakos 2004; Vrugt et al. 2005, 2006; Gourley & Vieux 2006; Lindenschmidt 2006; Ratto et al. 2007; Choi & Beven 2007). This abundance of literature does not imply that the modelling uncertainty from the change of model structure can be neglected (Beven et al. 2007). Indeed, structural uncertainty can be more significant than parameter and input data uncertainty, but such uncertainties are difficult to assess explicitly or to separate from other uncertainties during the calibration process (Beven & Binley 1992; Lindenschmidt et al. 2007). Furthermore, according to Beven (2001), model structures can only be identified uniquely when two components are specified: the perceptual model describing the dominant flow processes, and the conceptual model that is the

mathematical definition of those processes. Structural uncertainty is the modelling uncertainty due to the selection of an appropriate model, which includes the defined hydrological processes (perceptual model) and the mathematical description of these processes (conceptual model). In this context, the perceptual model might be more uncertain in comparison with the conceptual part, since it is usually formed based on a perceived lack of knowledge about the real processes, or a belief that the model abstracts and simplifies known processes (Neuman 2002; Beven 2001). For example, Newton's laws only resolve transfers of energy, matter and momentum through the environment. They do not resolve the processes that lead to changes in the storage and transfer of these elementary units. In practice, we are usually interested in the processes, as well as the transfers, because dominant process controls change through time and space.

Whereas the structural uncertainty is of more interest and importance, the range of schemes available for assessing the impact of model structure on modelling uncertainty is quite limited. Many investigations in model structures are mixed with other sensitivity or uncertainty analysis, such as parameter estimation, different discretizations or runtime errors (e.g. Uhlenbrook et al. 1999; Butts et al. 2004, Son & Sivapalan 2007; Ewen et al. 2006; Lindenschmidt et al. 2007). Some studies (e.g. Schuol & Abbaspour 2006) have discussed the impact of model structure and model complexity on model performance, but did not address the issues of structural uncertainty separately. Butts et al. (2004) explored ten model structures with different definitions in flow processes, built-in equations and spatial distributions; root mean square error (RMSE) and correlation (R) were used to assess the performance of model structure ensembles. Lindenschmidt et al. (2007) placed emphasis on the uncertainty in equations, and the quantification of structural uncertainty is quite case-specific as it is applied in a water quality modelling system. Yang et al. (2007) did not separate input and model structural uncertainty and concluded that a high fraction of uncertainty is due to input and model structure, comparing to parameter uncertainty.

In this study, we changed the model structure (mainly in perceptual models) to facilitate the structural uncertainty analysis. Different model structures were set up with PCRaster (Van Deursen 1995; Wesseling et al. 1996), a spatial modelling language and system. We explored the impact of different model structures on the discharge simulations for two catchments: Kielstau—a small lowland catchment (51.5 km^2) in northern Germany, and XitaoXi—a mesoscale mountainous basin (2271 km^2) in the south of China. With given model inputs, we focus on the uncertainty assessment in model structure. The results of the model ensembles are assessed against a number of performance criteria for the river discharge. The derived

uncertainty bounds are quantified and more detailed structural uncertainty analysis is performed using peak-flow/low-flow split testing.

With the development of a hydrological modelling framework that permits changes in the model structure and increases the model complexity within the same modelling tool, the objectives of this paper are: (a) to evaluate the performance of different model structures; (b) to identify the important hydrological processes or factors affecting model performance for each catchment; and (c) to estimate the structural uncertainty associated with river discharge simulation.

4.2 The study sites and data preparation

We report in this paper the estimates of daily streamflow of two representative basins differing in all main geohydrological features (Zhang et al. 2009). It is thought that the selection of two different basins would be useful in optimal exploitation of their perceptual model structures and of the flexibility of the employed modelling tool. This work is also one part of a Sino-German integrated geohydrological study of two basins, comprising hydrological and geophysical surveys, the collection of hydrometeorological and hydrochemical data, streamflow simulation, exploratory water quality investigation, model uncertainty, etc. It aimed to facilitate a systematic exploitation of the river water resources.

Figure 4.1 shows the approximate geographical locations and the digital elevation map of the two basins that were selected for the integrated geohydrological studies, namely the Kielstau basin and the XitaoXi basin.

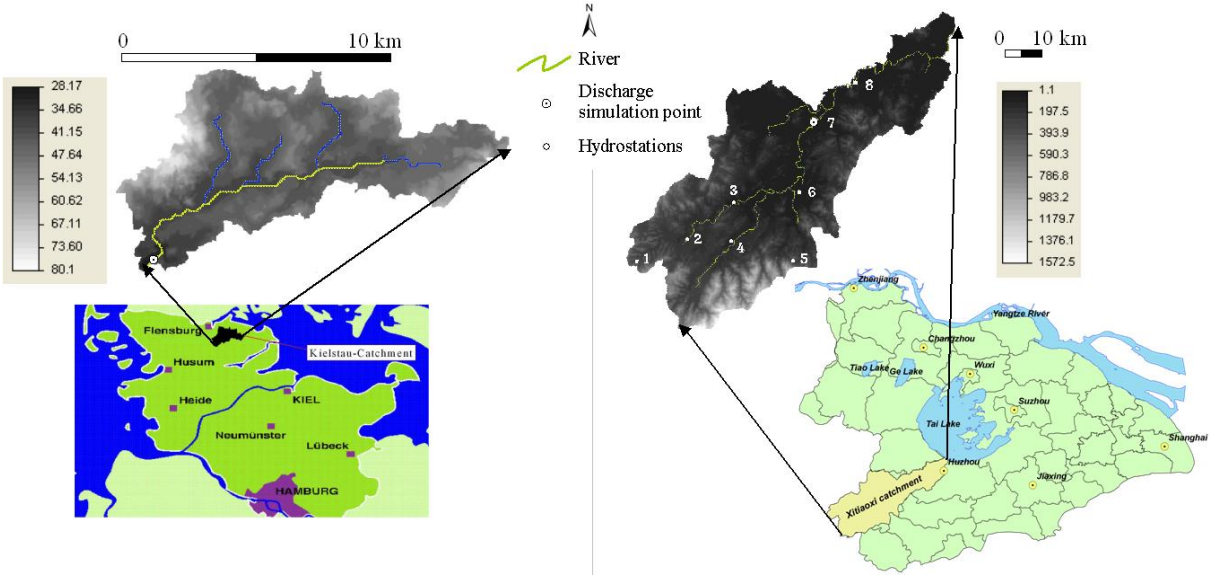

Figure 4.1 Location and DEM map of the two study catchments (Zhang et al. 2009) (discharge simulation point for Kielstau: Soltfelt; and for XitaoXi: Hengtangcun, hydrostation. 1: Tianjintang, 2: Hanggai, 3: Fushishuiku, 4: Laoshikan, 5: Yinkeng, 6: Dipu, 7: Hengtangcun, 8: Fanjiacun)

4.2.1 The Kielstau basin

The Kielstau basin is located in Schleswig-Holstein, northern Germany, and covers an area of 51.5 km^2. The River Kielstau, approx. 11 km long, is a small stream draining the basin from northeast to southwest. The landscape is distinguished by a rather flat relief, owing to the landform process under the influence of extensive glaciation during the Pleistocene epoch. The glaciers moved back and forth in turn over long periods of time creating on this small area a mixture of different types of moraine in close succession. The whole watershed has poor drainage due to the low gradient with a maximum altitude difference of 55 m (see Figure 4.1, left). Wedged between the North Sea and the Baltic Sea, the Kielstau catchment is characterized by moderate temperature and oceanic climate with mild, moist winters and cool, rainy summers. Snowfall is rare and occurs on average on 20 up to 25 days per winter. Average annual precipitation is around 860 mm, and actual evaporation around 400 mm (Schmidtke 1999). The geological basement of the basin is dominated by Pleistocene deposits, resulting in a wide variety of soil types and soil forms in this small area. Soils mainly consist of podzol, gleysol and luvisol, formed in the Saale and Weichsel ice ages, among which gleysol belongs to the major wetland soil types (Sponagel 2005). These are heavy soils having high field capacity and containing large proportions of clay and silt, which contribute to the formation of numerous scattered “Niedermoor” and “Hochmoor” (peatland or wetland) in the watershed. A large fraction of wetland area and near-surface groundwater level are observed in this region (Trepel 2004), but there are no accurate mapping data for this. The dynamics of near-surface groundwater are generally determined by precipitation, and, when close to the river, by stream water level as well. In most cases, groundwater levels in the riparian wetland are higher than those in the river. The interaction between surface water and groundwater is thus active for this region, especially in the riparian wetland area. During flood events, a reversal of the flow direction could occur if the close-to-river groundwater level is lower than the stream water level (Springer 2006).

4.2.2 The XitaoXi basin

The second study area, XitaoXi, is a 2271 km^2-sized mountainous basin located in southeast China. It is one of the major sub-basins of Taihu Lake. From the elevation map in Figure 4.1 (right), the topographic slope declines from southwest to northeast. In general, the whole XitaoXi basin can be characterized by three different areas with distinct topography: the upper reaches in the southeastern part are mountainous, with elevation over 600 m, accounting for about 15% of the total basin area; a 150–600-m-high low hilly area in the centre accounts for

40%; and in the remaining northeastern part the topograph turns into a flat outwash plain with a low hydraulic gradient. The dominant soil types are red soil and rocky soil. The ecologically and geologically diverse XitaoXi area is characterized by changing land-use patterns. The mountainous upper reaches are dominated by forest, of which about 75% has been planted with bamboo; in the middle hilly reaches, farmland and forest are in nearly equal percentage, while the downstream plain areas are mainly paddy fields (Wan et al. 2007). As it is situated in a semitropical climate zone, rainfall in the basin is monsoonal. The spatio-temporal variations in precipitation and evaporation distribution are statistically significant (Gao et al. 2006). Rainfall usually commences in the middle of May and continues mainly during June, July, August and September. Occasional showers occur in other months. There is usually more rainfall in the mountains than in the neighbouring plains. The average annual rainfall recorded at the eight hydrometeorological stations (Figure 4.1, right) in XitaoXi basin for the years 1979–1988 was found to be 1466 mm. The annual rainfall gradually decreased from the southwest mountain area (1800 mm) to the northeast plains (1200 mm). Annual open pan evaporation for this period was estimated as 800–900 mm. Evaporation intensity from the southwest to the northeast has shown an increasing trend (Zhang et al. 2006). The drainage pattern in the XitaoXi basin is of dendritic type. Two reservoirs—Fushishuiku and Laoshikan (near hydrostation no. 3 and no. 4 in Figure 4.1)—in the upsteam areas are used for flood control in rainy seasons. Available continuous streamflow data are only recorded at the Hengtangcun and Fanjiacun stations. The river runoff values at Fanjiacun were greatly influenced by the backflow from Taihu Lake, owing to its location in the lower outwash plain, close to the XitaoXi basin outlet to Taihu Lake. In order to facilitate the comparison of runoff simulations with the measured values, the Hengtangcun station, which covers the discharge basin area of 1524 km^2, was chosen in this study as the simulation point.

4.2.3 Data

The data used in the PCRaster model are: climatic data, DEM, soil and land-use data. The climatic data for Kielstau catchment were taken from the data set of Flenburg station, 9 km north of Kielstau basin (German Weather Service, Deutscher Wetterdienst, DWD). The DEM was provided by Landesvermessungsamt Kiel, and the LANU (Landesamt für Natur und Umwelt) provided river discharge values from 1983 to 1999 (at the official Soltfeld gauge station). Other spatial data such as land use and soil maps are from the BGR (Bundesamt für Geowissenschaften und Rohstoffe). Land use in the Kielstau basin is predominantly

agricultural (55.82%) and grass (26.14%). All maps were converted to a raster map with a cell length of 50 m.

Daily precipitation data in the XitaoXi basin are available from eight stations within the watershed area, while evaporation data are only recorded at two stations—Fushishuiku and Hengtangcun. The discharge data set from the selected Hengtangcun gauge station is available from 1978 to 1987. All data including land-use and soil maps were provided by the Administrative Bureau of TaiHu Basin. The cell length of the raster maps is 200 m.

A long-term hydrometeorological analysis was conducted for both basins. The values for annual precipitation, potential ET and river runoff of the two basins are presented in Figure 4.2, and Figure 4.3 shows the monthly mean values of rain and discharge which can be used to derive seasonal patterns for the two areas (Zhang et al. 2008). With the maritime climate environment in the Kielstau region, there is precipitation all the year round. Neither the annual variations in rainfall, nor the seasonal ones, extend to severe extremes. Meanwhile, a quite high evapotranspiration rate is shown during the summer season. The seasonal changes of rainfall and runoff are more distinct in the XitaoXi basin because of the monsoon climate, with 75% of rain falling between April and October. The average daily runoff of the XitaoXi River (35.09 m^3/s) is much higher than that of the Kielstau stream (0.45 m^3/s). The difference is also significant when considering the different discharge areas of the selected gauge stations for both basins. The runoff rate per unit area is 8.82 L s^{-1} km^{-2} for Kielstau, and 23.02 L s^{-1} km^{-2} for XitaoXi. Figure 4.3 also presents different patterns of the two watersheds in streamflow response to summer rains. To have a better look at their correlation, we calculated the runoff efficiency based on the ratio of monthly streamflow to monthly precipitation (Wu & Johnston 2008). The distribution of river runoff in the XitaoXi catchment is mainly controlled by rainfall. The runoff values kept in good correlation with the variation of rainfall, with runoff efficiencies ranging from 0.22 to 0.58. The runoff efficiencies calculated for the Kielstau basin have similar values for winter, with extremely low values for the summer months, e.g. 0.08 for the month of June, making the average value drop to 0.3. The larger variations in runoff efficiency of the Kielstau basin might be caused by high evapotranspiration in the wetland area of the watershed, and its capacity to impound surface runoff or to deter the streamflow events.

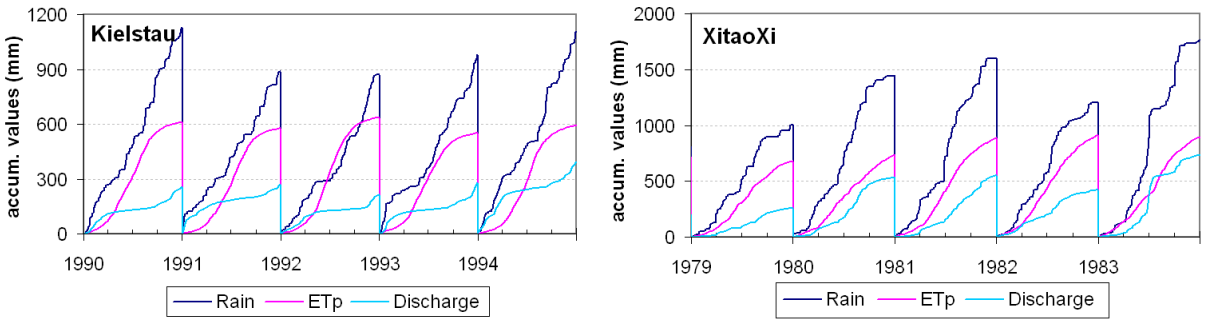

Figure 4.2 Annually accumulated climatic data for the Kielstau and XitaoXi catchments.

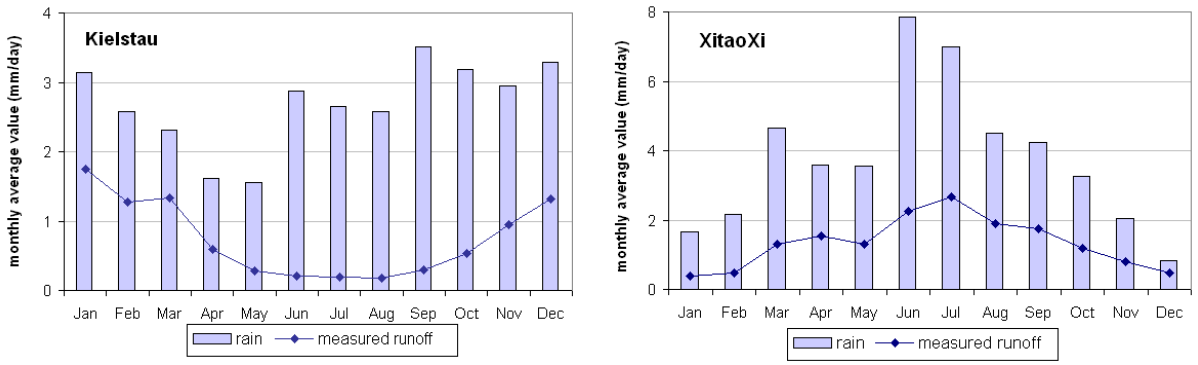

Figure 4.3 Monthly rain and discharge mean value, based on data from 1990 to 1999 (for Kielstau), and from 1979 to 1988 (for XitaoXi) (Zhang et al. 2008)

4.3 The procedure of uncertainty analysis

4.3.1 Basic module description

The basic hydrology module—KIDS (Kielstau Discharge Simulation model)—was developed for practical purposes to facilitate further research in nutrient leaching assessment, water protection and land-use evaluation in the Kielstau area. This implies that relatively simple model approaches were chosen to operate under restricted data availability. The model calculation is based upon the water balance equation (see equation 1), taking into account interception, precipitation, evapotranspiration, and the flows to other compartments. We use mm as the unit of measure for all the water amount expressions included herein, and calculate with a daily time step:

$$S_t = S_{t-1} + P_t - \mathrm{ET}_t - I_t - Q_{ot} - S_{pt} \quad (1)$$

where S is the soil water content, t is the modelling time step (d), P is precipitation, ET is evapotranspiration, I is interception, Q_o is surface runoff (overland flow), and S_p is percolation or seepage.

Precipitation and potential evapotranspiration are required as input data. The model calculates interception from canopy and litter, combined transpiration and evaporation and the water

fluxes in the soil column. The calculation of gravity-driven water percolation in the KIDS model follows the semi-empirical differential equation of Glugla (1969). Surface runoff Q_o is calculated according to equation (2). It describes soil percolation and storage calculation on the basis of derived soil parameters such as field capacity and infiltration rate of soil water deficit:

$$Q_o = \max\{[P - I - K_c(S_{fk} - S)], 0\} \quad (2)$$

where K_c is the infiltration parameter and S_{fk} is the wetness at field capacity.

The subsurface runoff or lateral flow for the soil column can be subdivided into several layers according to the soil database. This is simplified as one lumped uniform soil column for the basic KIDS model. We adjusted the amount of subsurface runoff with a lateral flow rate parameter as follows:

$$Q_s = K_s \times S \quad (3)$$

where Q_s is subsurface flow, and K_s is lateral flow rate.

Runoff is then composed of three parts: surface runoff, lateral flow and groundwater discharge from the groundwater layer, which is represented as a linear storage. In the basic model M for both basins, the value of parameter K_s is set equal to zero, whereas in the sub-module L, it is adjusted above zero for better comparison. More details of subsurface flow and groundwater calculation will be explained in Section 3.3.

Flow direction is then determined based on a DEM, and channel flow is modelled with fully dynamic runoff routing using kinematic wave function. The KIDS model represents a rather simple rainfall–runoff model. A very attractive feature is its applicability to small or large-scale areas, and flexibility to adapt model structures, whenever it is appropriate or necessary to take the internal variability of soil and vegetation characteristics, in particular of specific influence factors, into account. This could be done by means of additional sub-modules applied to the basic KIDS structure. Essential references are given in Hörmann et al. (2007) and Zhang et al. (2007).

4.3.2 Data processing

Owing to the different sizes of the two basins and the availability of data, it is important to handle data differently to fit in a more appropriate and regionalized model.

The basic module is implemented in the Kielstau basin with a single station for precipitation and ET. The only source of climatic data is from the neighbouring Flensburg weather station,

since long-term weather records within the Kielstau area were missing. One short-term data set obtained from field observations was compared with the long-term data set. The temporal variation of rainfall data was identical to the long-term records, except for some marginal differences in daily values. The spatial variation of rainfall may be considered homogeneously distributed around the local area on account of its flat topographical nature. The induced uncertainty is thus expected to be small resulting from the use of alternative climatic input data. As the soil water dynamics is described with the capacity based Glugla approach, the capacity parameters required by the model are attached to the model by external data files that are consistent with the German soil texture classification and their related capacity parameters in AG Boden 2005 (Sponagel 2005).

Meanwhile, deriving quantitative weather information is a more difficult task in mountainous regions like the XitaoXi basin. Spatially distributed rainfall or snow is important in a large and mountainous catchment for accurate hydrological prediction. Considering the XitaoXi climatic zone, only rainfall is the significant source in the hydrological cycle. Rainfall data from the eight weather stations within the study area were interpolated using Thiessen polygons. The network of ET gauges is less dense with only two stations in the area. ETp values were measured with Chinese pan method (Gao et al. 2006).

4.3.3 Development of the model structure ensembles

We used the following procedure to create the model ensemble, as shown in Figure 4.4. First, a basic module (abbreviated as M) and a group of sub-modules (represented by A, B, C etc.) are required as elementary components to build up a module pool. Secondly, the basic module M is combined with the other modules to create a group of "simple" models. These simple models are given the same letter as the sub-module. The methodology of "genetic algorithm" was applied to select fitter individuals for the optimization of the model structure combinations. Taking the performance of the basic module M as a reference, only the simple models with improvement in simulation results (according to the selected criteria) are included in the next step. Finally, the basic module M is combined with all other modules to form a series of "cross-models". They are identified with the ID combination of their sub-modules; thus, the main water flow processes of a model ensemble can be easily recognized from its name, and the number of the characters is an indicator of the complexity.

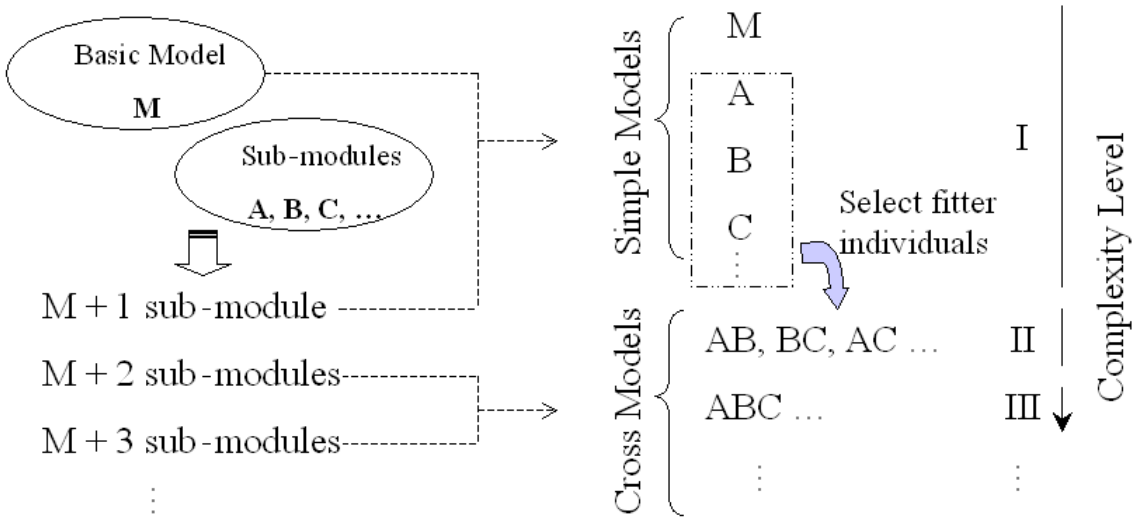

Figure 4.4 Schematic chart of the framework to develop model structure ensembles

We implemented a suite of model versions, representing the structural uncertainty of both watersheds. The basic KIDS model concept is taken as module M, and six sub-modules are developed for both Kielstau basin (H, L, T, G, D, W) and XitaoXi basin (P, E, G, L, T, R).

4.3.3.1 Model H & M - Kielstau

To describe the potential evapotranspiration (ET_p) two different approaches were used: calculation of ET_p with the empirical Haude formula (Haude 1958) in model H using crop-specific monthly coefficients, and calculation of a reference ET for grass with the FAO Penman-Monteith method (Allen et al., 1998) in the basic model M.

Traditionally the Haude evapotranspiration formula (equation (4)) was widely used in Germany with temperature (t in °C) and relative humidity (rH in %) measured at 14:00 h required as inputs. For different types of land use, monthly coefficients (a) for the Haude formula are given reflecting the state of the plants in an average annual growth cycle. Thus:

$$ET_p = a \times e_{s14} \times (1 - rH_{14}/100) \quad (4)$$

where a (-) is the Haude coefficient (from monthly tables, crop specific); e_{s14} (hPa) is saturated vapour pressure at 14:00 h local time, calculated based on temperature; and rH_{14} (%) is relative humidity at 14:00 h local time.

The FAO Penman-Monteith formula to estimate the reference evapotranspiration (ET_o) was derived by utilizing some assumed constant parameters and simplifying the air density term, as shown in equation (5). The equation requires standard climatological records of solar radiation (sunshine), air temperature, humidity, and wind speed:

$$ET_0 = \frac{0.408\Delta(R_n - G) + \gamma \frac{900}{T+273} u_2 (e_s - e_a)}{\Delta + \gamma(1 + 0.34u_2)} \quad (5)$$

where ET_o (mm d^{-1}) is reference evapotranspiration, R_n (MJ m^{-2} d^{-1}) is net radiation at the crop surface, G (MJ m^{-2} d^{-1}) is soil heat flux density, T (°C) is mean daily air temperature at 2 m height, u_2 (m s^{-1}) is wind speed at 2 m height, e_s (kPa) is saturated vapour pressure, e_a (kPa) is actual vapour pressure, $e_s - e_a$ (kPa) is the saturated vapour pressure deficit, Δ (kPa $°C^{-1}$) is the slope vapour pressure curve, and γ (kPa $°C^{-1}$) is a psychrometric constant.

The evapotranspiration estimate by the Haude approach was distinctly less satisfactory. The potential ET_p for Haude is only 51 mm $year^{-1}$ higher than the ET_a calculated by the M model. A further analysis of the monthly values shows that the summer evaporation is greatly underestimated and the growth of the plants starts earlier than predicted by the Haude method. The FAO Penman-Monteith method is thus recommended as the standard method for the definition and computation of the reference evapotranspiration to all other models of the Kielstau watershed.

4.3.3.2 Model G, L & T – Kielstau & XitaoXi

A threshold of groundwater outflow to river is set in model G, in order to restrict the impact of groundwater on discharge, as defined by:

$$G_t = G_{t-1} + I_{gt} - Q_{gt} \quad (6)$$
$$Q_g = \min(K_g G, G_m) \quad (7)$$

where G is groundwater storage, I_g the inflow to groundwater aquifer, Q_g the groundwater discharge to runoff, K_g the groundwater outflow rate, and G_m the maximum daily groundwater outflow or groundwater outflow threshold. Combining equations (6) and (7) yields the daily groundwater dynamics.

The lateral flow model L is adjusted with a positive value of the lateral flow rate K_s, as shown in equation (3). The evapotranspiration for different land-use types or crop surface is considered in model T. For Kielstau, we calculate the crop specific evapotranspiration ETc for other crops (equation 8) referring to Penman-Monteith method, with landuse coefficients (Kc) that relate ETc to ETo, the standard reference evapotranspiration.

$$ET_c = K_c\, ET_o \quad (8)$$

For XitaoXi, the potential evapotranspiration measured by pan method proved its practical value in Jin & Gao (2006). It has been used successfully to estimate reference evapotranspiration by observing the evaporation loss from a water surface and applying empirical coefficients to relate reference evapotranspiration to pan evaporation:

$$ET_r = K_p E_{pan} \quad (9)$$

where ET_r is the reference evapotranspiration in the XitaoXi area, K_p the pan coefficient, and E_{pan} the pan evaporation.

4.3.3.3 Model D & W - Kielstau

In Kielstau large areas of drainage were observed to combat the problem of water logging associated with flat topography and high water tables. The leakage of water from the network of water distribution through the manmade drainage channels is thus another important factor considered in model D, functioning as in equation (10). In this conceptual relationship, the soil types are the function controlling the curvature of drainage volume:

$$D = K_d S + L_d \quad (10)$$

where D is the drained water volume, K_d is a drainage factor, S is the available soil water storage, and L_d is the lateral inflow volume (lateral seepage from irrigation canals and drainage channels).

We introduced an additional wetland layer in model W. The dynamics of wetland water can be described as:

$$W_t = W_{t\text{-}1} + I_{wt} - E_{wt} - Q_{wt} \quad (11)$$

where W is wetland water storage; I_w the incoming water volume influenced by precipitation, interception and soil moisture; E_w the water loss from wetland, mainly evapotranspiration; and Q_w the wetland water seepage contributing to runoff.

Evaporation is frequently the most significant loss of water from a wetland as noted by Tagaki et al. (1998). This is also supported by a summery of studies on hydrological functions of wetlands (Bullock & Acreman 2003). Among all the collated reference studies, there is strong evidence that wetlands evaporate more water than other land types, such as grassland, forests or arable land. From the data analysis for Kielstau, the river runoff reveals a similar feature influenced by higher evaporation from wetlands. However, investigations into the wetland evaporation rate for Kielstau suffer from a lack of reliable measurements, as climatic

data are not collected routinely from wetland areas. In a review of evapotranspiration rates measured in a Danish wetland study, it was found that wetland evaporation is 1.3 to 1.5 times higher than grassland evaporation (Andersen 2003). Thus, within the framework provided by a water budget investigation, we set a factor of 1.3 times the reference evaporation for the wetland area, to model realistic wetland conditions in the KIDS model. The fraction of wetland is unknown. By reclassifying soil types Peat and Gley soil as wetland, it is estimated as 12%. Another consequential effect of water stagnation is substantial water storage within wetlands. This results in no limitation of available water to support the assumed higher potential evaporation transferring into actual evaporation. All these factors led to a transformation of the conceptual model from the basic one into the wetland model W.

4.3.3.4 Model P, E & M – XitaoXi

Three models with differences in spatial distribution of climatic input data are test for the XitaoXi catchment in order to compare the results. They are: model P—lumped precipitation distribution and two sub-basin distributed ET_p; model E—lumped ET_p distribution and eight sub-basin distributed precipitation; and model M—spatial distribution in both precipitation and ET_p.

4.3.3.5 Model R - XitaoXi

In the southeast upstream area of the XitaoXi catchment are the two reservoirs Fushishuiku and Laoshikan (near hydrostation 3 and 4 in Figure 4.1). They are primarily used for irrigation during the dry season and flood control during the rainy season. According to Jin & Gao (2006), the outflow from the reservoirs is controlled with some set-up water storage levels, as equation (13) suggests:

$$R_t = R_{t-1} + Pr_t - Qr_t \tag{12}$$

$$Qr = \begin{cases} 0 \ (R <= Qstrict) \\ x \ (Qstrict < R <= Qnormal) \\ y \ (Qnormal < R < Qmaximum) \\ z \ (R >= Qmaximum) \end{cases} \tag{13}$$

where R_t, R_{t-1} are reservoir storage at time t and $t - 1$; P_r is the net rainfall in the reservoir area; Q_r is the daily outflow from the reservoir; Q_{strict}, Q_{normal}, and Q_{max} denote conservative storage, normal storage, flood storage, and x, y, z are defined outflow amount from reservoir in different cases.

Both equations (12) and (13) describe the function of reservoir in our model R. Due to data restriction, it may be arguable that the large reservoirs are considered as points in the simulation (van der Knijff & de Roo 2008).

A short description of the main distinguishing features of all sub-modules is given in Table 4.1.

Table 4.1 Short description of sub-modules

Basin	ID	Module description
Kielstau	H	ETo calculated with Haude method (DVWK 1996)
	M	ETo calculated with Penman-Monteith method
	L	Subsurface water flow from soil layer to river runoff
	T	Spatial distributed ET adjusted with land-use coefficients referring to Penman Monteith method (Allen et al. 1998)
	G	Outflow threshold of groundwater flow to river discharge
	D	Subsurface drainage
	W	Additional wetland fraction (12%) in the soil zone, which has unlimited water support for evaporation as its actual ET equals the potential ET
XitaoXi	P	Lumped precipitation distribution and sub-basin distributed evapotranspiration
	E	Lumped evapotranspiration distribution and sub-basin distributed precipitation
	M	Sub-basin distributed precipitation and evapotranspiration
	G	Outflow threshold of groundwater flow to river discharge
	L	Subsurface water flow from soil layer to river runoff
	T	Spatial distributed evapotranspiration adjusted with land-use coefficients referring to Gao et al. (2006)
	R	Integration of two Reservoirs in the upstream area referring to Jin & Gao (2006)

4.3.4 Parameter calibration

This study is made to investigate model structure as one of the sources of uncertainty, but it was quite difficult to calculate explicitly (Radwan et al. 2004; Lindenschmidt et al. 2007). However, each simple or combined model here has a different set of parameters, which needs to be calibrated; hence a strict division of parameter and structural uncertainty was not quantified. An automatic parameter calibration scheme (Schmitz et al. 2009) was employed in the PCRaster language environment to optimize parameter estimations for each model. This is designed as searching for the optimal parametric values targeting a high Nash-Sutcliffe value (Nash & Sutcliffe 1970). Concerning that the calibration result may lead to significant parameter uncertainty and equifinality between parameter sets, ten parameters sets coming from the simulation runs are retained for each model in terms of model capability to reproduce measured data. Therefore the model is consistent and can be meaningful for further model structure analysis. In this case, attention is given to the uncertainty in the process description represented by the model orsub-module ensembles and less to the uncertainty in the parameters.

4.3.5 Criteria for uncertainty evaluation

Traditionally, model performance is evaluated with different numeric criteria (Gupta & Sorooshian 1998; Krause et al. 2005). For this study we used Nash-Sutcliffe index (NS, Nash & Sutcliffe 1970), regression coefficient R^2 and the difference of sum predicted and observed discharge values per year. These represent modelling efficiency, the match to the shape of the hydrographs and the water balance error respectively. The combination of these three criteria is also used to decide which sub-modules will be included to form the cross models.

We use two measures to quantify the deduced model prediction uncertainty. A normalized measure of the dispersion in the simulation ensemble was selected to indicate the influence of the variances in model structures on the uncertainty in flow simulations. This measure, termed *R* factor (Schuol & Abbaspour 2006), was defined as the average thickness of the prediction uncertainty among all ensemble runoff values at each time step normalized by the standard deviation of the measure data within a selected period. Another measure quantifying the strength of the model uncertainty is *P* factor (Abbaspour et al. 2004), which is the percentage of measured data bracketed by the band of prediction uncertainty.

The ideal situation would be to have an *R* factor value close to zero, and in the meantime to bracket most of the measured data within the uncertainty band. This method is suitable for comparing ensemble dispersion of different scenarios and it is independent of the shape of the observed flows. The different contribution of the simulation uncertainty in low-flow and peak-flow seasons to the overall structural uncertainty will be assessed by examining patterns of behaviour in the measure *R* factor.

4.4 Results and discussion

4.4.1 Performance of model structure ensemble

According to the three criteria, the performances of all model structures of the two study basins are shown in Figure 4.5. There are seventeen models tested for each watershed, including seven simple and ten cross-models.

For the Kielstau basin, two simple models—H and T—did not perform as well as the basic module in any of the three criteria. Both models failed because of the evapotranspiration estimation. As expected, the Penman-Monteith method used in the basic model M can achieve a better result than the simple empirical Haude approach to calculate the potential evaporation. This may suggest that the Haude formula, especially the embraced monthly coefficients, needs further verification for a specific region before it can be applied in a model. This study shows that the summer evaporation is greatly underestimated and the

growth of the plants starts earlier than predicted by the Haude method. The model T with an integration of land-use adjusted ET_o has similar problems. The land-use coefficients referring to Penman-Monteith method did not help much to make a good estimation of the high evaporation rate at summer seasons. Models L and G could induce only little changes in model performance, with a minor improvement in the water balance error as the model G restrains groundwater recharging. Comparing the performance of all simple models shows that the influence of drainage and wetland fraction makes a great difference in model efficiency. The drainage process used in model D gives the most significant improvement. This can be observed in the performances of cross models as well: models including drainage achieve relatively higher NS value and less water balance error. The combination of drainage and wetland fractions—model DW—outperformed hydrological simulations from the entire cross models. Note that the Kielstau region is a very flat landscape with open drainage ditches and a large area covered by wetlands; these must be indispensable elements in the local hydrological cycle. Moreover, the analysis of the Kielstau data set shows a low runoff to precipitation ratio with an average value of 0.318, whereas for Schleswig-Holstein, runoff is typically slightly below 50% of precipitation (Schmidtke 1999). A possible explanation for the lower discharge in summer and autumn (see Figure 4.3) could be: either additional water loss by drainage and extra evapotranspiration is underestimated, or the hydrological functions of e.g. wetland are ignored, or a part of both. Further data requirements and analysis are needed in support of the justification of these assumptions. The method of modelling with simple structure assumption here may provide useful information on the modelling uniqueness in this study area for any subsequent model applications. The well performing DW model shows that the integration of drainage and wetland fraction in the model creates a better fit of the simulated and measured runoff for the Kielstau basin. It decreases the large amount of excess runoff during the low flow periods. Water is extracted by the additional wetland storage mostly, drainage and high evaporation during summer and autumn seasons. It could thus represent the observed low runoff/precipitation characteristics in a better way. This may be the most appropriate model structure in all tested models for the catchment.

For the XitaoXi basin, the results of simple models demonstrate a strong link between the model performance and the spatial distribution of input climatic data. The model M with sub-basin distributed evaporation and precipitation has better performance than the model P and E in all three criteria. It is clear from the results that the regionalization of all hydroclimatological inputs should be handled with extreme care for large and mountainous watersheds like the XitaoXi basin. Therefore P and E were excluded from the cross model

procedure. Just two ET observation stations in model M can not provide sufficient information to quantify the spatial distribution of ET in the basin. Model T has shown further improvements in simulation results by updating ET data with land-use information. Furthermore, no significant enhancement in model simulation is observed in model L, the lateral flow model. This may suggest that the river discharge mainly comes from surface runoff since the dominant soil types are red soil and rocky soil, which tend to have limited water storage capacity and low permeability. A study from Xu et al. (2007) also indicates that saturation excess surface runoff is probably the dominant process for the XitaoXi catchment. The inclusion of two large reservoirs in the upstream basin (model R) did not improve the results drastically; it only decreased some peak discharges. The fact that large reservoirs are only modelled as points in the simulation may contribute to this, as significantly higher evaporation losses from the reservoir areas may be ignored. Among all the models, best performance is achieved by the model GT, which is coupled with groundwater outflow threshold, and spatial distribution of evaporation adjusted with land-use coefficients. It does not make a distinct increase in NS value, but a high R^2 value and close-to-zero balance error may indicate that the runoff producing process of model GT suits the best to match the shape of hydrographs. This indicates to a certain extent that an appropriate input tranformaiton process for the heterogeneous XitaoXi basin is a crucial step in model simulation, and the influence from the groundwater in the hilly region is very limited. The GT model structure may better capture the hydrological mechanisms reflected in the performance assessment.

Figure 4.5 also shows the complexity level of model structure indicated by the number of characters on its model ID. The model prediction ability is increasing to some extent with the model complexity level. At the first stage, the simple perceptual rainfall-runoff models perform relatively poorly for both watersheds. However, the most complicated model, which is coupled with all available sub-modules, does not necessarily report the best simulation result. Model performance depends strongly on model structure, but there is a trade-off between model complexity and simulation quality. The results demonstrate that the importance of various model structures is to a high degree case-dependent. The modules for the most significant improvement of model performance are different for two basins.

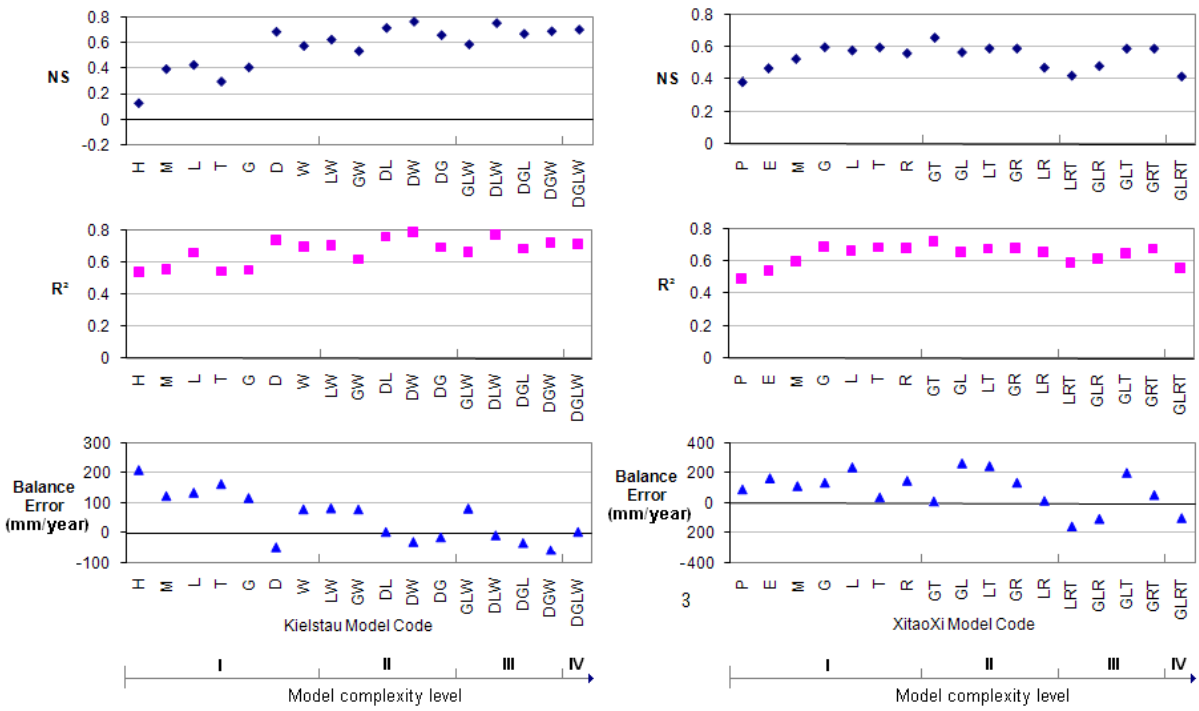

Figure 4.5 Results of model efficiency NS, R^2 and summed water balance for all model structures

4.4.2 Model structural uncertainty analysis

An important goal for this paper is to highlight an example of structural uncertainty. Although it would be desirable to break down the total uncertainty into its various components, it is quite difficult to do so and, as far as the authors are aware, no reliable procedure yet exists. However, it is generally impossible to exclude uncertainties from other sources owing to the inherent interrelations of all factors in any modelling procedure. For example, when the model structure is changed in any part of process description, it would unavoidably involve changes associated with system input and calibration procedures. We can find a typical example of this, such as the sub-modules P, E and M in the XitaoXi models, which were more concerned with input data changes than with model structure. All the changes contribute to aggregate uncertainty so that it is difficult to tell the individual effect from each source. Therefore the uncertainty generated here account for all uncertainties.

However, this study endeavoured to focus on model structural analysis by investigating different perceptual models and to the most extent eliminating influences from other uncertainty sources. In this context, these prediction uncertainties are closely linked to the model structural errors arising from the aggregation of real world process into a modelling simplification.

The uncertainties are reflected in the discharge simulation presented in Figure 4.6. The simulation results show a substantial variation in the hydrographs produced by the different

model structures. This variation can be used as an estimate of the structure uncertainty of the selected models.

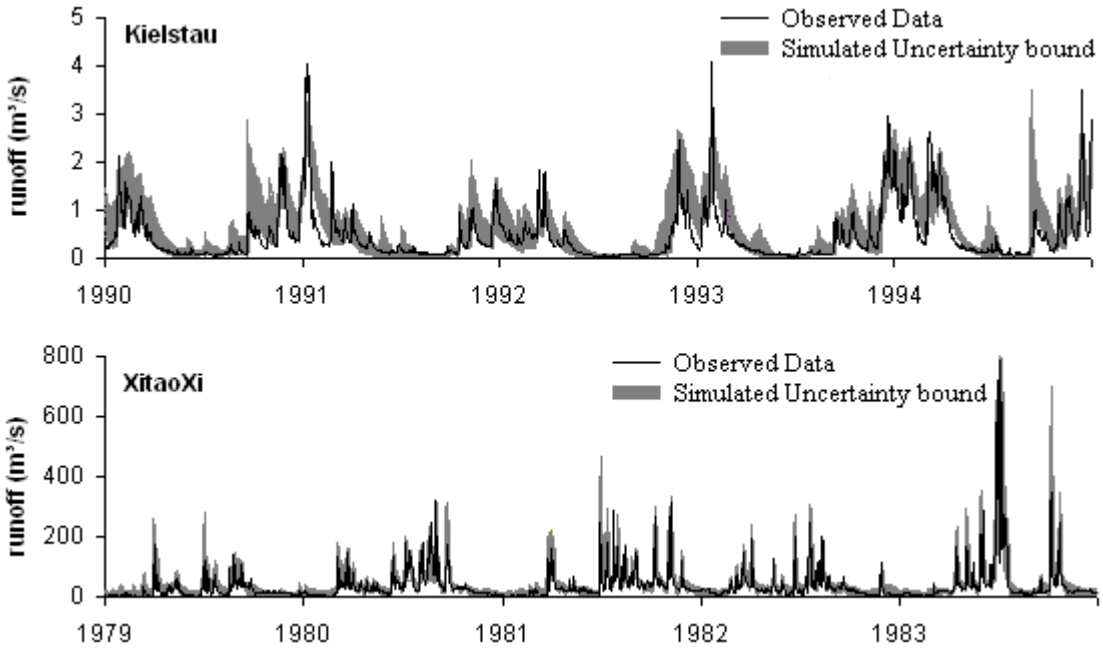

Figure 4.6 Simulation results of different model structures for two study basins, with the shaded area showing the uncertainty intervals along with the measured discharge

The shaded area in Figure 4.6 represents the predicted simulation uncertainty for the years 1990–1995 in the Kielstau catchment, and for the years 1979–1983 in the XitaoXi basin. There is a high variation in model simulations caused by the different model structures. For the Kielstau catchment, 52.31% of the observed data (*P* factor) is bracketed by the uncertainty bound. The other measure, *R* factor, is calculated as 0.58, which quantifies the thickness of the uncertainty bound. The predicted uncertainty band for the XitaoXi basin bracketed 61.54% of the observations, with an *R* factor of 0.51. It is notable that the huge differences in runoff scales for the two basins in Figure 4.6, which may explain why the dispersions of the ensemble model structures in the two basins are so different by visual comparison. The variation of all model simulations for the Kielstau catchment looks wider than that for the XitaoXi catchment. As these hydrographs for the Kielstau basin indicate, there is always a certain amount of diffusion and dispersion in the low flows, especially during summer seasons, and around the peaks. This gives rise to attenuation and modifications in the peak amplitude and shape, respectively, while the XitaoXi hydrographs give much tighter uncertainty bounds, and are generally centred on the observations. It has better results in the timing and magnitude of variations at any flow stages, with most of the peaks covered by the uncertainty band. However, the results for both basins are quantitatively similar. Judging from the two uncertainty measures, the derived perceptual model uncertainty bounds exhibit

appropriate coverage (*P* factors >50%), and *R* factors are in the acceptable range (when it is small than 1, cf. Schuol & Abbaspour 2006). These reproduce the aggregation of all uncertainties, with explicitly accounting for model structural errors. More accurate uncertainty bound may be obtained by fitting distributions around the prediction of appropriate individual models, which would be a further parameter uncertainty research in future work.

4.4.3 Peak-flow low-flow split testing

To examine the uncertainty behaviour further, we use peak-flow low-flow split testing to take a closer look at the patterns of structural uncertainty. For comparison the monthly mean discharge data are plotted instead of the daily values. All months are divided into peak-flow and low-flow seasons by the average discharge value of all years. Then the *R* factor is calculated for each season and the result is shown in Figure 4.7. It reveals a clear pattern of how much each flow period contributed to the overall uncertainty during the whole period. Significantly smaller values are noted for the peak-flow months in Kielstau basin and higher values for low-flows. An analogous pattern is also observed for the completely different XitaoXi basin. Apparently low-flow seasons contribute more to the overall uncertainty than peak-flow seasons. It seems be more difficult to simulate river discharges at low-flow seasons. The results highlight problems related to the simulation of low flow. Worth mentioning is, that in a lot of papers about hydrological modelling (e.g. Yang et al. 2007) the authors argued that baseflow is easier to simulate. Because in the peak-flow season, river flow may come from surface runoff, interflow and groundwater discharge; while in low-flow season, it is mainly dependant on groundwater discharge. It is obviously recognised that more factors have impacts on runoff generation during peak-flow time, but more uncertainty sources do not necessarily produce more prediction uncertainty in hydrological modelling. The power of influence from each factor on model simulation must be considered as well. Rainfall generally has the most significant impact on runoff generation, particularly in peak-flow season. And the relationship between rainfall and runoff is the most essential structure in all hydrological modelling. This rainfall–runoff relationship is thus better understood and implemented than other runoff-influencing factors such as groundwater and lateral flows. And in most cases rainfall is the major factor influencing runoff processes in peak-flow seasons. For those model structures with dominating rainfall–runoff relationship, the peak-flows can be better reproduced. This is why we suggest that there are some other factors contributing to model uncertainty for low-flow seasons that need further investigation.

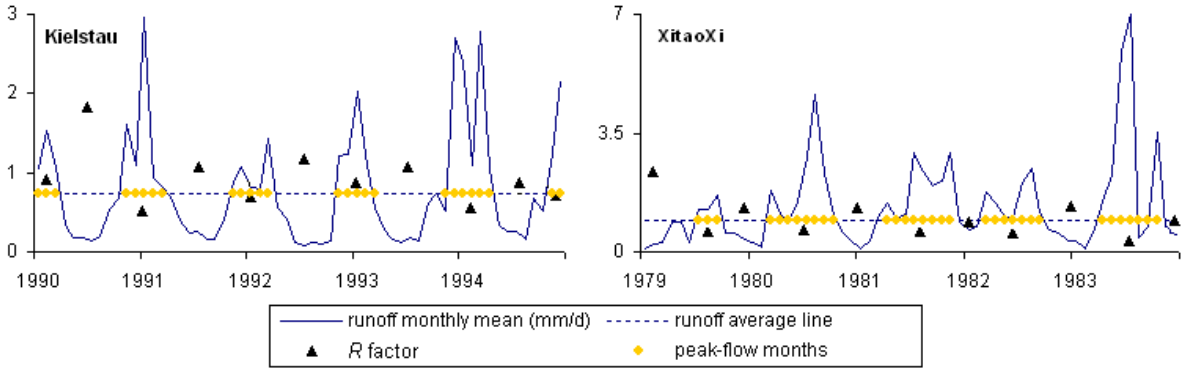

Figure 4.7 *R* factor values for low-flow and peak-flow periods in two study areas

4.5 Conclusions

Modelling uncertainty associated with model structure errors is difficult to assess, not only theoretically, but also technically. This study developed a hydrological modelling framework that allows changes in model structure complexity, and investigated the structural uncertainty associated with river runoff simulations.

The simple KIDS hydrological model was *tested* for two watersheds with completely different characteristics. An extension of model structures with ensemble sub-modules was successfully applied to the implementation of KIDS model. These models are plausible alternatives for the discharge simulation incorporating the main processes occurring in the selected river basins. We examined the impact of model structure on the hydrological simulations and evaluated the different model structures against a number of performance criteria for two study basins. Relating topological, geological and physical characteristics of the Kielstau River basin to the runoff simulation is essential for assessing the hydrological impacts of low gradient, wetland and high groundwater table in this basin. Since it is difficult to do such work with insufficient relevant data, some simplifying or assumptions are often necessary. Within the selected modelling framework, model DW performed better than other ones as it considered the possible influence of drainage and wetland. For the XitaoXi basin, accurate distributions of precipitation and evapotranspiration are two of the determining factors for the success of the river flow simulations. Two case studies indicated that hydrological model needs careful site-specific priors and adaptations for a sound runoff simulation. It can also be concluded from the results that the extended KIDS model ensemble is generally applicable as model structure test method for hydrological simulations under significantly different watershed conditions.

The related model structural uncertainty is estimated through the dispersion range of flow simulation ensembles around the observed data. Our approach leads to an acceptable

mechanical and statistical description of simulation uncertainty, as quantified by the two measures—*P* factor and *R* factor. A peak-flow low-flow split testing shows a similar pattern in both catchments: the uncertainties in baseflow are higher than in peak-flow periods. The reason for this is that, during the peak-flow or wet periods, the influence of other factors such as soil moisture, groundwater discharge is marginal, because of dominant influence of rainfall, which is the factor best accounted for runoff generation in our models.

Although some simplifications or assumptions in the model structure exploration might be arguable, we presented an effective method for practical model structural uncertainty estimations for the two study basins. Here it proved that assumption and its model simplification (like wetland in Kielstau or ET distribution in XitaoXi) are more critical than it may seem. In addition, all the adaptations in this paper have been based on field observations and data investigations. It facilitates model analysis a lot. Important information can be withdrawn from the result include that, wetlands must be a critical part of integrated water resources management in the Kielstau river basin, and more refined climatological data would greatly increase model reliability for the XitaoXi catchment.

Finally, the variations in model simulations provided by the different model structures are interpreted as a result of the uncertainty in model structure. This incorporates a challenging problem of how to separate and define the model structural uncertainty explicitly. When only structural errors are inferred, the produced simulation uncertainties do not represent structural errors exclusively and are also contaminated by parameter estimation errors and input data errors. Hence for this study, the simulation variations are considered to represent uncertainties mainly from structural errors but with influences from other uncertainty sources. Future work is also recommended for further uncertainty investigation when considering other sources of uncertainty, like parameter uncertainty and input data uncertainty. An attempt is made in this paper to strengthens the view that it is of great importance to explore different model structures to improve the overall accuracy of the simulations and to assess modelling uncertainty.

Acknowledgments

The authors thank Kiel University for financial support of this programme. We appreciate help from our colleagues of the Ecology Centre, Kiel University for access to their research data. We thank Nanjing Institute of Geography and Limnology, Chinese Academy of Sciences for the providing the XitaoXi data. Part of this work is sponsored by the National Research Program (no. 2008CB418106) of the Chinese Ministry of Science and Technology; and by the Key Project (no. KZCX1-YW-14-6) of the Chinese Academy of Sciences. In addition, detailed reviews of two anonymous reviewers greatly improved the original manuscript.

References

Abbaspour, K. C., Johnson, C. A., & van Genuchten, M. T. 2004 Estimating uncertain flow and transport parameters using a sequential uncertainty fitting procedure, *Vadose Zone J.* 3, 1340–1352.

Allen, R.G., Pereira, L.S., Raes, D. & Smith, M. 1998 Crop evapotranspiration - Guidelines for computing crop water requirements - *FAO Irrigation and drainage paper 56.* Rome: Food and Agriculture Organization, ISBN 92-5-104219-5.

Andersen, H.E. 2003 Hydrology, nutrient processes and vegetation in floodplain wetlands. PhD thesis. National Environmental Research Institute, Denmark.

Beven, K. 2001 Rainfall–Runoff Modelling: The Primer: Chichester, Wiley.

Beven, K. & Binley, A. 1992 The Future Of Distributed Models - Model Calibration And Uncertainty Prediction. *Hydrol. Process.* 6 (3), 279-298.

Beven, K. & Freer, J. 2001 Equifinality, data assimilation, and uncertainty estimation in mechanistic modelling of complex environmental systems using the GLUE methodology. *Journal of Hydrology* 249 (1–4), 11–29.

Beven, K., Smith, P. & Freer, J. 2007 Comment on "Hydrological forecasting uncertainty assessment: Incoherence of the GLUE methodology" by P. Mantovan and E. Todini. *J. Hydrol.* 338, 315– 318.

Brown, J.D. & Heuvelink, G.B. 2005 Assessing uncertainty propagation through physically based models of soil water flow and solute transport. In: *Encyclopedia of Hydrological Sciences* (M. G. Anderson, ed.), Chichester, Wiley, 1181-1196.

Bullock, A. & Acreman, M. 2003 The role of wetlands in the hydrological cycle. *Hydrol. Earth System Sci.* 7 (2), 358-389.

Butts, M.B., Payne, J.T., Kristensen, M. & Madsen, H. 2004 An evaluation of the impact of model structure on hydrological modelling uncertainty for streamflow simulation. *J. Hydrol.* 298, 242–266.

Carpenter, T. M. & Georgakakos, K.P. 2004 Impacts of parametric and radar rainfall uncertainty on the ensemble streamflow simulations of a distributed hydrologic model. *J. Hydrol.* 298, 202–221.

Choi, H. T. & Beven, K.J. 2007 Multi-period and multi-criteria model conditioning to reduce prediction uncertainty in an application of TOPMODEL within the GLUE framework. *J. Hydrol.* 332, 316– 336.

Christiaens, K. & Feyen, J. 2002 Constraining soil hydraulic parameter and output uncertainty of the distributed hydrological MIKE SHE model using the GLUE framework. *Hydrol. Process.* 16, 373–391.

Clausnitzer, V., Hopmans, J.W. & Starr, J.L. 1998 Parameter uncertainty analysis of common infiltration models. *Soil Sci. Soc. Am. J.* 62, 1477–1487.

DVWK (Deutscher Verband für Wasserwirtschaft und Kulturbau e.V.) 1996 Ermittlung der Verdunstung von Land- und Wasserflächen. Bonn: DVWK, Merkblätter zur Wasserwirtschaft, Heft 238, 135p.

Ewen, J., O'Donnell, G., Burton, A. & O'Connell, E. 2006 Errors and uncertainty in physically-based rainfall-runoff modelling of catchment change effects. *J. Hydrol.* 330 (3-4), 641-650.

Gao, J., Lu, G., Zhao, G. & Li, J. 2006 Watershed data model: a case study of Xitiaoxi sub-waterhed, Taihu Basin (in Chinese, with English abstract). *J. Lake Sciences*, 18 (3), 312-318.

Glugla, G. 1969 Berechnungsverfahren zur Ermittlung des aktuellen Wassergehalts und Gravitationswasserabflusses im Boden. *Albrecht-Thaer-Archiv*, 13 (4), 371-376.

Gourley, J. & Vieux, B. 2006. A method for identifying sources of model uncertainty in rainfall–runoff simulations. *J. Hydrol.* 327, 68-80.

Gupta, H.V. & Sorooshian, S. 1998 Toward improved calibration of hydrologic models: multiple and noncommensurable measures of information. *Water Resour. Res*. 34 (4), 751-763.

Gupta, H.V., Beven, K.J. & Wagener, T. 2005 Model calibration and uncertainty estimation. In: *Encyclopedia of Hydrologic Sciences* (M. Anderson, ed.). Chichester: Wiley.

Haan, C.T., Storm, D.E., Al-Issa, T., Prabhu, S., Sabbagh, G.J. & Edwards, D.R. 1998 Effect of parameter distributions on uncertainty analysis of hydrologic models. *Trans. Am. Soc. Agric. Engrs*, 41, 65–70.

Hansen, S., Thorsen, M., Pebesma, E.J., Kleeschulte, S. & Svendsen, H. 1999 Uncertainty in simulated nitrate leaching due to uncertainty in input data. A case study. *Soil Use Manage.* 15, 167–175.

Haude, W. 1958 Ueber die Verwendung verschiedener Klimafaktoren zur Berechnung der Evaporation und Evapotranspiration, *Meteorologische Rundschau*, 11, 96-99.

Hörmann, G., Zhang, X.Y. & Fohrer, N. 2007 Comparison of a simple and a spatially distributed hydrologic model for the simulation of a lowland catchment in Northern Germany. *Ecolog. Model.* 209 (1), 21-28.

Jin, X. & Gao, J. 2006 Modelling of human activities impacts to hydrological processes-based on distributed hydrological model (in Chinese, with English abstract). MSc Thesis, Nanjing Institute of Geography & Limnology, Chinese Academy of Sciences.

Krause, P., Boyle, D.P. & Baese, F. 2005 Comparison of different efficiency criteria for hydrological model assessment. *Adv. Geosci*. 5, 89–97.

Lindenschmidt, K.E. 2006 The effect of complexity on parameter sensitivity and model uncertainty in river water quality modelling, *Ecolog. Model.* 190, 72-86.

Lindenschmidt, K.E., Fleischbein, K. & Baborowski, M. 2007 Structural uncertainty in a river water quality modelling system. *Ecolog. Model.* 204, 289–300.

Melching, C.S. 1995 Reliability estimation. In: *Computer Models of Watershed Hydrology* (V. Singh, ed.), Littleton, CO: Water Resources Publications, 69–118.

Nash, J.E. & Sutcliffe, J.V. 1970 River flow forecasting through conceptual models. Part I: A discussion on principles. *J Hydrol.* 10, 282-290.

Neuman, S.P. 2002 Accounting for conceptual model uncertainty via maximum likelihood Bayesian model averaging. *Acta Univ. Carolinae Geologica*, 46(2/3), 529–534.

Radwan, M., Willems, P. & Berlamont, J. 2004 Sensitivity and uncertainty analysis for river quality modelling. *J. Hydroinform*. 6, 83–99.

Ratto, M., Young, P.C., Romanowicz, R., Pappenberger, F., Saltelli, A. & Pagano, A. 2007 Uncertainty, sensitivity analysis and the role of data based mechanistic modelling in hydrology. *Hydrol. Earth System Sci*. 11, 1249-1266.

Rogers, C.C.M., Beven, K.J., Morris, E.M. & Anderson, M.G. 1985 Sensitivity analysis, calibration and predictive uncertainty of the institute of hydrology distributed model. *J. Hydrol.* 81, 179-191.

Schmidtke, K.D. 1999 *Land im Wind—Wetter und Klima in Schleswig-Holstein*. Wachholtz Verlag.

Schmitz, O., Karssenberg, D., van Deursen, W.P.A. & Wesseling, C.G. 2009 Linking external components to a spatio-temporal modelling framework: coupling MODFLOW and PCRaster. *Environ. Modell. Softw.* 24, 1088-1099.

Schuol, J. & Abbaspour, K.C. 2006 Calibration and uncertainty issues of a hydrological model (SWAT) applied to West Africa. *Adv. Geosci*. 9, 137–143.

Son, K. & Sivapalan, M. 2007 Improving model structure and reducing parameter uncertainty in conceptual water balance models through the use of auxiliary data. *Water Resour. Res.* 43 (1) W01415, 1-18.

Sponagel, H. 2005 Bodenkundliche Kartieranleitung. Hannover: Adhocarbeitsgruppe Boden der Staatlichen Geologischen Dienste und der Bundesanstalt für Geowissenschaften und Rohstoffe. 5.Verbesserte und erweiterte Auflage.

Springer, P. 2006 Analyse der Interaktion zwischen Oberflächenwasser und Grundwasser am Beispiel einer Flussniederung im Norddeutschen Tiefland. Diplomarbeit, Fach Geographie, Christian-Albrechts-Universität zu Kiel, Germany.

Takagi, K., Tsuboya, T. & Takahashi, H. 1998 Diurnal hystereses of stomatal and bulk surface conductances in relation to vapor pressure deficit in a cool temperate wetland. *Agric. For. Met*. 91, 177–191.

Trepel, M. 2004 Development and application of a GIS-based peatland inventory for Schleswig Holstein (Germany). In: Päivänen, J., ed. *Proceedings of the 12th International Peat Congress—Wise Use of Peatlands*, vol. 2, 931–936.

Uhlenbrook, S., Seibert, J., Leibundgut, Ch. & Rodhe, A. 1999 Prediction uncertainty of conceptual rainfall–runoff models caused by problems to identify model parameters and structure. *Hydrol. Sci. J*., 44 (5), 279-299.

Van der Knijff, J. & de Roo, A. 2008 *LISFLOOD Distributed Water Balance and Flood Simulation Model*, Revised user manual. Luxembourg: Office for Official Publications of the European Communities, EUR 22166 EN/2.

Van Deursen, W.P.A. 1995 Geographical Information Systems and Dynamic Models: development and application of a prototype spatial modelling language. Netherlands Geographic Studies, issue 190, 195p.

Vrugt, J. A., Diks, C. G. H., Gupta, H. V., Bouten, W. & Verstraten, J. M. 2005 Improved treatment of uncertainty in hydrologic modelling: combining the strengths of global optimization and data assimilation. *Water Resour. Res.* 41 (1), 1-17.

Vrugt, J.A., Clark, M.P. & Diks, C.G.H. 2006 Multi-objective calibration of forecast ensembles using Bayesian model averaging. *Geophys. Res. Lett*. 33 (19), 1-6.

Wan, R., Yang, G., Li, H. & Yang, L. 2007 Simulating flood events in a mesoscale watershed: a case study from River Xitiaoxi Watershed in the upper region of Taihu basin. *J. Lake Science*. 19 (2), 170–176.

Wesseling, C.G., Karssenberg, D.J., Burrough, P.A., Van Deursen, W.P.A. 1996 Integrated dynamic environmental models in GIS: The development of a Dynamic Modelling language. *Trans. GIS* 1 (1), 40–48.

Wu, K. & Johnston, C. A. 2008 Hydrologic comparison between a forested and a wetland/lake dominated watershed using SWAT. *Hydrol. Process.* 22, 1431–1442.

Xu, L., Zhang, Q., Li, H., Viney, N.R., Xu, J. & Liu, J. 2007 Modelling of surface runoff in Xitiaoxi catchment, China. *Water Resour. Manage.* 21, 1313–1323.

Yang, J., Reichert, P. & Abbaspour, K.C. 2007 Bayesian uncertainty analysis in distributed hydrologic modelling: a case study in the Thur River basin (Switzerland), *Water Resour. Res*., 43, W10401, 1-13.

Zhang, Q., Li, H. & Xu, L. 2006 Surface runof modelling for Xitiaoxi catchment, Taihu Basin. *J. Lake Science.* 18 (4), 401–406.

Zhang, X.Y., Hörmann, G. & Fohrer, N. 2007 The Effects of Different Model Complexity on the Quality of Discharge Simulation for a Lowland Catchment in Northern Germany. Heft 20.07 ‘Einfluss von Bewirtschaftung und Klima auf Wasser- und Stoffhaushalt von Gewässern’ (2007), Band 2, *Forum für Hydrologie und Wasserbewirtschaftung*, 111-114.

Zhang, X.Y., Hörmann, G. & Fohrer, N. 2008 An investigation of the effects of model structure on model performance to reduce discharge simulation uncertainty in two catchments. Adv. Geosci. 18, 31–35.

Zhang, X.Y., Hörmann, G. & Fohrer, N. 2009 Hydrologic comparison between a lowland catchment (Kielstau, Germany) and a mountainous catchment (XitaoXi, China) using KIDS model in PCRaster. Adv. Geosci. 21, 125–130.

Chapter 5

Parameter calibration and uncertainty estimation of a simple rainfall-runoff model in two case studies

X.Y. Zhang, G. Hörmann, N. Fohrer and J.F. Gao
Journal of Hydroinformatics, accepted 16 Dec 2011, forthcoming

Abstract

The simple rainfall-runoff conceptual model KIDS (Kielstau Discharge Simulations) using PCRaster is applied to simulate continuously daily discharge of two river basins: the small lowland Kielstau catchment (51.5 km²) in Germany and the mesoscale mountainous XitaoXi basin (2271 km²) in China. With the given model structure, this work focuses on the parameter calibration procedure and, in particular, the assessment of model prediction uncertainty. We employ a simplistic analysis routine SUFI-2 (Sequential Uncertainty Fitting, ver. 2, Abbaspour et al. 2004) coupled with the implementation of a Monte Carlo based sampling strategy for the joint investigation of parameter calibration and uncertainty estimation. The degree of uncertainty is quantified by two measures referred as *P* factor and *R* factor (Schuol & Abbaspour 2006). The scatter plots of model performance and parameter exhibits high equifinality of parameter sets in fitting the observations, while their histogram

distribution patterns imply that most parameters can be well defined. This study investigates the parameter sensitivities and finds interesting local results: soil and groundwater parameters are more sensitive in Kielstau models than in XitaoXi models, and only the soil parameters 'S_{fk}' and 'K_c' are found strongly correlated. Finally, the uncertainty bounds are always thin and the global shape of the hydrograph is well approximated for both basins. As the validated uncertainty bounds also represent the desired coverage (*P* factor >50%) of the observations, and the calculated *R* factor values are in the targeted range (*R* factor<1), it demonstrates the efficiency and suitability of this revised SUFI method for the two case studies.

Keywords: Hydrologic modelling; KIDS model; Kielstau, Germany; parameter uncertainty estimation; random sampling; XitaoXi, China.

5.1 Introduction

In the last few decades, there has been an increasing use of dynamic simulation in hydrological models. In order to improve the accuracy of model simulations, many calibration methodologies were developed intending to locate the values of unknown parameters and to verify the usefulness and power of models. The laborious nature of conventional manual calibration in the 'trial and error' adjustment style has motivated the development of automatic calibration techniques, including gradient-based methods like the Gauss-Levenberg-Marquardt method (Doherty & Johnston 2003), population-evolution-based algorithms like Shuffled Complex Evolution method (Duan et al. 1992), and regionalization or spatial generalization (Lamb & Kay 2004). The main difficulties preventing the determination of the best parameter set by any automatic calibration schemes are the presence of non-uniqueness in parameter optimization, nonlinear parameter interaction and the complex shape of the response surface defined by the objective function (Feyen et al. 2007). Moreover, since process-based hydrological models consist, at least partially, of an empirical combination of mathematical relationships describing some observable features of idealized hydrological processes (Kuczera & Parent 1998), parameter estimates are subject to uncertainty, which leads to uncertainty in model predictions. To overcome these problems, many studies have shifted the research emphasis on identifying the model prediction uncertainty, instead of searching for one absolute global optimum. Parameter calibration and prediction uncertainty of a model are then intimately related (Blasone et al. 2008; Laloy et al. 2010).

A large number of methods have come out recently to derive feasible calibration techniques and uncertainty analysis in hydrologic modelling, involving the optimization algorithms such as shuffled complex evolution algorithm (Duan et al. 1992; Vrugt et al. 2003a; Feyen et al. 2007), simulated annealing (Sumner et al. 1997) and genetic algorithms (Wang 1997; Cheng et al. 2006). Aiming to simulate various important characteristics of the observed data, automatic routines using multiple criteria or objective have been introduced in solving the calibration problem (Yapo et al. 1998; Madsen 2000; Boyle et al. 2000; Cheng et al. 2002; Vrugt et al. 2003b; Schuol & Abbaspour 2006; Li et al. 2010). Other approaches focusing on assessing global uncertainty in rainfall-runoff modelling include the (pseudo-) bayesian methods (Freer & Beven 1996; Thiemann et al. 2001), such as the generalized likelihood uncertainty (GLUE) framework (Beven & Binley 1992; Aronica et al. 2002; Uhlenbrook & Sieber 2005; Blasone et al. 2008), and the meta-Gaussian approach (Krzysztofowicz & Kelly 2000; Montanari & Brath 2004). Those methods contributed the development of more complex or sophisticated uncertainty analysis tools, but some weaknesses may be inevitable at the same time, like global algorithms are mostly complex and computationally expensive (Li et al. 2010), and other approaches such as GLUE also requires a large sample of model runs and adequate reliable data describing watershed characteristics (Choi & Beven 2007).

In practice, however, the complex approaches do not always provide more accurate results relative to simpler and low-dimensional estimation problems, depending on the watershed scale, the number of parameters to calibrate, the quantity and quality of calibration data. A simple approach may be adequate and efficient in the cases of ungauged basins, or lumped models with less parameters.

Abbaspour et al. (2004) proposed a simple inverse modelling routine SUFI-2 (Sequential Uncertainty Fitting, version 2) for an uncertainty estimation of the SWAT model (Arnold et al. 1998). Another application in Schuol & Abbaspour (2006) showed that SUFI-2 is an efficient parameter optimization-uncertainty analysis procedure for a multi-site large-scale water quantity investigation. The sequential fitting scheme in SUFI-2 helps to maintain an appropriate sampling density in the Monte-Carlo based sampling mothod. The easy-to-setup approach is attractive for low-dimensional uncertainty estimation problems, such as modelling with restricted data availability, a relatively simple model structure, or less parameters. The calibration procedure we have applied in this paper belongs to this group, but with adjustments adapted to PCRaster modelling environment (Van Deursen 1995; Wesseling et al. 1996). The current study has two objectives. First, we test the SUFI-2 method with a simple rainfall-runoff conceptual model KIDS (Hörmann et al. 2007; Zhang et al.

2007). The KIDS model is raster based using a dynamic modelling language PCRaster, which has more flexibility in input data requirements and less complexity in model structure than the SWAT model applied in Abbaspour et al. 2004. Second, we assess the parameter uncertainty for the KIDS model and quantify its effects on model simulations for daily discharge of two river basins. One is a small lowland Kielstau catchment in Germany, and the other is a mesoscale mountainous XitaoXi basin in China. We hypothesize that, the approach in this two-site comparison would better examine the influence pattern of each parameter on model performance, and yield better results in uncertainty assessment than one could get from extrapolating parameters from a single site. To evaluate our hypothesis, we select six main parameters for each basin, compare their distribution patterns and correlations, and apply the adapted SUFI-2 methodology to map and quantify simulation uncertainty in the modelling process onto the parameter space.

5.2 Sites description and data processing

The study sites include two basins with remarkable differences in hydrologic features – Kielstau in Germany and XitaoXi in China.

Kielstau is a lowland watershed in Northern Germany, with a drainage area of 51.5 km² (see Figure 5.1a). As the development of the landscape was mainly influenced by the Saale and the Weichselian ice ages (Eggemann et al. 2001), the whole catchment is rather flat, with elevation ranging from sea level to 50m. Land use is dominated by agricultural (55.8%) and grassland (26.1%). Mean annual precipitation is ca. 800mm, and evaporation app. 400mm (Schmidtke 1999). The main soil texture is sandy loam and the dominating soil types are Gleysol and Luvisol (Sponagel 2005). A large fraction of wetland area and the near-surface groundwater level are observed in this region.

The second study watershed XitaoXi is a 2271 km^2 sized mountainous basin (Figure 5.1b), which is located in the semitropical monsoon zone in Southern China. It is a sub-basin of the Taihu Lake. In the XitaoXi region, 63.4% of land use is forest and grass, 20% paddy rice land (Wan et al. 2007). Average precipitation in the watershed is 1466mm annually, with 75% of rain falling between April and October. And average evaporation from water surface ranges from 800mm to 900mm annually. The dominant soil types are red soil and rocky soil. Since these soils tend to have limited water storage capacity, most portions of the river discharge are probably from the saturation excess surface runoff (Xu et al. 2007).

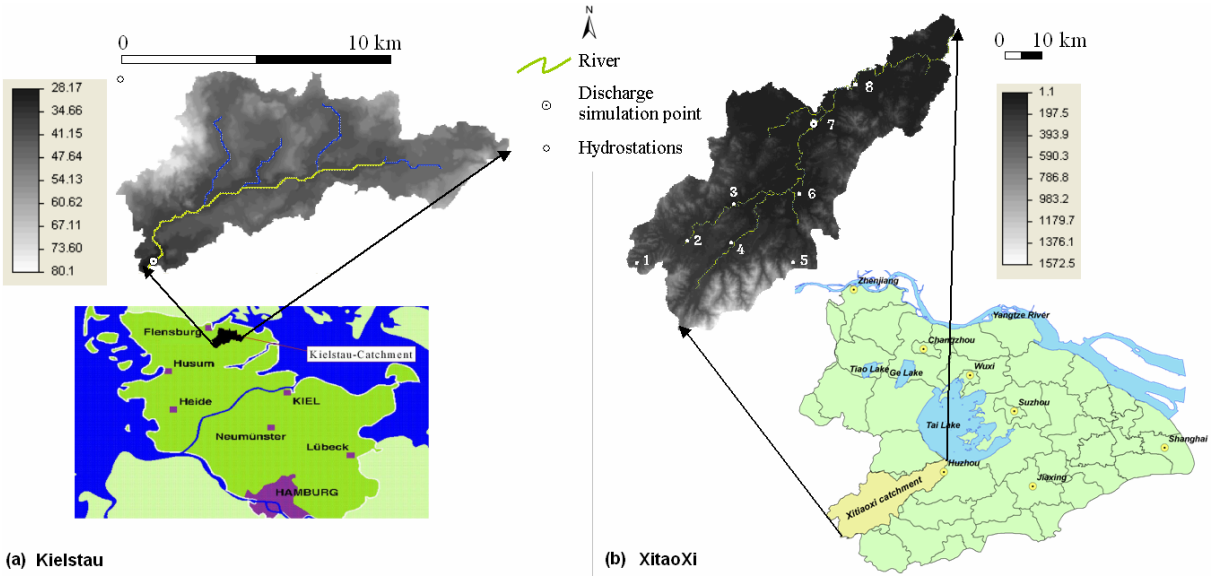

Figure 5.1. Location of (a) the Kielstau catchment and (b) the XitaoXi catchment, with grey-scale overlay of the topography (discharge simulation point: Soltfelt-Kielstau, Hengtangcu-XitaoXi; weather station in Kielstau – Flensburg, hydrostations in XitaoXi - 1: Tianjintang, 2: Hanggai, 3: Fushishuiku, 4: Laoshikan, 5: Yinkeng, 6: Dipu, 7: Hengtangcun, 8: Fanjiacun).

The KIDS model in PCRaster requires climatic and topographic data as basic data input for all model runs. The DEMs are derived originally from the topographic maps provided by local authorities (Landesvermessungsamt Kiel and the Administrative Bureau of TaiHu Basin) and gridded with an resolution of 50 m for the Kielstau basin and 200 m for the XitaoXi basin according to the input dap scale. Although the drainages in Kielstau area are relatively indistinct due to the flatness of the basin surface, the KIDS model still allows for efficient runoff routing based on the flow accumulation calculated from DEM.

The climatic data for Kielstau catchment are taken from the data set of Flenburg station, the official weather station nearest Kielstau basin. The LANU (Landesamt für Natur und Umwelt) provided river discharge values from 1983 to 1999 (at the official Soltfeld gauge station). Daily precipitation data in the XitaoXi basin are available from eight stations within the watershed area, while evaporation data are only recorded at two stations—Fushishuiku and Hengtangcun. The discharge data set from the selected Hengtangcun gauge station is available from 1978 to 1987. The reason to select Hengtangcun instead of the river outlet as discharge simulation point is that, Hengtangcun is the nearest station to river outlet and are not greatly influenced by the backflow from Taihu Lake. Only the contributing area is considered in the model calculation. Other data including land-use and soil maps are converted from its originally coarser data resolution to a raster map with the same cell length of DEM.

The Kielstau and XitaoXi watersheds have quite different hydrologic regimes (Zhang et al. 2009), thereby providing diverse data sets to test the adapted SUFI-2 method used in this

study. For example, the average daily runoff of the XitaoXi river (35.09 m^3/s) is much higher than that of the Kielstau stream (0.45 m^3/s). The difference is significant as well when considering the different discharge area: the runoff rate per unit area is 23.02 l/s/km² for XitaoXi, and 8.82 l/s/km² for Kielstau. The calibration data considered in this paper are the daily records of river discharge (m^3/s) at the selected gauge station. The current work also serves as one part of a Sino German integrated geohydrological study of these two basins. All analysis steps will be made parallel for the Kielstau and XitaoXi catchments.

5.3 KIDS hydrologic model

The KIDS model (Kielstau Discharge Simulation model, Hörmann et al. 2007; Zhang et al. 2007, 2011) is a simple rainfall-runoff model developed for practical purposes to facilitate water resource management in the field of Kielstau. It is basically driven by elevation map and meteorological input data, and then simulates river discharge in given river basins as a dynamic function of spatial information using PCRaster modelling language. Additional inputs like soils and land cover can be integrated as extended submodels to the basic model structure. All derived models form the KIDS model ensembles. Figure 5.2 gives an overview of the basic model structure with solid lines and added submodels in dashed lines. The model is spatially distributed and space was discretized in 50 m by 50 m grid size for Kielstau and 200 m by 200 m for XitaoXi.

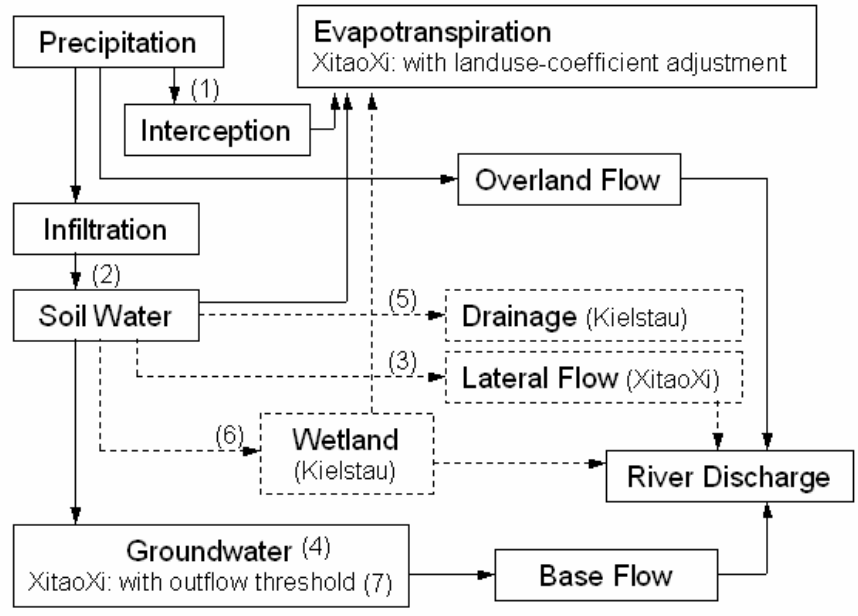

Figure 5.2 Illustration of the KIDS model structure.

Runoff is calculated on each grid cell based on the water balance equation (see equation 1), taking into account interception, precipitation, evapotranspiration, and the flows to other compartments. We use 'mm' as unit of measure for all the water amount expressions included in equations of this paper, and calculate with a daily time step.

$$S_t = S_{t-1} + P_t - ET_t - I_t - Qo_t - Sp_t \quad (1)$$

Where S is the soil water content, t is the modelling time step (daily), P is precipitation and ET is evapotranspiration, I is interception, Qo is surface runoff (overland flow), Sp is percolation or seepage.

Precipitation and potential evapotranspiration are input forcing data. Interception is calculated with the parameter 'I*m*' (equation 2).

$$I_t = \min (P_t, Im) \quad (2)$$

Where I*m* is the maximum interception amount of vegetation cover.

Surface runoff 'Qo' (see equation 3) describes soil percolation and storage calculation on the basis of derived soil parameters like field capacity and infiltration rate of soil water deficit.

$$Qo_t = \max \{[P_t - I_t - K_c(S_{fk} - S_t)], 0\} \quad (3)$$

Where Qo represents the surface runoff, K_c is the infiltration parameter, and S_{fk} is the wetness at field capacity.

The whole river basin is assumed to have one soil type with unified water storage capacity in the basic model structure. Sub-surface flow is modeled as 1D bucket flow with a lateral flow rate parameter 'K_s', as shown in equation 4. The value of parameter K_s is set equal to zero in the basic model for both basins.

$$Qs_t = K_s S_t \quad (4)$$

Where Qs is subsurface flow, and K_s is lateral flow rate.

The groundwater layer is represented as linear storage and its discharge is set with a groundwater outflow rate 'Kg'. Combining equations 5, 6 and 7 yields the daily groundwater dynamics.

$$G_t = G_{t-1} + Ig_t - Qg_t \quad (5)$$

$$Ig_t = \rho S_t \quad (6)$$

$$Qg_t = K_g G_t \quad (7)$$

Where G is groundwater storage, Ig the inflow to groundwater aquifer, Qg the groundwater discharge to runoff, ρ the water seepage rate from soil to groundwater, K_g the groundwater outflow rate.

The flow path is then derived from topography through a flow accumulation grid calculated in PCRaster. The routing of the runoff is modeled with the fully dynamic kinematic wave function (Chow et al. 1988).

Considering the greatly differing hydrology of the two basins, the appropriate model structure for each basin is selected from the KIDS model ensembles respectively (Zhang et al. 2008, 2011): Model 'DW' for Kielstau – basic KIDS model with drainage (equation 8) and integration of wetland (equation 9); Model 'LTG' for XitaoXi – basic KIDS model with landuse-coefficient adjusted ET distribution, additional subsurface flow with $K_s>0$ and groundwater outflow threshold (equation 10).

$$D_t = K_d * S_t + L_d \quad (8)$$

Where D is the drained water volume, K_d is drainage factor, S is available soil water storage, L_d is the lateral inflow volume (lateral seepage from irrigation canals and drainage channels).

$$W_t = W_{t-1} + Iw_t – Ew_t - Qw_t \quad (9)$$

Where W is wetland water storage; Iw the incoming water volume influenced by precipitation, interception and soil moisture; Ew the water loss from wetland, mainly evapotranspiration; Qw the wetland water seepage contributing to runoff.

$$Qg_t = Min (K_g * G_t, Gm) \quad (10)$$

Where Gm is the maximum daily groundwater outflow or groundwater outflow threshold.

Owing to the general nature and flexible structure of the KIDS model, its application to any study area requires that certain parameters be identified for the particular basin. In the current model version, six main parameters need to be determined by calibration using daily discharge observations. Table 5.1 lists an overview of the calibration parameters with their upper and lower value ranges.

Table 5.1 Description of parameters included in the KIDS hydrological model calibration procedure, with their upper and lower bounds

Parameter (unit)	**Range**	**Definition**
Im [mm]	0 – 10	Maximum water amount intercepted by vegetation cover
S_{fk} [mm]	1 – 800	Soil water storage capacity
K_c [-]	0.01 – 0.6	Soil Infiltration parameter
ρ [-]	0 – 0.5	Water seepage rate from soil to groundwater
K_q [-]	0.001 – 0.1	Groundwater discharge rate to the river baseflow
K_d [-] in Kielstau	0 – 0.01	Water drainage rate from available soil water storage
K_s [-] in XitaoXi	0 – 0.05	Soil water percolation rate to river discharge

5.4 Calibration scheme

5.4.1 SUFI-2 revised with random sampling strategy

The SUFI-2 scheme (Abbaspour et al. 2004) is designed to perform multi-site, semi-automated global search procedure with the SWAT hydrologic models (Arnold et al. 1998). Schuol & Abbaspour (2006) provided another application example using SUFI-2 for large-scale water quantity investigations. It combines parameter calibration and uncertainty prediction. The procedure is simple and the uncertainty is worked out by calculating the likelihood of the parameter set using the simulated and observed discharge. The choice of the likelihood function relies on the user-defined hypothesis. However, the Nash-Sutcliffe efficiency (Nash & Sutcliffe 1970) is assumed as the informal likelihood measure, which is widely used as a performance measure in hydrological modelling (Beven et al. 2007). Each set of parameters is assigned a likelihood value (the NS index) to quantify how well that particular parameter combination simulates the system. Higher NS values typically indicate better correspondence between the model prediction and observations. A preliminary sensitivity test of six parameters is conducted to decide the initial sampling space (as shown in Table 5.1) by sequentially varying one parameter while keeping all other constant. In order to adapt the sampling scheme in SUFI-2 to PCRaster environmental modelling language, Schmitz (2009) has developed a specialized client-server software toolbox for the KIDS model. It has extendable interfaces and a Python binding allowing to add calibration algorithms and to define specific objective functions by the user. This software framework is suited for PCRaster environment to assign the KIDS model files, and it is applied to the parameter sampling in this study. It is a Monte Carlo based method as it evaluates the objective function at randomly spaced points in the defined parameter space. This random sampling scheme is easy-to-install and requires two assumptions when usesd in practical applications: low-parameterized models, and the uniform prior distributions for the tested parameters. Our conjecture is that, the random sampling scheme adopted here can provide a sufficiently large sample of solutions for the simple KIDS models with relative low-dimensional parameter estimation problems.

5.4.2 Analysis procedure

The process of parameter calibration and uncertainty analysis of the SUFI-2 algorithm is depicted graphically in Figure 5.3. Starting from models with the initially large parameter sampling range, each iteration run generates 2000 model simulations (s=2000). With the purpose of identifying a group of behavioral parameter sets within the resulting possible

model parameter combinations from the first iteration, we derived a subjective method to differentiate between behavioral and non-behavioral simulations. The term 'behavioral' is used here to characterize those parameter sets that are judged to be 'acceptable' on the basis of available data and knowledge (Tang et al. 2007). As each parameter set is assigned with a NS value, we sorted the sample population in order of decreasing NS value, and choose half of the results (s/2=1000) with higher NS values as behavioral parameter combinations. From the chosen 1000 simulations result, the parameter distribution pattern, parameter correlation and identifiability can be inferred. In SUFI-2, parameter uncertainty is depicted as uniform distributions. We construct the probability distributions for each parameter by dividing its sampling range into ten equivalents. When a further iteration is required, we narrow the parameter sampling range by neglecting those parameter value ranges that has low probability (it is defined here <5%). The resettled parameter value range is used as the new sampling range in the next SUFI-2 iteration.

Two measures are defined in SUFI-2 to quantify the model uncertainty and to decide the calibration target: *P* factor and *R* factor (equation 11 and 12). The percentage of measured data bracketed by the 90% simulation uncertainty bound is referred as the *P* factor. From the simulation results of each sampling run, the 90% uncertainty bound can be derived by calculating the 0.05- and 0.95-quantiles of the simulated discharge values. We defined the associated parametric uncertainty *R* factor as the ratio of the average distance of the 90% uncertainty intervals and the standard deviation of the measured data. The ideal situation is to have an *R* factor value close to zero, while at the same time to cover all the observation data within the 90% prediction uncertainty bounds (*P* factor=100%).

$$P\ \text{factor} = \frac{m}{n} \times 100\% \tag{11}$$

where m is the number of model time steps counted when the observed river discharge value is within the modeled simulation uncertainty bounds, n is the time steps of the selected flow period.

$$R\ \text{factor} = \frac{\sum_{i=1}^{n} \left[\left(S_{95} - S_5\right)_1 + \left(S_{95} - S_5\right)_2 + \ldots + \left(S_{95} - S_5\right)_n \right] / n}{stdev\{Q1, Q2, \ldots, Qn\}} \tag{12}$$

where S_{95} and S_5 denote the 95% and 5% percentiles for each simulated variables; n is the time steps of the selected flow period; stdev is standard deviation of the observed flows within the selected period.

The values of *P* factor and *R* factor reflect the uncertainty about the model parameters after taking into account the discharge observations. These two measures also specify the stopping rules of SUFI iterations. When the calculated *R* factor value reaches a small ratio – usually less than 1, and most of the observations (>50%) can be bracketed inside the uncertainty bound, we defined it as a state of being sufficiently calibrated. The sampling run will be iterated several times by resettling, usually narrowing the parameter space though the posterior parameter distribution, until the calibration target is achieved.

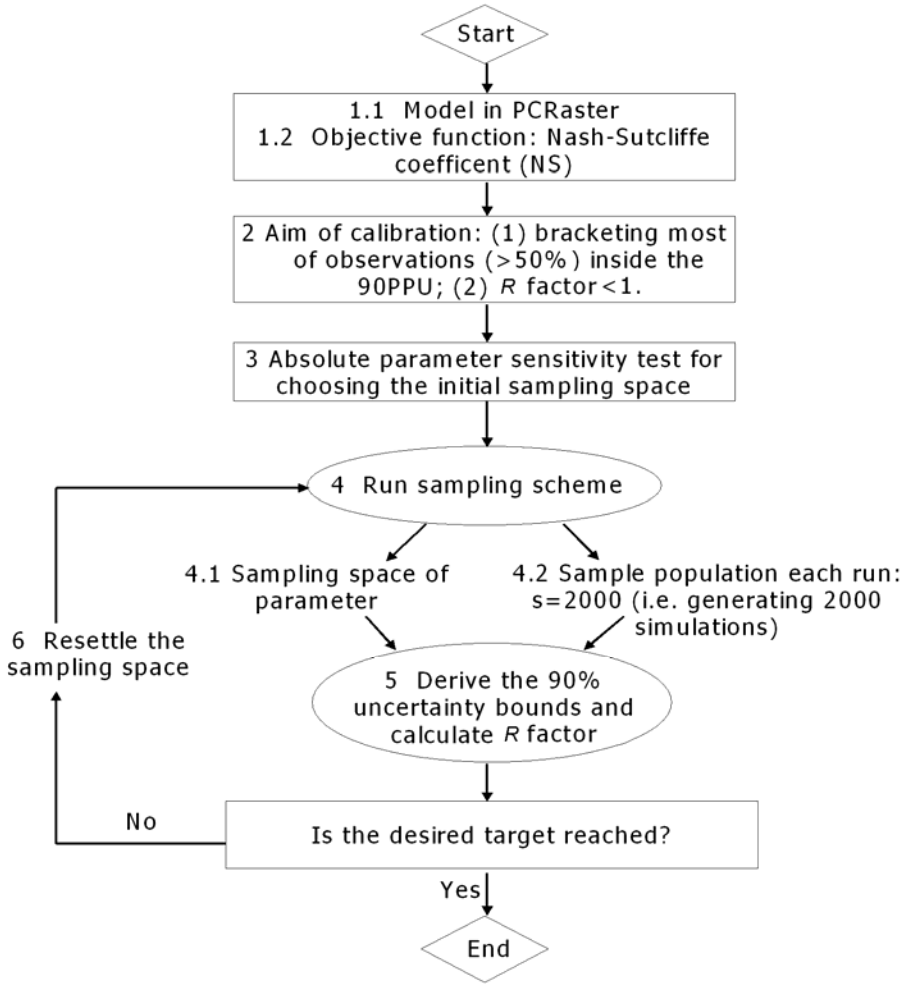

Figure 5.3 Flowchart of the calibration strategy.

5.5 Results and discussion

The SUFI-2 scheme is implemented for the Kielstau and XitaoXi basin. Staring from initially large parameter sampling space, the calibration procedure was iterated three times until the desired target was reached. This section presents analyses for the last iteration that reaches the desired calibration targets.

5.5.1 Parameter uncertainty and correlation

The result of the last iteration is plotted in Figure 5.4 (Figure 5.4a for Kielstau and Figure 5.4b for XitaoXi) to assess the parameter behavior on model performance in Nash-Sutcliffe values. In general, the scatter plots of model performance versus parameter values exhibit a high degree of equifinality of parameter sets in fitting the observations. It indicates that a wide range of parameter values can be included in behavioral parameter sets to make the model's performance similar close to optimal. This equifinality problem has been universal found and accepted as a working paradigm in hydrological models (Zak & Beven 1999; Beven 2007; Li et al. 2009).

For Kielstau, the parameter 'ρ' (water seepage rate from soil to groundwater) is the most sensitive to model performance, with a peaked band of dots ranging [0.05, 0.1]. This means that better model performances occurred for parameter sets having 'ρ' values between 0.05 and 0.1. For XitaoXi, a tendency of achieving better results is observed when the parameter 'K_c' and 'ρ' have small values. The maximum efficiency occurred in Kielstau model with the parameter 'S_{fk}' has higher value (around 450mm), while in XitaoXi model with lower value of 'S_{fk}' near 225mm. An inspection of other plots in Figure 5.4 reveals low sensitivity of those parameters, where smooth response surfaces are clearly displayed. The scatter plots describe adequately the high equifinality of acceptable parameter sets, and imply a large uncertainty from parameter estimations. The high uncertainty depicted in the figures is mainly due to the iteration, which leads to a narrower sampling space taken from a wide interval of possible parameter values. Further explorations are thus needed by examining parameter distributions and calculating associated uncertainty bounds.

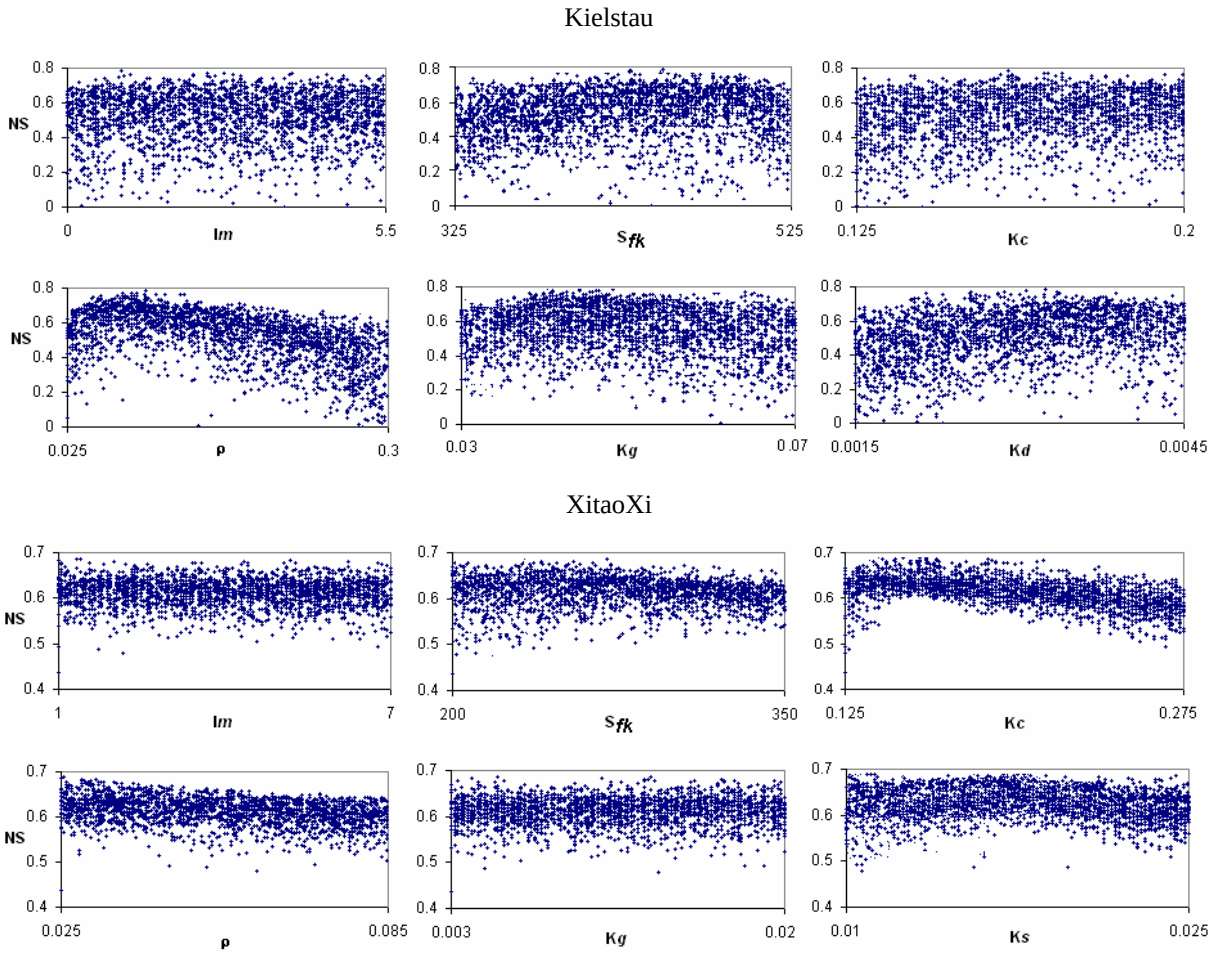

Figure 5.4 Scatter plots of model performance in Nash-Sutcliffe index within the parameter space of the last sampling iteration.

For a closer look in the parameter distribution pattern, we construct the posterior parameter distribution from the result of the last iteration by setting a subjective cutoff threshold (50% of all simulations) for behavior parameter sets. This posterior distribution can be used to directly resettle, usually narrow the parameter sampling space when a further iteration is needed. Figure 5.5 presents the probability distributions for the calibration parameters constructed using the top-ranked (NS-index) 1000 samples. For a good comparison of the two study basins, results for the same parameter are plotted in one diagram, where the x-axis depicts its original bound range stated in Table 5.1. The upper and lower boundary values of each parameter in its distribution histogram are showed along the x-axis, where numbers with brackets are values for the XitaoXi basin. The response surface of each parameter can help to identify its optimum value range.

The approximately flat response surface for the interception parameter 'I*m*' corresponds to a uniform distribution for both basins. It indicates a nearly negligible influence contribution of this part in water processes to the overall model performance. The distributions of soil field capacity parameter 'S_{fk}' and hydraulic infiltration parameter 'K_c' show a log-normal shape.

Given that the peak of their posterior distribution around the most likely value is sharp or nearly sharp, these parameters are well defined for the study area. The most likely value of the soil water storage capacity parameter 'S_{fk}' is well defined but its optimal value range differs in the two basins. Most acceptable simulations are achieved when the 'S_{fk}' in XitaoXi has lower values in [230, 275], while in Kielstau it is in the higher values ranging [405, 485]. Owing to the very different soil types in two basins, it reflects the relatively high water storage capacity of the loamy soils or wetland soils in the lowland area of Kielstau, and meanwhile limited soil water capacity of the typical red soil and rocky soil in the mountainous region of XitaoXi. Distributions of another soil parameter 'K_c' still have a large probability at their peaks indicating more uncertainty on their most likely value for both basins. The density of the soil groundwater flux parameters 'ρ' approximates a normal distribution centered around the sharp peak, despite that its left lower boundary is truncated by the limits of the x-axis. The higher 'ρ' optimal values in Kielstau reveals a more interactive relationship between soil and groundwater layers. Moreover, the most likely value of groundwater recharge parameter 'K_g' is not well identifiable in XitaoXi, but in Kielstau it shows a moderate normal distribution. It indicates that groundwater in Kielstau plays a more important role in river runoff producing precesses. Furthermore, the added submodel parameters describing drainage rate 'K_d' in Kielstau and lateral flow rate 'K_s' in XitaoXi have high possibilities in small values comparing their original bound ranges. The optimal value of 'K_d' is well defined, but the distribution of 'K_s' is slightly bimodal. One must also note that for all parameters, the intervals between the lower and upper bounds are not identical for different study basins, in order to have a good comparison on the same range of the x-axis.

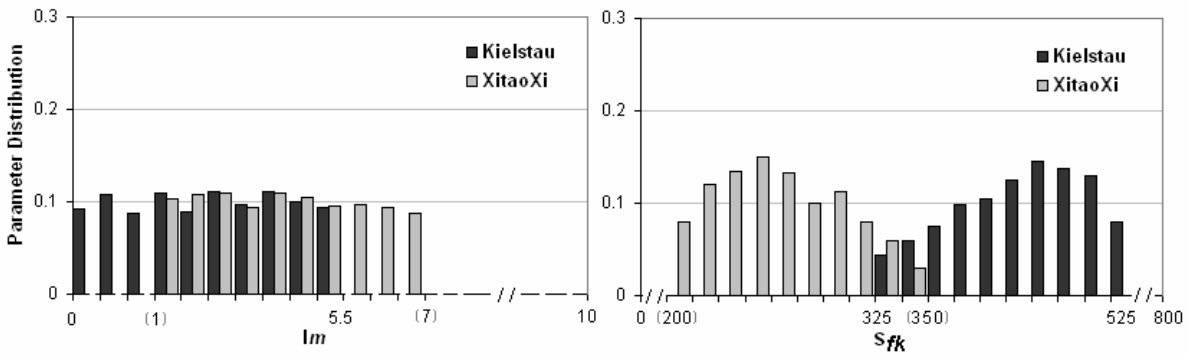

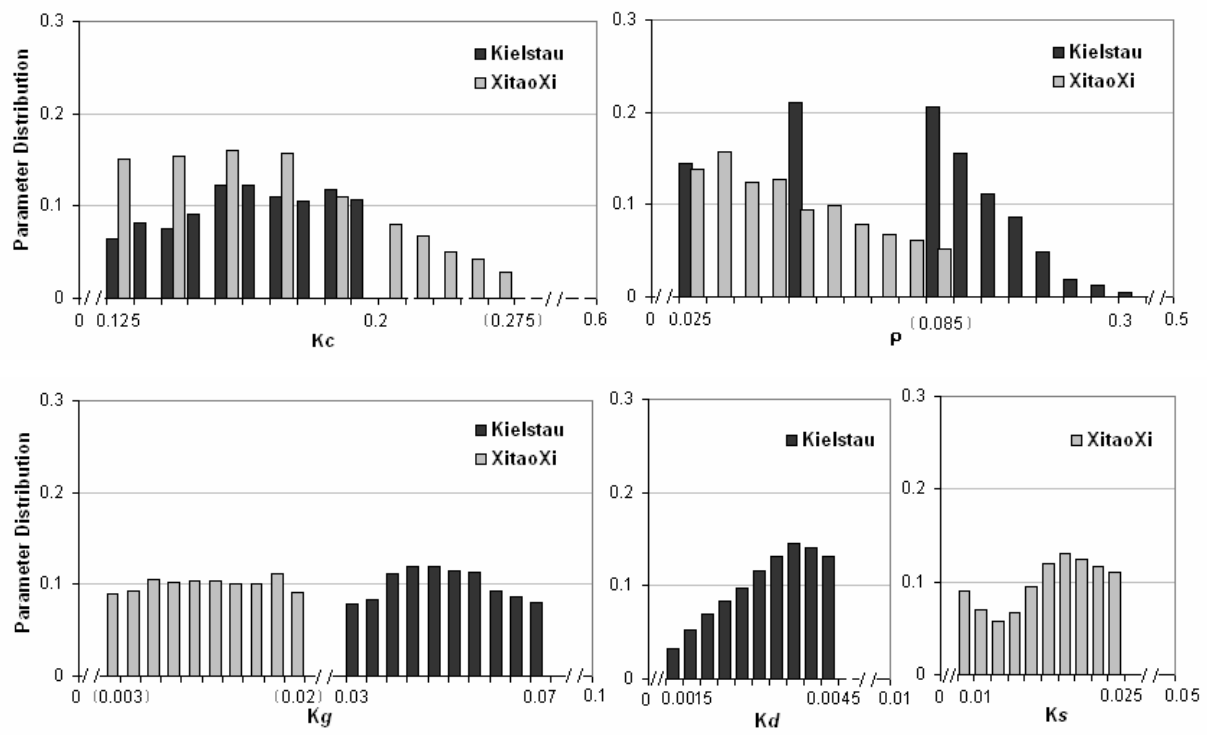

Figure 5.5 Histograms of parameter distribution in the comparison of two study basins (Parameter units are listed in Table 5.1).

As an illustration, Figure 5.6 presents correlation plots in two dimensions of parameter space obtained from samples with good performance (10% of the maximum NS) in two study areas. It indicates that moderate to strong linear correlations exist between some parameters. For example, the plots of soil parameters {'S_{fk}', 'K_c'} show a clear negative correlation in both cases. It is especially closer related in XitaoXi catchment. The two parameters affect the fast response of the model either through overland flow or subsurface runoff. We also note in panels {'S_{fk}', 'K_d'} for Kielstau and {'S_{fk}', 'K_s'} for XitaoXi, these parameters are slightly negative correlated, while in {'K_c', 'K_d'} for Kielstau and {'K_c', 'K_s} for XitaoXi, they are slightly positive correlated. It can be directly explained by their effect on model response. Indeed, an increase of 'S_{fk}' will have the same effect on runoff production as a decrease of 'K_c', or 'K_d' for Kielstau ('K_s for XitaoXi). The plots for Parameter 'ρ' in both basins are restrained within the half range of lower values, suggesting a high probability to have optimal values near lower boundary. Other plots concerning parameters 'Im' and 'K_g' show very low correlations, which is consistent with their large uncertainty demonstrated in Figure 5.4 and Figure 5.5.

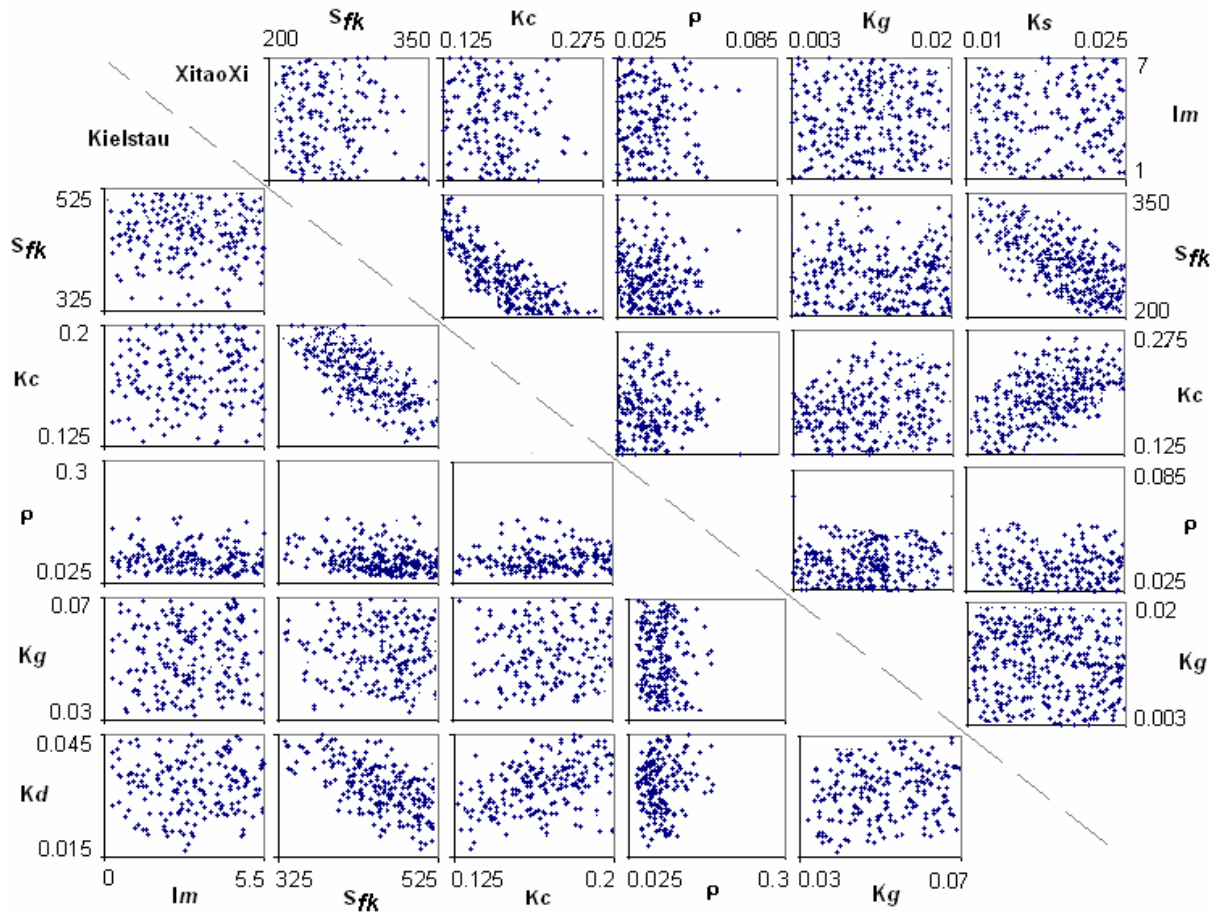

Figure 5.6 Correlation plots of parameters in two study areas (lower left: Kielstau, upper right: XitaoXi).

5.5.2 The SUFI-2 uncertainty bounds in calibration and validation results

Accurate probabilistic forecasting requires that the uncertainty bounds are statistically meaningful and exhibit the appropriate coverage. Instead of focusing on the goodness-of-fit of the median output estimate, we examine the properties of each iteration result by checking if the two measures of *P* factor and *R* factor could reach the desired targets. When the calculated results from the total generated simulations of the last SUFI-2 iteration meet our calibration targets, the same run was conducted for validation. The calibration and validation results for both study basins are derived here in the sense that they represent the desired range of simulation uncertainty instead of one 'optimum' parameter set. The 90% uncertainty bound describes the parameter uncertainty resulting from the non-uniqueness of effective model parameters. As we can see from Figure 5.7 and Figure 5.8, hydrograph simulations obtained from the 90% uncertainty bounds can reproduce the observed discharges with reasonable accuracy for both catchments. The calculated values of *P* factor and *R* factor are also shown in the figures. It exhibits the appropriate coverage, i.e. the simulations bracket the observations most of the time (*P* factor>50%) with acceptable *R* factor values (*R* factor<*1*). The plot

reveals that there is a tendency for small discharges to be underestimated in Kielstau during the summer time, but overestimated in XitaoXi at its spring seasons. For example at the beginning of calibration period in Kielstau, the low runoff is underestimated during the months of July and August. It can be partly owing to the recorded dry season, and partly because of the relatively low water storage modeled in wetland or groundwater aquifers accumulated from previous calibration years, which is supposed to be important baseflow sources in low-rain seasons. Meanwhile in XitaoXi, the river discharges are slightly overpredicted around the month of March for both calibration and validation. It can happen given the great complexity in water management (like irrigation) of such periods for which plants are growing with low precipitations (Gao 2006). However, the global shape of the hydrograph is nevertheless well approximated. When comparing the calibration and validation results for the Kielstau basins, it is noticeable that better *P* factor and *R* factor values are achieved for the validation period. As we can see from Figure 5.7, the validation year included more peak flows, while a longer period of low flow was presented during the calibration year. The pattern is consistent with the inference that low-flow seasons contribute more to the overall uncertainty than peak-flow seasons (Zhang et al. 2011). Regarding the XitaoXi catchment, the total uncertainty bounds are relatively thin despite similar *R* factor values, indicating a good model performance. This could partly due to the much larger scales in y-axis of the XitaoXi river discharge amount comparing to the small Kielstau streamflow. As the calibration and validation results show accepted accuracy for both basins, it clearly indicates that the data is adequate to capture the scale of local hydrologic processes in spite of different resolution data used for each catchment.

Finally, the simulated uncertainty bounds in Figure 5.7 and Figure 5.8 using SUFI-2 are mainly associated with parameter estimation but account for all sources of uncertainties such as model structure and input data (Abbaspour et al. 2004). The fact that the parameter uncertainty is relatively narrow but does not always bracket the observations indicates that model structure may need further improvement. However, such advantage of a more complex model is limited and may be outweighed by an increase in model uncertainty with added processes and information.

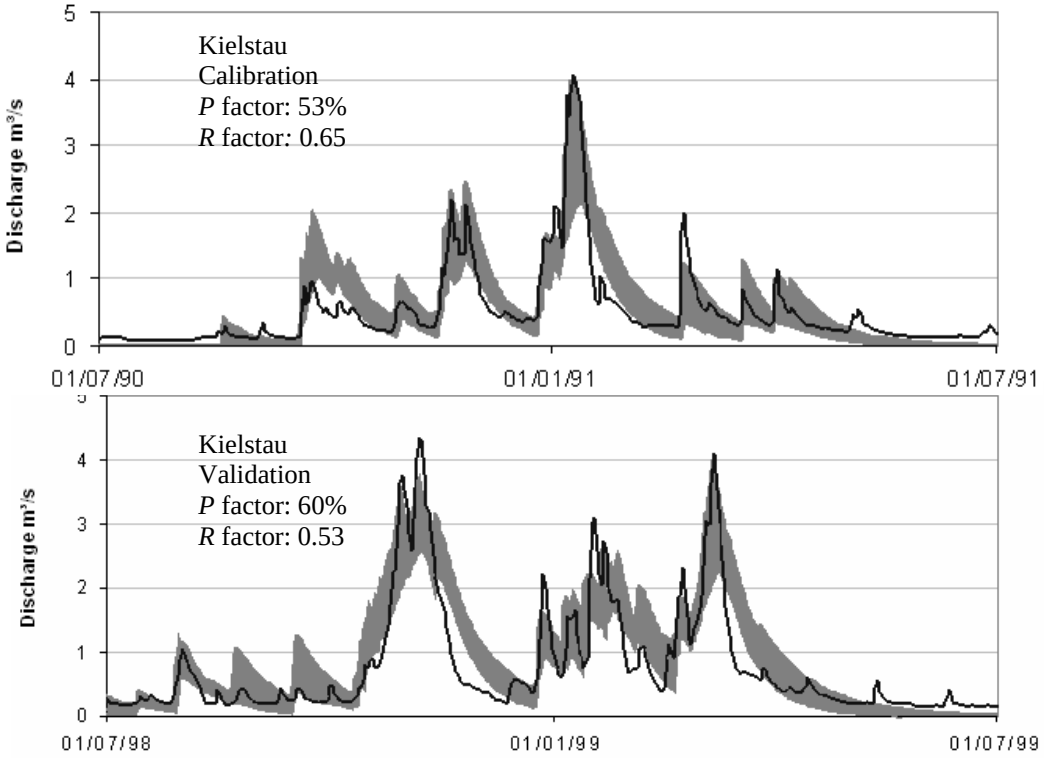

Figure 5.7 Calibration and validation results for Kielstau basins showing the 90% simulation uncertainty intervals (gray shadow) along with the measured discharge (black line).

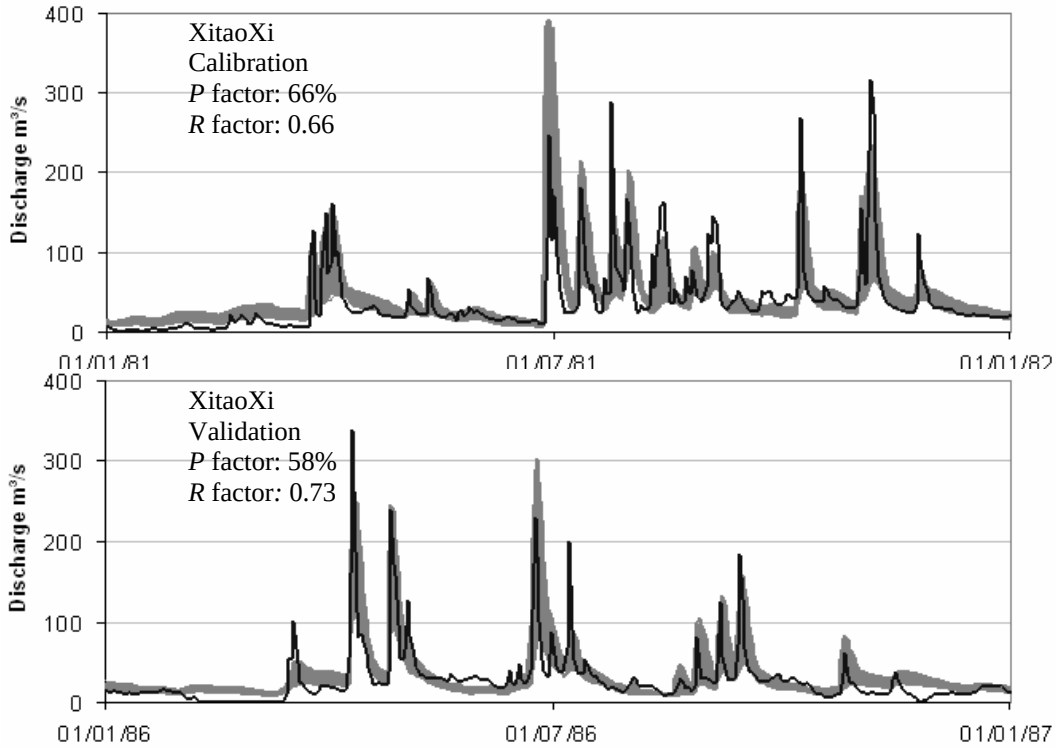

Figure 5.8 Calibration and validation results for XitaoXi basins showing the 90% simulation uncertainty intervals (gray shadow) along with the measured discharge (black line).

5.6 Conclusion

A simple and iterative parameter optimization-uncertainty analysis routine SUFI-2 has been successfully used to sample the parameter spaces in the KIDS model and to find the associated simulation uncertainty from the non-unique parameter sets. The random sampling scheme adopted in our approach is proved to be adequate and efficient for relative simple low-dimensional sampling problems, as the applications in two very-differing study basins demonstrated here.

The scatter plots of parameter values versus model performance (NS) highly exhibit equifinality where many possible parameter sets can provide acceptable simulations of the catchment response. This also implies a large uncertainty from parameter estimations. It ensures the assumptions that a meaningful calibration should include the uncertainty estimation instead of identifying a unique set of parameter values. Further investigation into the posterior parameter distribution functions reveals a clearer distribution pattern for each parameter. Among them, most of their optimal values can be well defined. Two parameters – 'I*m*' and 'K_g' - have a relatively smooth response surface and therefore not so well identifiable for a good model performance. This is in consistence with the results of parameter correlations, that these two parameters are not close-correlated with others. Soil and groundwater parameters like 'ρ' and 'K_g' are more sensitive in Kielstau models. It may reflect the active soil-groundwater interactions in Kielstau region because of the near-surface groundwater level and the large fraction of wetland area. A strong negative correlation was found between soil parameters 'S_{fk}' and 'K_c' due to their effect on model performance. The validated hydrograph shows an acceptable simulation uncertainty range (*R* factor*<1*) for both catchments, which can bracket the observations most of the time (*P* factor>50%). Despite that some simulations are less accurate during low-flow periods, the global shape of the hydrograph is reasonably well approximated for both basins, and the 90% uncertainty bounds are always narrow. However, the parameter uncertainty bounds do not always cover the measured data during the validation periods. It indicates that further improvements in the model structure may be required for more accurate predictions in future researches.

Acknowledgments

The authors thank the Kiel University for financial support of this program. We appreciate help from our colleagues of Institute for the Conservation of Natural Resources, Kiel University for access to their research data. We thank Nanjing Institute of Geography and Limnology, Chinese Academy of Sciences for the provision of XitaoXi data. Part of this work is sponsored by the National Research Program (No.: 2008CB418106) from Chinese Ministry of Science and Technology; and by the Key project (No.: KZCX1-YW-14-6) from Chinese Academy of Sciences.

References

Abbaspour, K., Johnson, C. & van Genuchten, M. 2004 Estimating uncertain flow and transport parameters using a sequential uncertainty fitting procedure, *Vadose Zone J.* 3, 1340–1352.

Arnold, J., Srinivasan, R., Muttiah, R. & Williams, J. 1998 Large area hydrologic modelling and assessment-Part I: model development. *J. Am. Water Resour. Assoc.* 34 (1), 73-89.

Aronica, G., Bates, P. & Horritt, M. 2002 Assessing the uncertainty in distributed model predictions using observed binary pattern information within GLUE. *Hydrol. Process.* 16 (10), 2001–2016.

Beven, K. 2007 Towards integrated environmental models of everywhere: uncertainty, data and modelling as a learning process. *Hydrol. Earth Syst. Sci.* 11 (1), 460-467.

Beven, K., Smith, P. & Freer, J. 2007 Comment on ‘‘Hydrological forecasting uncertainty assessment: Incoherence of the GLUE methodology’’ by Pietro Mantovan and Ezio Todini. *J. Hydrol.* 338, 315– 318.

Blasone, R., Vrugt, J., Madsen, H., Rosbjerg, D., Robinson, B. & Zyvoloski, G. 2008 Generalized likelihood uncertainty estimation (GLUE) using adaptive Markov Chain Monte Carlo sampling. *Adv. Water Resour*. 31 (4), 630-648.

Boyle, D., Gupta, H. & Sorooshian, S. 2000 Toward improved calibration of hydrological models: combining the strengths of manual and automatic methods. *Water Resources Res.* 36 (12), 3663–3674.

Cheng, C., Ou, C. & Chau, K. 2002 Combining a fuzzy optimal model with a genetic algorithm to solve multi-objective rainfall–runoff model calibration. *J. Hydrol.* 268, 72–86.

Cheng, C., Zhao, M., Chau, K. & Wu, X. 2006 Using genetic algorithm and TOPSIS for Xinanjiang model calibration with a single procedure. *J. Hydrol.* 316, 129–140.

Choi, H. & Beven, K. 2007 Multi-period and multi-criteria model conditioning to reduce prediction uncertainty in an application of TOPMODEL within the GLUE framework. *J. Hydrol.* 332, 316– 336.

Chow, V., Maidment, D. & Mays, L. 1988 *Applied Hydrology.* McGraw-Hill, New York, USA.

Doherty, J. & Johnston, J. 2003 Methodologies for calibration and predictive analysis of a watershed model. *J. Am. Water Resour. Assoc.* 39 (2), 251–265.

Duan, Q., Sorooshian, S & Gupta, V. 1992 Effective and efficient global optimization for conceptual rainfall–runoff models. *Water Resour. Res.* 28 (4), 1015–1031.

Eggemann, G., Sterr, H. & Kuhnt, G. 2001 *Geomorphologie SchleswigHolsteins.* (unpublished), Kiel, 140p.

Feyen, L., Vrugt, J., Ó Nualláin, B., van der Knijff, J. & De Roo, A. 2007 Parameter optimization and uncertainty assessment for large scale streamflow simulation with the LISFLOOD model. *J. Hydrol.* 332, 276–289.

Freer, J., Beven, K. & Ambroise, B. 1996 Bayesian estimation of uncertainty in runoff prediction and the value of data: an application of the GLUE approach. *Water Resour. Res.*32 (7), 2161–2173.

Gao, J., Lu, G., Zhao, G. & Li, J. 2006 Watershed data model: a case study of Xitiaoxi sub-waterhed, Taihu Basin (in Chinese, with English abstract). *J. Lake Science.* 18 (3), 312-318.

Glugla, G. 1969 Berechnungsverfahren zur Ermittlung des aktuellen Wassergehalts und Gravitationswasserabflusses im Boden. *Albrecht-Thaer-Archiv,* 13 (4), 371-376.

Hörmann, G., Zhang, X. & Fohrer, N. 2007 Comparison of a simple and a spatially distributed hydrologic model for the simulation of a lowland catchment in Northern Germany. *Ecolog. Model.* 209 (1), 21-28.

Krzysztofowicz, R. & Kelly, K. 2000 Hydrologic uncertainty processor for probabilistic river stage forecasting. *Water Resour. Res.* 36 (11), 3265–3277.

Kuczera, G. & Parent, E. 1998 Monte Carlo assessment of parameter uncertainty in conceptual catchment models: the Metropolis algorithm. *J. Hydrol.* 211, 69–85.

Laloy, E., Fasbender, D. & Bielders, C. 2010 Parameter optimization and uncertainty analysis for plot-scale continuous modelling of runoff using a formal Bayesian approach. *J. Hydrol.* 380, 82–93.

Lamb, R. & Kay, A. 2004 Confidence intervals for a spatially generalized, continuous simulation flood frequency model for Great Britain. *Water Resour. Res.* 40 (7), 1-13.

Li, L., Xia, J., Xu, C., Chu, J. & Wang, R. 2009 Analyse the sources of equifinality in hydrological model using GLUE methodology. *Hydroinformatics in Hydrology, Hydrogeology and Water Resources.* IAHS Publ. 331, 130-138.

Li, X., Weller, D. & Jordan, T. 2010 Watershed model calibration using multi-objective optimisation and multi-site averaging. *J. Hydrol.* 380, 277–288.

Madsen, H. 2003 Parameter estimation in distributed hydrological catchment modelling using automatic calibration with multiple objectives. *Adv. Water Resour.* 26, 205–16.

Montanari, A. & Brath, A. 2004 A stochastic approach for assessing the uncertainty of rainfall-runoff simulations. *Water Resour. Res.* 40, 1-11.

Nash, J. & Sutcliffe, J. 1970 River flow forecasting through conceptual models. Part I: A discussion on principles. *J. Hydrol.* 10, 282-290.

Schmidtke, K. 1999 *Land im Wind, Wetter und Klima in Schleswig-Holstein.* Wachholtz Verlag, 119p.

Schmitz, O., Karssenberg, D., van Deursen, W.P.A. & Wesseling, C. 2009 Linking external components to a spatio-temporal modelling framework: Coupling MODFLOW and PCRaster. *Environ. Modell. Softw.* 24, 1088-1099.

Schuol, J. & Abbaspour, K. 2006 Calibration and uncertainty issues of a hydrological model (SWAT) applied to West Africa. *Adv. Geosci.* 9, 137–143.

Sponagel, H. 2005 *Bodenkundliche Kartieranleitung.* ADHOCARBEITSGRUPPE BODEN der Staatlichen Geologischen Dienste und der Bundesanstalt für Geowissenschaften und Rohstoffe. 5.verbesserte und erweiterte Auflage, Hannover, 438p.

Sumner, N., Fleming, P. & Bates, B. 1997 Calibration of a modified SFB model for twenty-five Australian catchments using simulated annealing. *J. Hydrol.* 197, 166–188.

Tang, Y., Reed, P., Wagener, T. & Werkhoven, K. 2007 Comparing sensitivity analysis methods to advance lumped watershed model identification and evaluation. *Hydrol. Earth Syst. Sci.* 11, 793–817.

Thiemann, M., Trosset, M., Gupta, H. & Sorooshian, S. 2001 Bayesian recursive parameter estimation for hydrological models. *Water Resour. Res.* 37(10), 2521–35.

Uhlenbrook, S. & Sieber, A. 2005 On the value of experimental data to reduce the prediction uncertainty of a process-oriented catchment model. *Environ. Modell. Softw.* 20, 19-32.

Van Deursen, W.P.A. 1995 Geographical Information Systems and Dynamic Models: development and application of a prototype spatial modelling language. *Netherlands Geographic Studies*, issue 190, 195p.

Vrugt, J., Gupta, H., Bouten, W. & Sorooshian, S. 2003a A Shuffled Complex Evolution Metropolis algorithm for optimization and uncertainty assessment of hydrologic model parameters. *Water Resour. Res.* 39 (8), 1201-1213.

Vrugt, J., Gupta, H., Bastidas, L. Bouten, W. & Sorooshian, S. 2003b Effective and efficient algorithm for multi-objective optimization of hydrologic models. *Water Resour. Res.* 39 (8), 1214-1232.

Wan, R. Yang, G., Li, H. & Yang, L. 2007 Simulating flood events in mesoscale watershed: a case study from River Xitiaoxi Watershed in the upper region of Taihu Basin. *J. Lake Science.* 19 (2), 170-176.

Wang, Q. 1997 Using genetic algorithms to optimize model parameters. *Environ. Modell. Softw.* 12 (1), 27–34.

Wesseling, C., Karssenberg, D., Burrough, P. & Van Deursen, W.P.A. 1996 Integrated dynamic environmental models in GIS: The development of a Dynamic Modelling language. *Transactions in GIS*, 1 (1), 40–48.

Xu, L., Zhang, Q., Li, H., Viney, N., Xu, J. & Liu, J. 2007 Modelling of Surface Runoff in Xitiaoxi Catchment, China. *Water Resour. Manag.* 21, 1313–1323.

Yapo, P., Gupta, H. & Sorooshian, S. 1998 Multi-objective global optimization for hydrological models. *J. Hydrol.* 204, 83–97.

Zak, S. & Beven, K. 1999 Equifinality, sensitivity and predictive uncertainty in the estimation of critical loads. *The Science of the Total Environment*, 236, 191-214.

Zhang, X.Y., Hörmann, G. & Fohrer, N. 2007 The Effects of Different Model Complexity on the Quality of Discharge Simulation for a Lowland Catchment in Northern Germany. Heft 20.07 ‘Einfluss von Bewirtschaftung und Klima auf Wasser- und Stoffhaushalt von Gewässern’ (2007), Band 2, *Forum für Hydrologie und Wasserbewirtschaftung*, 111-114.

Zhang, X.Y., Hörmann, G. & Fohrer, N. 2008 An investigation of the effects of model structure on model performance to reduce discharge simulation uncertainty in two catchments. *Adv. Geosci.* 18, 31–35.

Zhang, X.Y., Hörmann, G. & Fohrer, N. 2009 Hydrologic comparison between a lowland catchment (Kielstau, Germany) and a mountainous catchment (XitaoXi, China) using KIDS model in PCRaster. *Adv. Geosci.* 21, 125–130.

Zhang, X.Y., Hörmann, G., Gao, J.F. & Fohrer, N. 2011 Structural uncertainty assessment in a discharge simulation model. *Hydrol. Sci. J.* 56 (5), 854-869.

Chapter 6

Estimating the impacts and uncertainty of changing spatial input data resolutions on streamflow simulations in two basins

X.Y. Zhang, G. Hörmann, N. Fohrer and J.F. Gao
Journal of Hydroinformatics, accepted 11 Dec 2011, forthcoming

Abstract

Impact of different grid resolutions of spatial input data on modelled river runoff are investigated using the simple rainfall-runoff model KIDS (Kielstau Discharge Simulations) in PCRaster modelling language for two watersheds - Kielstau and XitaoXi. In this study, the grid based spatial data are aggregated to coarser resolutions to support the multi-resolution, multi-calibration and multi-site analysis for grid-scale investigations. Daily streamflow is simulated and model parameters are calibrated at each spatial resolution. The study suggests that re-calibration is critically needed when the grid resolution is changed. Altering grid sizes have apparent impact on the parameter distribution patterns. Resolution uncertainty bands obtained by the overlapping hydrographs generated with different resolutions of input data are reported with a sufficient coverage of the observations for both basins. The analysis of model

efficiency in terms of IC-ratio (a ratio between the input grid area and the catchment area) indicates that coarser resolutions with IC-ratio<0.001 may be used as an effective alternative for conducting preliminary analyses in streamflow simulation for the Kielstau basin. The modelling outputs are more sensitive to the spatial distribution of input data at the XitaoXi watershed, showing that accurate input data are required to achieve optimum modelling performance.

Keywords: grid size upscaling; hydrological modelling; IC-ratio; parameter sensitivity; resolution uncertainty.

6.1 Introduction

Distributed hydrological models as well as process-based models deal with the interactions of their spatial patterns and processes on a variety of scales. Grid resolutions are often used in spatially explicit models to account for detailed watershed heterogeneity, like spatial information on topography, soil and vegetation properties. The scale and resolution issues became more significant as physically based models are widely used. The choice of an appropriate scale is considered to be in the first instance aiming on attaining optimal model performance.

Many researchers have investigated the issues that are related to the impact of resolution on model parameters and the predictions of catchment modelling. As the higher resolution database usually represents better landscape information required in model application, several studies found that the finer grid size gave more accurate results (Quinn et al. 1991; Moore et al. 1993; Wolock & Price 1994; Bruneau et al. 1995; Kuo et al. 1999). But a large effort to improve model performance by increasing data discretization level is mostly not justified when above a certain threshold of resolution. Zhang & Montgomery (1994) examined the effect of digital elevation model (DEM) grid size on the portrayal of the land surface and hydrologic simulations. Elevation data gridded at 2-, 4-, 10-, 30-, 90-m scales significantly affects computed topographic parameters and hydrographs. The result revealed that the 10-m grid size provides a substantial improvement over 30- and 90-m data, but 2- or 4-m data provide only marginal additional improvement for the study areas. Vazquez et al. (2002), Vazquez & Feyen (2003) demonstrated that different input data resolutions with the MIKE SHE model code (Refsgaard & Storm 1996; DHI 1998) lead to significant differences in both effective parameter values and model performance. They found that an acceptable compromise between accuracy of model predictions and computational time was reached

when using a grid size of 600 m for the Gete catchment in Belgium. A subsequent study with the same hydrologic code focuses on the impact assessment of different DEM gridding method on basin runoff modelling (Vazquez & Feyen 2007). Bormann (2006) indicates that an aggregation of input data for the calculation of regional water balances using TOPLATS type models (Famiglietti & Wood 1994) does not lead to significant errors up to a grid size of 300 m. Shrestha et al. (2006) evaluated the model performance by comparing observed discharge against simulated discharge for a range of IC-ratio values. The IC-ratio is defined as the ratio of the input forcing resolution to catchment size (equation 1)

$$IC - ratio = \frac{C^2}{A} \tag{1}$$

Where C [m] is grid cell size, A [m^2] is catchment area.

The IC-ratio range 0.05 – 0.1 is found to be the optimum performance range considering the data and resource demands of distributed models.

Possible reason could be that highly resolved data often contain redundant information; therefore a higher data resolution does not always produce a better modelling result. Furthermore, the benefit of increased data resolution strongly depends on the applied model philosophies and catchment specific characteristics. Beven (2001) described the problem of scaling as the difficulty to apply a hydrological model to a particular catchment with its own, unique characteristics. Bormann et al. (2009) investigated model sensitivity to data aggregation using different catchment models. They concluded that aggregation effects are partly model and case study dependent. The results presented that high quality of input data is more important than high spatial resolution of data for the calculation of regional water balances. With regard to the quality of input data, it is a highly subjective terminology as it should be appropriate to the resolution of model disaggregation and the scales of hydrological significance patterns like topography, forcing data spatial discretization etc.

Additional challenges arising from the scaling issues in hydrological modelling are the induced predictive uncertainty (Shrestha et al. 2006). A number of recent studies provided evidence of the effects of input data on model sensitivity and uncertainty. Lindenschmidt et al. (2005) conducted an uncertainty analysis for different degrees of model complexity in scale discretization and compared at different basin scales. It indicated that the model sensitivity increases with the discretization level since the inclusion of additional processes brings with it additional parameters and data input. Hebeler & Purves (2008) assessed the impact of scaling on models from different resolution, and concluded that tested models had clear dependencies on scale, terrain roughness and variations of parameter thresholds. Bogena

et al. (2005) focused on model uncertainty analysis in the simulation of groundwater recharge at different scales.

In summary, choosing an appropriate resolution is a key task in hydrology (Hebeler & Purves 2008). The scaling dilemma exists when approaching better model performance with higher resolution data: the limited effect to bring more accurate results after a certain resolution threshold and the massive demand of storage capacity and computer time required by high resolved data (Vazquez et al. 2002; Omer et al. 2003; Cullmann et al. 2006). Even when a detailed data base is preferred, it is not always available for every catchment of interest.

Despite those efforts in literature to investigate the impact of data resolution, it is still a difficult task to find a suitable solution for different hydrological models or different sites. This is not only because results are mostly not transferable, but also the assessment will usually demand the considerations of various aspects such as data assessment, parameter errors, modelling uncertainty. Therefore, this study elaborates the effects of grid aggregation on the streamflow simulation, parameter estimation and modelling uncertainty for model application in two case studies. The hydrological model in this study is set up with a GIS-based dynamic modelling language PCRaster (Van Deursen 1995; Wesseling et al. 1996). River runoffs are simulated for two watersheds: the small lowland Kielstau catchment (51.5 km²) in Germany and the medium sized mountainous XitaoXi basin (2271 km²) in China. With regard to the scale issues, previous studies using PCRaster based models such as Zhao et al. (2009) examined the impacts of spatial data resolution on discharge simulation for the XitaoXi basin. It concluded that an aggregation of input data does not lead to significant errors up to a grid size of 1km. However, it did not address explicitly either the effects on parameter behavior or the assessment of model uncertainty. Furthermore, discussion about the results comparison between small and medium sized watersheds is not common in previous publications. In this paper, we intend to inspect how the modelling process is affected by changing input data resolutions (grid upscaling) in terms of the effective parameter values and of the modelling performance in the two watersheds. Thus the objectives of this study are (1) to simulate daily stream flow at different grid resolutions for Kielstau and XitaoXi watersheds using hydrological model (namely KIDS model) in PCRaster; (2) to examine the grid-size impact on effective parameter values; (3) to assess the extent of modelling uncertainty caused by varying resolutions; (4) to compare the model efficiency at changing input data resolutions for the two watersheds in terms of the IC-ratio, and therefore to investigate the suitable resolution level for runoff simulation.

6.2 Data, model and methods

6.2.1 The study sites

We consider two catchments in this study including the Kielstau basin in Germany and the XitaoXi basin in China. These two basins are the subject catchments of a Sino German integrated geohydrological study.

Kielstau is a lowland watershed in the Northern Germany, with a drainage area of 51.5 km² (see Figure 6.1a). As the development of the landscape was mainly influenced by the Saale and the Weichselian ice ages (Eggemann et al. 2001), the whole catchment is rather flat, with the maximum altitude difference of about 52m. Wedged between the North Sea and the Baltic Sea, the Kielstau catchment is characterized by moderate temperature and oceanic climate with soft moist winters and cool rainy summers. Snowfall is rare and occurs on average at 20 up to 25 days per winter. Mean annual precipitation is about 800 mm, and actual evaporation 400 mm approximately (Schmidtke 1999). Land use is dominated by agriculture (55.8%) and grassland (26.1%). The geological underground of the basin is dominated by pleistocene deposits, resulting in a wide variety of soil types and soil forms in this small area. Soils are mainly consisting of Podzol, Gleysol and Luvisol formed in the Saale and Weichsel ice ages, among which Gleysol belongs to the major wetland soil types (Sponagel 2005; Liu et al. 2009). These are heavy soils having high field capacity and containing large percentages of clay and silt, which contribute to forming numerous scattered wetland areas in the watershed. A large fraction of wetland area (estimated as 30% of land surface area, Treple 2004) and the near-surface groundwater level are observed in this region. Dynamics of near-surface groundwater are generally determined by precipitation, and when close to the river by stream water level as well. Groundwater levels in the riparian wetland are in most cases higher than those in the river. The interaction between surface water and groundwater is thus active, especially in the riparian wetland area for this region. During flood events, a reversion of the flow direction could happen if the close-to-river groundwater level is lower than the stream water level (Springer 2006).

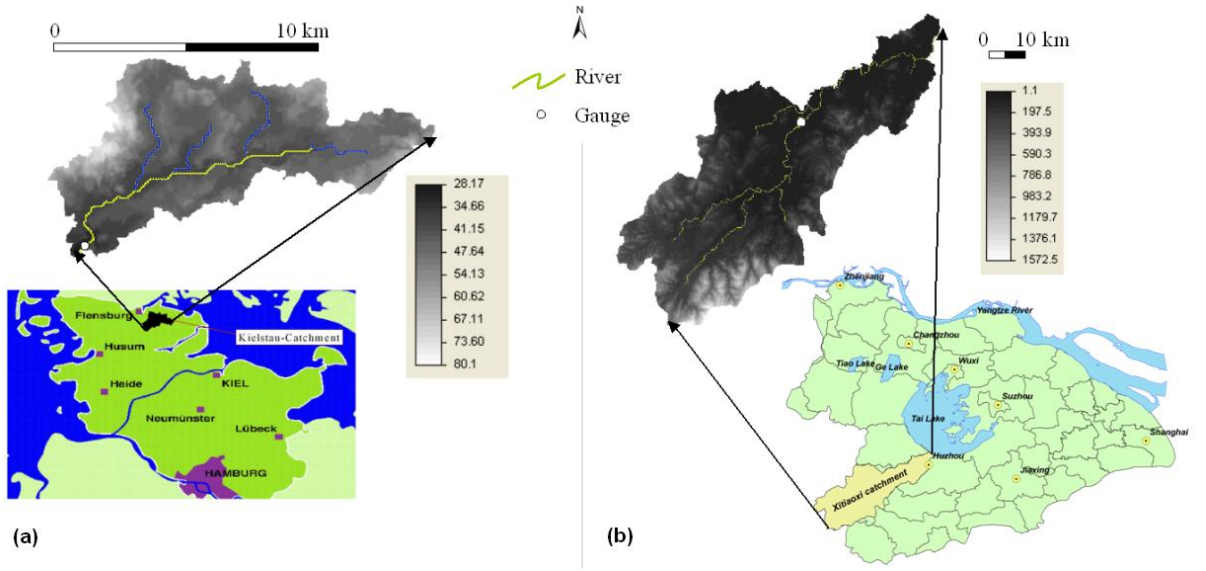

Figure 6.1 Geographic location and elevation map for (a) the Kielstau basin and (b) the XitaoXi basin.

The second study watershed XitaoXi is a 2271 km^2 sized mountainous basin, which is located in the semitropical monsoon zone in the Southern China (see Figure 6.1b). It is one of major sub-basins that drain into Taihu Lake. The spatio-temporal variations in precipitation and evaporation distributions are statistically significant. Average precipitation in the watershed is 1466mm annually, with 75% of rain falling between April and October (Gao et al. 2006). The annual rainfall was gradually decreasing from the southwest mountain area of 1800mm to the northeast plains of 1200mm. Average evaporation from water surface ranges from 800 mm to 900 mm annually. Evaporation intensity from the southwest to the northeast has shown an increasing trend (Zhang et al. 2006). The XitaoXi basin is characterised by three different topographic areas from southwest to northeast. The upper reaches in southeast part are mountainous area, with elevation over 600 m accounting for about 15% of the total basin area. The following sections are 150-600 m part of low hills area in the central accounting for 40%. And the rest northeast part turns into a flat outwash plain with a low hydraulic gradient. The dominant soil types are red soil and rocky soil. These soils tend to have limited water storage capacity. In the XitaoXi region, 63.4% of land use is forest and grass, 20% paddy rice land (Wan et al. 2007). Most portions of the river discharge are assumed mainly from the saturation excess surface runoff, with limited influence from the deeper, regional groundwater (Xu et al. 2007).

The Kielstau and XitaoXi watersheds have quite different hydrologic characteristics in catchment scale, topography, soil properties, landuse and weather conditions (Zhang et al. 2009). Those features also illustrate their noticeable differences in the extent of catchment

heterogeneity. The mountainous XitaoXi basin is more heterogeneous in catchment spatial features than the small flat Kielstau watershed. These two areas thus provide a good data set to compare the impacts of different grid-scales.

6.2.2 KIDS model description

The KIDS model (Kielstau Discharge Simulation model, Hörmann et al. 2007; Zhang et al. 2007) is a simple rainfall-runoff model developed in PCRaster modelling language. It was used at first for practical purposes to facilitate water resource management in the Kielstau basin. The main advantage of the KIDS model in PCRaster is its flexibility of model structure complexity in lumped or physically distributed model. It is basically driven by digital elevation model (DEM) and meteorological input data, and then simulates river discharge in given river basins. To fit model results to local conditions, it also allows the extension of the model with additional inputs like soils and land cover as submodels (Zhang et al. 2008, 2011). All derived models form the KIDS model ensembles. The model is spatially distributed and space was originally discretized at a 50 m by 50 m grid size for Kielstau and 200 m by 200 m for XitaoXi using the best available resolution data.

In the framework of KIDS model, runoff is calculated on each grid cell based on the water balance equation (see equation 1), taking into account interception, precipitation, evapotranspiration, and the flows to other compartments. We use ‘mm’ as unit of measure for all the water amount expressions included in equations of this paper, and calculate with a daily time step. The model is a simplified approximation of complex water cycles, with detailed calculation steps stated below.

$$S_t = S_{t-1} + P_t - ET_t - I_t - Qo_t - Sp_t \quad (2)$$

Where S is the soil water content, t is the modelling time step (daily), P is precipitation and ET is evapotranspiration, I is interception, Qo is surface runoff (overland flow), Sp is a lumped term of water seepage loss.

Precipitation and potential evapotranspiration are required as input data. The model calculates interception from vegetation layer, with the parameter ‘I*m*’ as shown in equation 3. Surface runoff ‘Qo’ is calculated according to equation 4. It describes satur

and storage calculation on the basis of derived soil parameters like field capacity and infiltration rate of soil water deficit. The parameter ‘Sp’ is the expression of water loss which comprises percolation or seepage, lateral flows and other aggregate model errors.

$$I_t = \min (P_t, Im) \quad (3)$$

Where I*m* is the maximum interception amount of vegetation cover.

$$Qo_t = \max \{[P_t - I_t - K_c(S_{fk} - S_t)], 0\} \quad (4)$$

Where Qo represents the surface runoff, K_c is the infiltration parameter, and S_{fk} is the wetness at field capacity.

The whole river basin is set up with one lump soil layer in the basic structure. The current soil map can be sub-parameterized or more soil layers can be added if required. And sub-surface flow is modelled as 1D bucket flow with a lateral flow rate parameter 'K_s' as equation 5 shows. The value of parameter 'K_s' is set equal to zero in the basic model for both basins, however, it can be adjusted above zero for further modifications.

$$Qs_t = K_s S_t \quad (5)$$

Where Qs is subsurface flow, and K_s is lateral flow rate.

The groundwater layer is represented as linear storage. Combining equations 6, 7 and 8 yields the daily groundwater dynamics.

$$G_t = G_{t-1} + Ig_t - Qg_t \quad (6)$$

$$Ig_t = \rho S_t \quad (7)$$

$$Qg_t = K_g G_t \quad (8)$$

Where G is groundwater storage, Ig the inflow to groundwater aquifer, Qg the groundwater discharge to runoff, ρ the water seepage rate from soil to groundwater, K_g the groundwater outflow rate.

Runoff is then composed of three parts: surface runoff, lateral flow and groundwater discharge. The flow path is then derived from topography through a flow accumulation grid calculated in PCRaster. The routing of surface and subsurface runoff water flows is modelled with the fully dynamic kinematic wave function (Chow et al. 1988).

The basic KIDS model and equations as described above represent a simple rainfall–runoff model. The basic model can be easily adapted for a wide range of hydrological modelling applications by means of integrating sub-modules into basic structure in order to take some specific influence factors into account. Considering the greatly differing hydrology of the two basins, the appropriate model structure for each basin is selected from the KIDS model ensembles respectively (Zhang et al. 2011): Model 'DW' for Kielstau – basic KIDS model with drainage (equation 9) and integration of wetland (equation 10); Model 'GLT' for XitaoXi – basic KIDS model with groundwater outflow threshold (equation 11), subsurface flow and landuse-coefficient adjusted ET distribution.

$$D_t = K_d S_t + L_d \quad (9)$$

Where D is the drained water volume, K_d is drainage factor, S is available soil water storage, L_d is the lateral inflow volume (lateral seepage from irrigation canals and drainage channels).

$$W_t = W_{t-1} + Iw_t - Ew_t - Qw_t \quad (10)$$

Where W is wetland water storage; Iw the incoming water volume influenced by precipitation, interception and soil moisture; Ew the water loss from wetland, mainly evapotranspiration; Qw the wetland water seepage contributing to runoff.

$$Qg_t = \text{Min}(K_g G_t, Gm) \quad (11)$$

Where Gm is the maximum daily groundwater outflow or groundwater outflow threshold.

Owing to the general nature and flexible structure of the KIDS model, its application to any study area requires certain parameters be identified for the particular basin. In the current model version, six main parameters need to be determined by calibration using daily discharge observations. Table 6.1 lists an overview of the calibration parameters with the upper and lower value ranges, which are decided based on a preliminary parameter sensitivity test (Zhang et al. 2009) and also considering empirical scales of physical parameters.

Table 6.1 Description of parameters included in the KIDS hydrological model calibration procedure, with their upper and lower bounds.

Parameter (unit)	**Range**	**Definition**
I*m* [mm]	0 – 10	Maximum water amount intercepted by vegetation cover
S_{fk} [mm]	1 – 800	Soil water storage capacity
K_c [-]	0.01 – 0.6	Soil Infiltration parameter
ρ [-]	0 – 0.5	Water seepage rate from soil to groundwater
K_g [-]	0.001 – 0.1	Groundwater discharge rate to the river baseflow
K_d [-] in Kielstau	0 – 0.01	Water drainage rate from available soil water storage
K_s [-] in XitaoXi	0 – 0.05	Soil water percolation rate to river discharge

6.2.3 Experimental data processing and analyses steps

To investigate the effects of varying resolutions on model simulation, we need to generate input forcing data with different grid sizes. The initial and finest dataset in this study is at 50×50 m^2 resolution for Kielstau, 200×200 m^2 for XitaoXi. It was used to acquire a set of experimental data set at different spatial resolutions, namely 2, 4, 8, 12, and 20 times coarser resolution, over the two study basins. Aggregation is done with an upscaling operation in PCRaster system using averaged parameter values. Figure 6.2 shows an example of the data aggregation process with the basic spatial data of DEM over the Kielstau watershed at six different grid sizes. Other spatial data or system required map data are converted into coarser resolutions using the same process. The time series data (TSS files) including the daily precipitation data and streamflow data at all six spatial resolutions are consistent with each other.

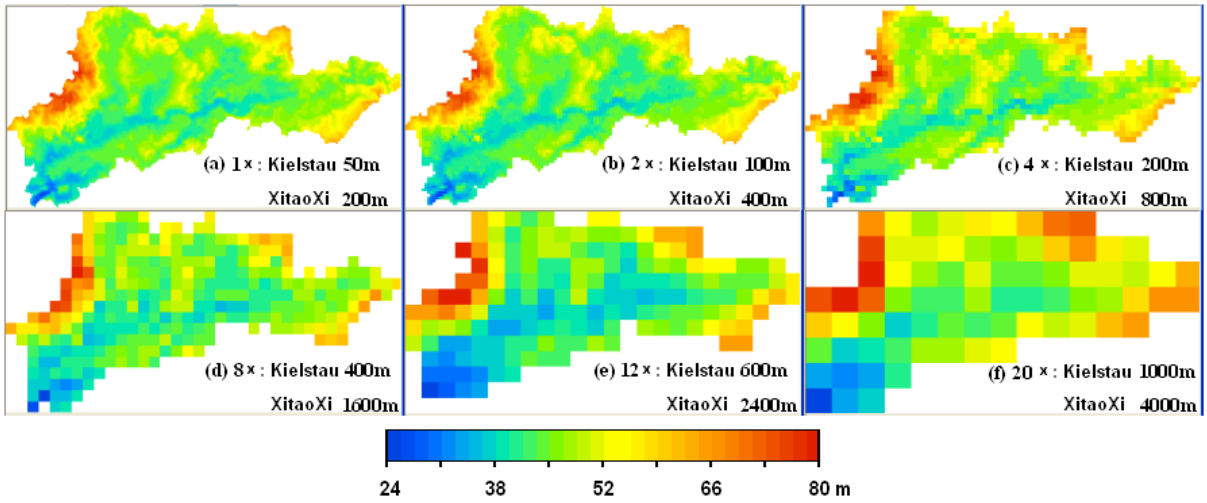

Figure 6.2 An example of spatial data DEM over the Kielstau basin at resolutions of (a) 1x – grid size 50 m for Kielstau, 200 m for XitaoXi, (b) 2x, (c) 4x, (d) 8x, (e) 12x, (f) 20x and their corresponding grid sizes.

The resolution coarsening process results in the change of overall watershed area (Bruneau et al. 1995; Kuo et al. 1999), as it is clearly illustrated in Figure 6.2. We adjust the border cells for forcing input data of rainfall and ET to keep the modelled area consistent, so that only the portion inside the watershed defined in 1x resolution data is considered in modelling. Other data and parameters are aggregated to different spatial resolutions in PCRaster system based on the average cell value of continuous data or the most common value for categorical data. The grid cell aggregation process inevitably leads to loss of information and an increase in the errors in the data.

To facilitate model evaluation, three statistical criteria are used to evaluate the impact of model calibrations considering the strengths and weaknesses of each technique for their applications in watershed model evaluation (Gupta & Sorooshian 1998; Moriasi et al. 2007). They are the Nash Sutcliffe (NS) coefficient (Nash & Sutcliffe 1970), the root mean squared error (RMSE), and the regression coefficient (r^2):

$$NS = 1 - \frac{\sum_{i=1}^{n}(P_i - O_i)^2}{\sum_{i=1}^{n}(O_i - \overline{O})^2} \tag{12}$$

$$RMSE = \sqrt{\frac{\sum_{i=1}^{n}(P_i - O_i)^2}{n}} \tag{13}$$

$$r^2 = \left[\frac{\sum_{i=1}^{n} (O_i - \overline{O})(P_i - \overline{P})}{\sqrt{\sum_{i=1}^{n} (O_i - \overline{O})^2} \sqrt{\sum_{i=1}^{n} (P_i - \overline{P})^2}} \right]^2 \quad (14)$$

where P_i and O_i denote the predicted value and observed value *i*, $\overline{P}$ and $\overline{O}$ are their means over the study time period, and *n* is the total number of simulation time steps.

With the establishment of required data at different resolution levels for the two catchments, a multi-resolution (MR), multi-calibration (MC) and multi-site (MS) test approach was conducted.

First, the model at the initial resolution level is calibrated to obtain optimal model performance based on daily streamflow data. The derived parameter values are directly transferred into other models at different resolutions for river discharge simulation. This is the multi-resolution test to analyse the model performance results as a starting step in the process. An automatic parameter estimation method is used for the KIDS model calibration. This software framework developed by Schmitz et al. (2009) is suited for PCRaster environment to assign the KIDS model files. It allows adding calibration algorithms by the user and evaluates the objective function at randomly spaced points in the defined parameter space. For each calibration process it will generate 3000 model simulations with different parameter values. The Nash Sutcliffe coefficient (NS) is used as the objective function to get a quick overview of model performance evaluation in this step. The optimal value of NS is 1.0 and the feasible range of variation is $-\infty<NS\leq1.0$.

Second, models with the five coarser resolutions are subjected to identical parameter calibration process in the framework of the multi-calibration (MC) test. As each set of calibrated parameters is assigned with a NS value, we choose the parameter combinations whose NS value is higher than 0.5 (NS>0.5) as the sample population for the parameter behavior analysis. The parameter distribution pattern will be generated for each model by dividing the parameter sampling range into twenty equivalents. The results will then be compared to assess the relationships among effective parameter values and grid size. For the river discharge simulation, an optimal model behavior can be obtained for all the grid sizes after calibration. This will yield a band of overlapping hydrographs generated from various input data resolutions in both catchments. Two measures are defined here to quantify the band width which represent model sensitivity or uncertainty of changing input data resolution (Abbaspour et al. 2004; Schuol & Abbaspour 2006). The first measure is referred as *R* factor, the ratio of the average distance of the simulation intervals from different grid sizes and the

standard deviation of the measured data, as equation (15) shows. The other is *P* factor, the percentage of measured data bracketed by the simulation uncertainty bounds (equation 16). The ideal situation is to have an *R* factor value close to zero, while at the same time to cover all the observation data within the simulation uncertainty bounds (*P* factor=100%). The values of *P* factor and *R* factor reflect the uncertainty of varying grid sizes after taking into account the discharge observations.

$$R\ \text{factor} = \frac{\sum_{i=1}^{n}\left[\left(S_{\max}-S_{\min}\right)_1+\left(S_{\max}-S_{\min}\right)_2+\ldots+\left(S_{\max}-S_{\min}\right)_n\right]/n}{stdev\{Q1,Q2,\ldots,Qn\}} \tag{15}$$

where S_{max} and S_{min} denote the maximum and minimal values for each simulated variables; n is the time steps of the selected flow period; stdev is standard deviation of the observed flows within the selected period.

$$P\ \text{factor} = \frac{m}{n}\times 100\% \tag{16}$$

where m is the number of model time steps counted when the observed river discharge value is within the modelled simulation uncertainty bounds, n is the time steps of the selected flow period.

Finally, a multi-site (MS) evaluation test is also performed to investigate how the results differ between the small lowland Kielstau basin and the medium sized mountainous XitaoXi basin. The MS test mainly includes an analysis of the model performances for the selection of an appropriate input data grid resolution in the context of IC-ratio. Shrestha et al. (2002, 2006) used the IC-ratio to investigate the effects of input data resolution on discharge.

Other results comparisons for the two study areas in the MR and MC analysis steps are considered as part of the MS test. Figure 6.3 describes the evaluation framework of the proposed MR-MC-MS test approach in this study.

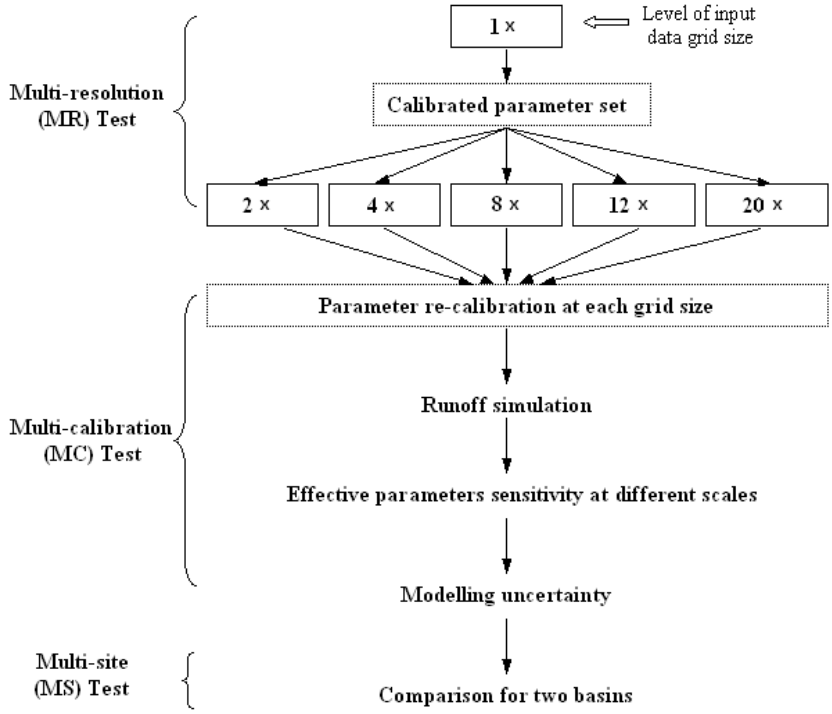

Figure 6.3 Flowchart of the MR-MC-MS approach for the investigation of grid-scale issues.

6.3 Results and discussion

6.3.1 Multi-resolution test and multi-calibration test

The KIDS model performances at various resolution level in the multi-resolution (MR) and multi-calibration (MC) tests are summarized by the NS index in Figure 6.4. The simulation results with the base-line data present acceptable accuracy – 0.8 NS value for 50 m Kielstau model and 0.75 for 200 m XitaoXi model. The result for Kielstau shows that the NS values (ranging between 0.74 and 0.79) at the four different spatial resolutions of 1x, 2x, 4x, and 8x are similar to each other for both MR and MC tests. The NS values at 12x and 20x resolutions are significantly lower than those at the other four resolutions. However, different patterns of the behaviours in NS values are observed for the XitaoXi basin. It drops dramatically at 2x resolution (400 m grid size) even after calibration. All the calibrated (MC) results seem to have better NS values than the MR test. This indicates the necessity of parameter calibration, especially for the XitaoXi catchment as suggested by the larger gap between the NS values of the MR and MC test. The somewhat distinct model behaviours of the two basins are mainly due to the significantly large differences in the effect of spatial variability. The 51.5 km² small lowland Kielstau catchment is more homogeneous characterized in hydrometeorological features (such as topography, soil properties and spatial variation of precipitation) than the 2271 km² mountainous XitaoXi basin. Model simulation and parameter estimation will be

more sensitive to the upscaling grid cells operation in XitaoXi, as the aggregation of input data causes important information losses for the runoff modelling.

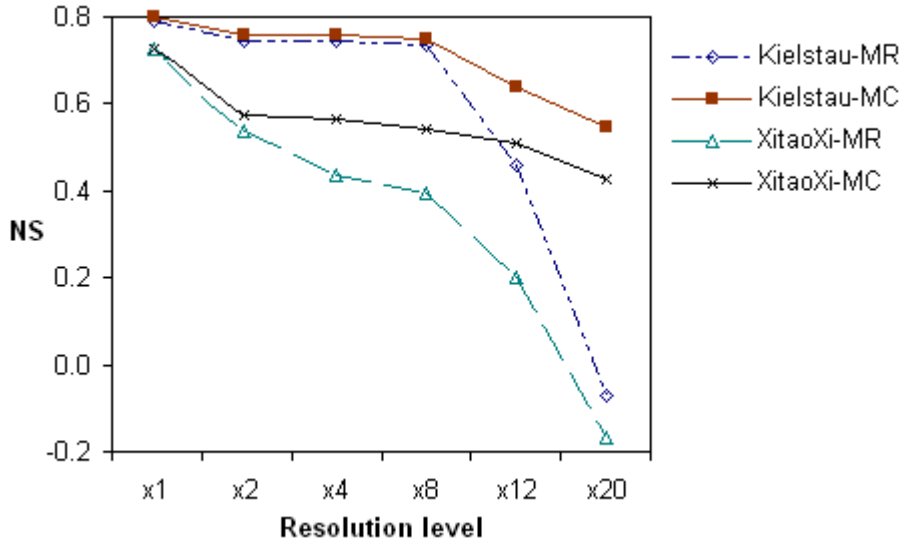

Figure 6.4 Variations of model performance (NS) at different resolution levels for the MR and MC tests.

Furthermore, Figure 6.5 illustrates that the outcomes of two other statistics RMSE and r^2 for the calibrated models also show similar patterns as the NS values in Figure 6.4. The evaluation analysis using three criteria reveals an acceptable agreement to compare simulated output with measured data. This combination of statistical indexes are presented together to establish a platform for model evaluation in the multi-calibration test.

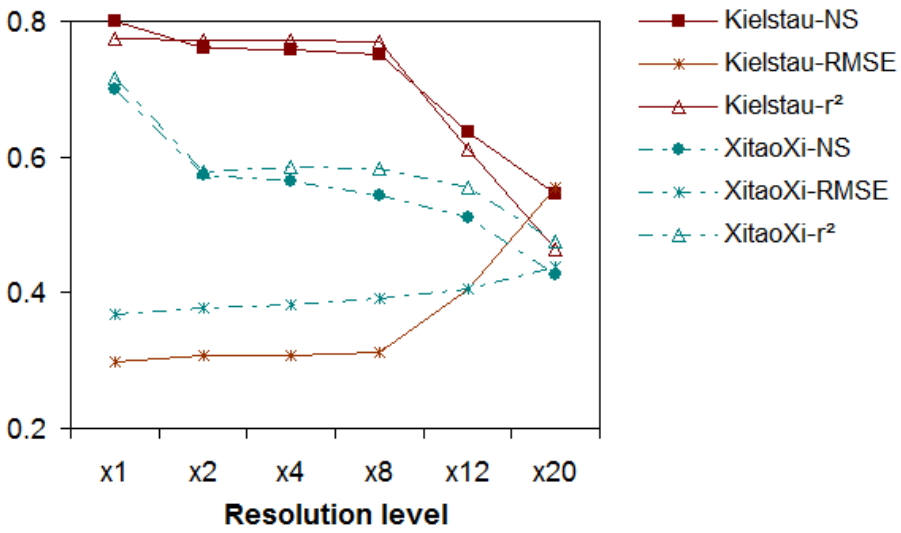

Figure 6.5 Simulation results of NS, RMSE, r^2 of calibrated models for Kielstau (solid lines) and XitaoXi basins (dashed lines).

6.3.2 Parameter sensitivity

In this section we examine the change of parameter distribution patterns with different grid sizes using the random sampling techniques. It is automated model calibration with variation

of random combinations of parameters rather than each parameter individually to perform the parameter sensitivity analysis. As the result show that some parameters (like I*m,* the maximum interception) have low sensitivity to varying input data resolution, we construct the probability distributions only for effective parameters. These are presented for the parameters including, S_{fk} [mm] the wetness at field capacity, ρ [-] water seepage parameter from soil to groundwater, K_g [-] groundwater outflow rate, K_d [-] drainage factor in the Kielstau catchment (Figure 6.6); and S_{fk} [mm] the wetness at field capacity, ρ [-] water seepage parameter from soil to groundwater, K_c [-] infiltration parameter, K_s [-] lateral flow rate factor in the XitaoXi catchment (Figure 6.7). Moreover, the result of models at four different resolution levels of 1x, 2x, 4x, and 12x are selected in the plots for a better view of comparison. It suggests the models of K50, K100, K200, K600 for Kielstau, and X200, X400, X800, X 2400 for XitaoXi. We designate a series of standard abbreviations for the modelling results using different resolution data in the two basins – 'K' is Kielstau, 'X' is XitaoXi, then followed by a number representing the grid cell size (50 means 50x50 m² resolution).

As illustrations for the Kielstau basin in Figure 6.6, the distribution patterns are qualitatively similar for parameter S_{fk}, but with increasing peak values as the grid cells aggregate. As we can see from its Figure 6.6a, the peak value is around 240 for K50 curve, and then increases to 480 for K600. Second, most of the distribution curves for model with finer resolution data (e.g. K50 model) are narrower and peakier than other models with coarser data input. This feature is especially apparent for parameter ρ: the lines are getting more flat as the grid size increases, which result in higher equifinality of parameter estimation. It indicates that the optimal parameter values become less identifiable with upscaling resolutions, which will also introduce increasing parameter estimation uncertainty. Finally, while the model K50 derived parameter distribution curves are usually single well-defined mode (the desired result), coarser data derived curves become more multi-modal, like the K600 curve for parameter K_g and $K_{d.}$ However, differences between the curves for these two parameters are relatively small. For example, the dotted lines of K100 and K200 are very close to each other. It suggests that parameter K_g and K_d are not so sensitive to input data resolution as the other parameters like S_{fk} and ρ.

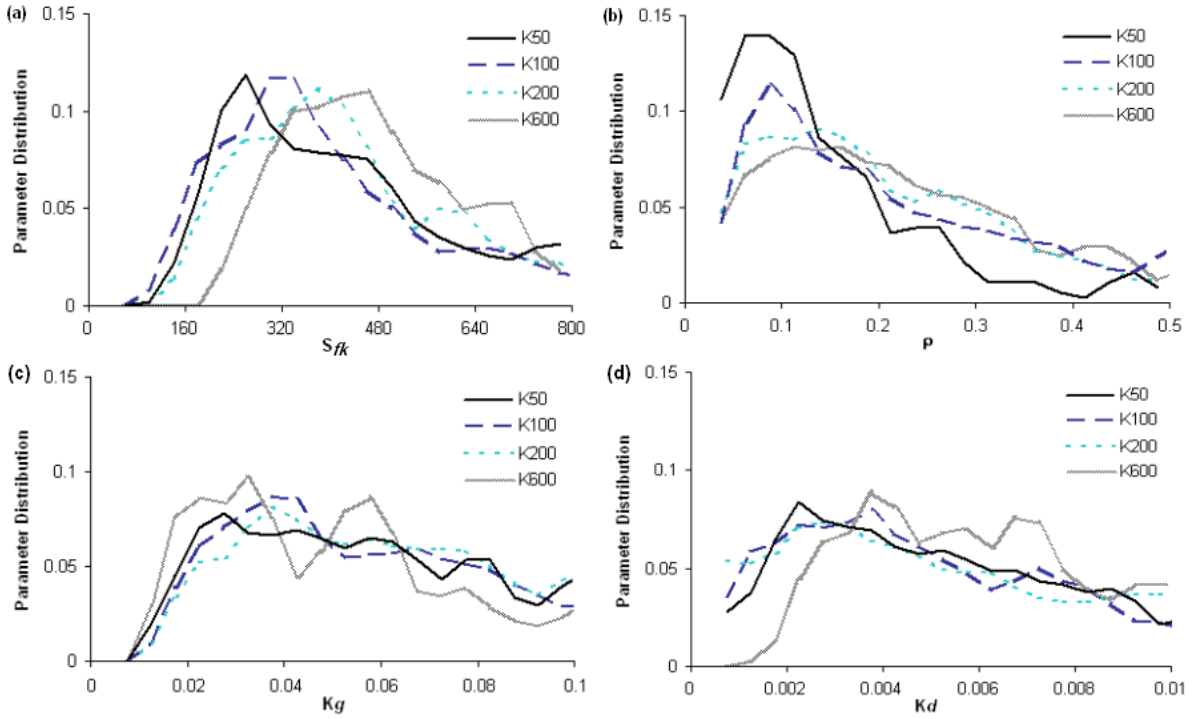

Figure 6.6 Variations of probability distributions with different spatial resolutions for the effective parameters in Kielstau catchment.

Similar conclusions are also applicable to the XitaoXi basin as observed in Figure 6.7. Concerning the limited influence of groundwater layer in the modelled area of XitaoXi basin, the parameter K_g reveals low sensitivity to resolution and therefore is not included in this plot. It is noticeable that, with respect to the parameter S*fk*, not only the peak values of derived functions deviate from the optimal value of model X200, but also the curves become more smooth and flat with increasing grid cell sizes. The distribution functions of parameter ρ in XitaoXi models show less resolution dependency comparing those of the same parameter in Kielstau. This is consistent with the observations in the Kielstau area that high groundwater activities can affect the sensitivity of soil groundwater parameter ρ. The distribution patterns of the parameter K_c and K_s are unstable and their curves (e.g. the X400 X800 curves of parameter K_s) deviate much further away from that of model X200. The distinct differences among the distribution patterns obtained from various resolution levels show the parameters of XitaoXi are not so well identifiable as those of Kielstau, and exhibits more resolution dependency or sensitivity for the effective parameter in XitaoXi models.

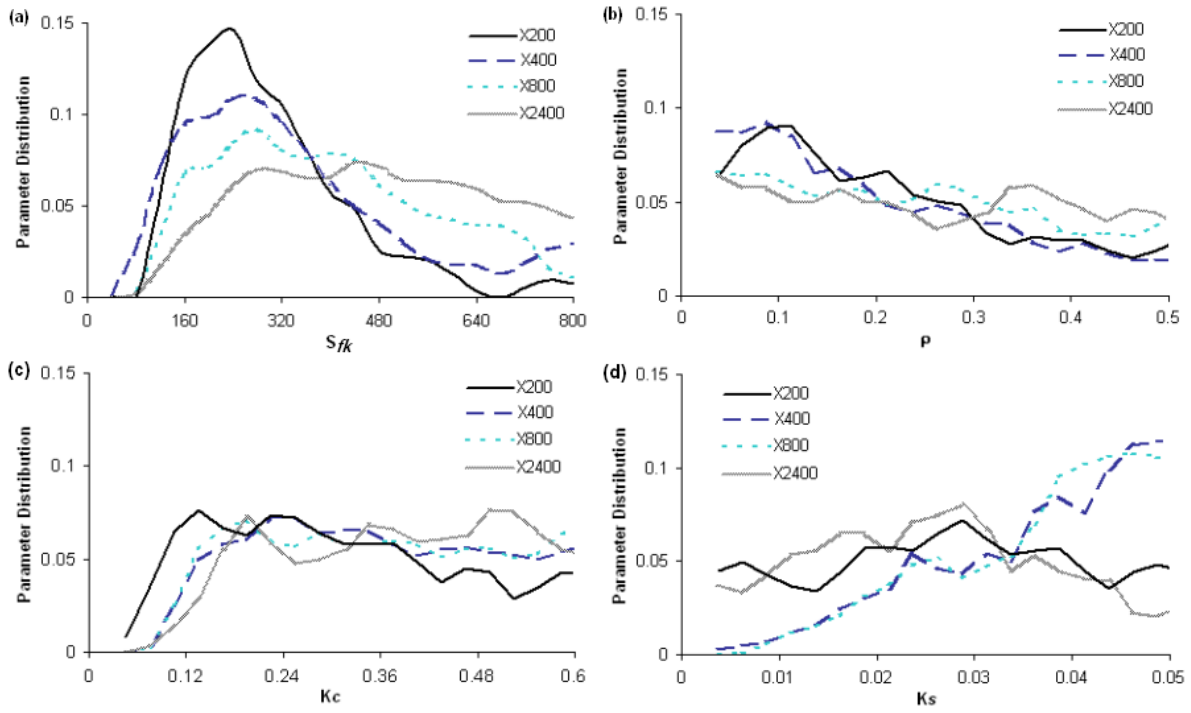

Figure 6.7 Variations of probability distributions with different spatial resolutions for the effective parameters in XitaoXi catchment.

6.3.3 Discharge simulation results and derived resolution uncertainty

The initial input data and the generated experimental data with five coarser resolutions are integrated into the KIDS model to simulate discharge in both study basins. The model yields different simulation results as the input data resolution changes. Overlapping the hydrographs obtained from different resolutions of input data produces a simulation band, which indicates the derived resolution uncertainty. Figure 6.8 (Kielstau catchment) and Figure 6.9 (XitaoXi watershed) present time-series plots of observed streamflow data versus simulated hydrograph band in the calibration and validation periods for a representative portion of the historical record. Figures 6.8 and 6.9 show that, in general, models can reproduce acceptable simulation bands centred on the observations with data at various resolution levels. In broad terms, the peak flows are better simulated, while the low flows are mostly underestimated for Kielstau and overestimated for XitaoXi. The quantitative measures of *R* factor and *P* factor are also calculated for both basins. The *R* factor indexes, which depict the average width of the simulated hydrograph bands along the observations, are 0.45 (calibration) and 0.41 (validation) for Kielstau, 0.50 (calibration) and 0.55 (validation) for XitaoXi. This exhibits moderately better simulation performance in the small Kielstau catchment, resulting in less spread of the uncertainty bands due to resolution changes. The values of *P* factor, the percentage of observations falling inside the uncertainty bands, are statistically meaningful (larger than 50%) and exhibit appropriate coverage.

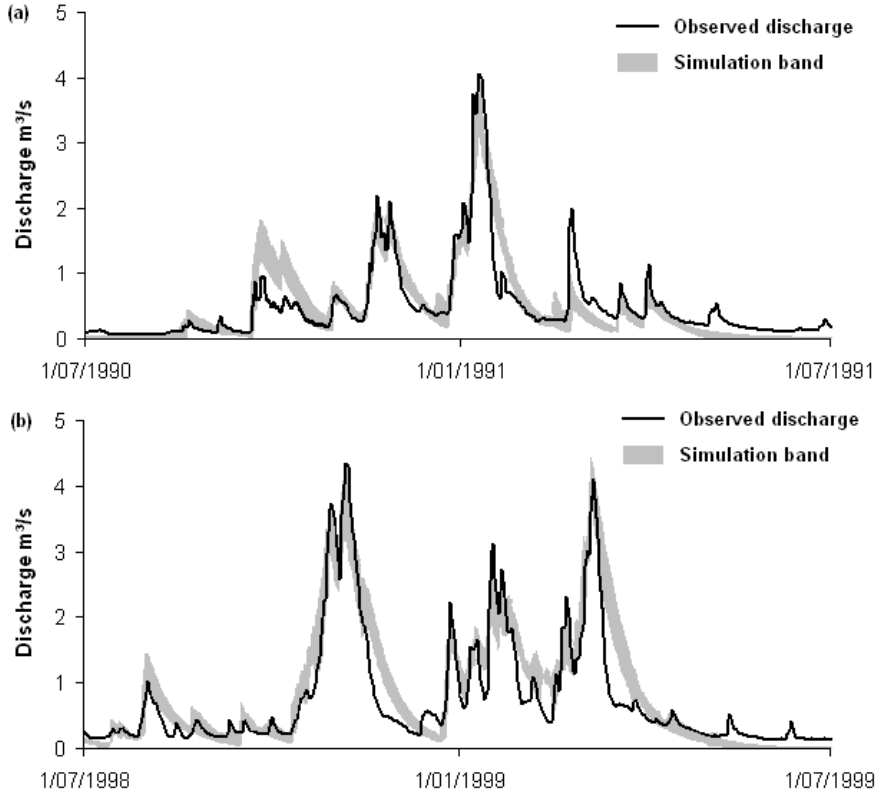

Figure 6.8 Simulation bands showing the uncertainty intervals for the Kielstau basin using different resolution data with 50 m, 100 m, 200 m, 400 m, 600 m, and 1000 m grid size in periods of (a) calibration, with *R* factor = 0.45 and *P* factor = 56.7%; (b) validation, with *R* factor = 0.41 and *P* factor = 53.9%.

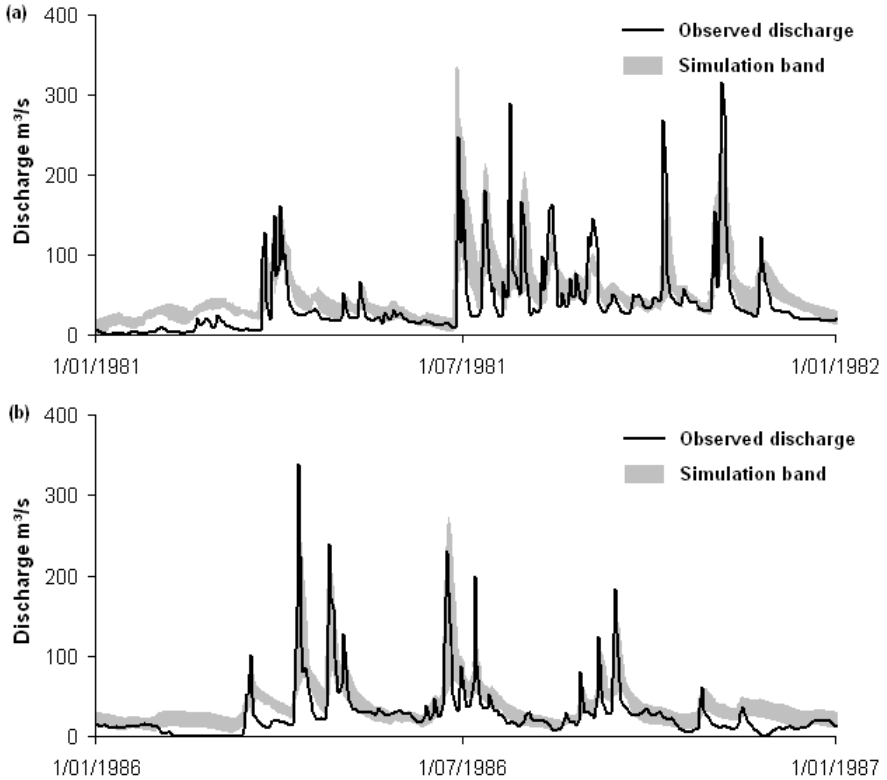

Figure 6.9 Simulation bands showing the uncertainty intervals for the XitaoXi basin using different resolution data with 200 m, 400 m, 800 m, 1600 m, 2400 m, and 4000 m grid size in periods of (a) calibration, with *R* factor = 0.50 and *P* factor = 53.4%; (b) validation, with *R* factor = 0.55 and *P* factor = 54.8%.

The simulated runoff at different resolution levels is further demonstrated in Figure 6.10, where the discharges simulated by various resolution input data are compared with the discharge simulation by the finest resolution data (K50 for Kielstau and X200 for XitaoXi) in a selected period representing the runoff simulations. From the deviated runoff simulations by other data, we can see that, using coarse resolution input data could give very different runoff to that obtained using fine resolution input data. It is especially obvious for large catchment, owing to the massive information loss caused by grid cells aggregation. The hydrograph peaks are particularly affected as shown in the plots of the XitaoXi catchment. Therefore resolution issues need careful consideration in discharge simulations.

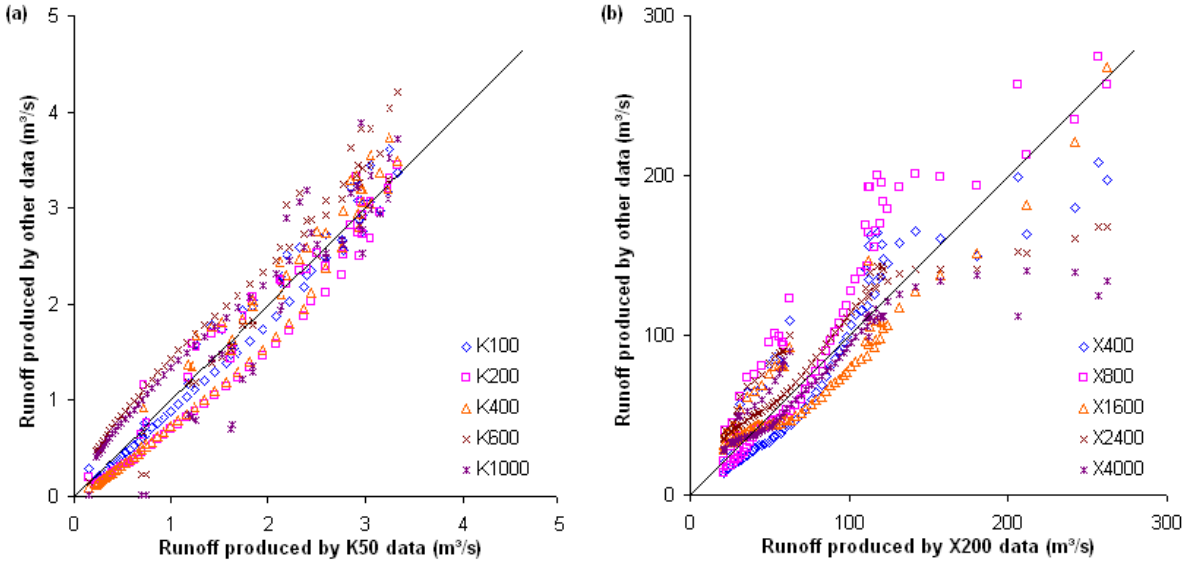

Figure 6.10 Deviation of simulated discharge due to change in resolutions of input data at (a) Kielstau (51.5 km²) for the period of 10/10/98 ~ 20/12/98, (b) XitaoXi (2271 km²) for the period of 10/06/86 ~ 20/08/86.

6.3.4 Comparison of modelling efficiency in terms of IC-ratio

To compare modelling components or simulation results in different catchments is not an easy task (Beven 2002). It is hard to find suitable indices for testing against forcing data resolutions and scale issues. The IC-ratio is proved to be a useful index for investigating the effects of input data resolution on discharge (Shrestha et al. 2006). All the tested spatial resolution levels for both basins in this study are expressed as the decimal IC-ratio (0<IC-ratio $\leqslant$1), where a lower value corresponds to a finer resolution of input for a given catchment. Concise information on the changes in the model performance in response to the altered resolution of forcing data using the IC-ratio index is represented in Figure 6.11. The IC-ratio facilitates the comparison of responses at various scales of catchment size. Along with the model performances in NS values, the modelling time for each simulation at various resolution levels is also plotted on Figure 6.11. Since the modelling cost is likely to increase

dramatically with an increase in resolution, the model running time is presented here to give an idea of the probably changed cost. Although the comprehensive cost is hard to be quantified, the optimum performance range can be appreciated from the curves in Figure 6.11, bearing in mind that there are huge data handling requirements and a lot of model set-up cost involved when selecting a higher resolution. From Figure 6.11, model performance for Kielstau is found to be consistently good when the IC-ratio is lower than 0.001. That is noticed to be the resolution range that can provide a satisfactory simulation result, when considering the crossed cost curve. Comparatively, the simulation results for XitaoXi deteriorate significantly as the input resolution starts to become coarser. It suggests that coarser resolution hydro-meteorological datasets do not satisfy the need of runoff simulation in the XitaoXi basin. It is better to keep the current resolution level or even to try finer data. However, the cost may increase geometrically for that case, as the steepness of the time-cost curve is higher than that of the Kielstau catchment. The distinction in the result of both basins indicates that, smaller, more homogenous-distributed catchment may be modelled successfully at coarser scale but larger heterogeneous field like the XitaoXi basin need finer input data. This, in general, raised the point that, it is preferred to investigate both the most appropriate data resolution and model representations that fit best the natural scales of hydrological significance (Shrestha et al. 2006). Based on the previous study on model structures (Zhang et al. 2011), we have applied different models to Kielstau and XitaoXi basins which are considered to match the hydrological patterns, e.g. basin size, climate, underlying physiography, topography, land cover, drainage, etc. The results obtained in this study indicate that, the best-fit input data resolution is not necessarily finer-resolution data but detailed enough to represent the river basin information in every model simulation. With respect to a further increase in resolution, it can be impractical effort in the case of the small homogenous Kielstau area, but beneficial for the heterogeneous XitaoXi basin.

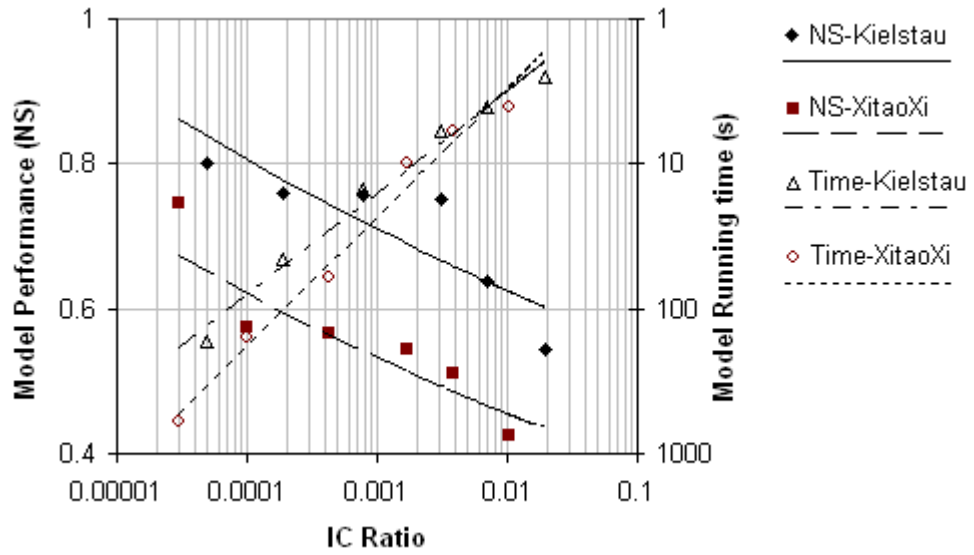

Figure 6.11 Model performance versus simulation time at different scales expressed in IC-Ratio for the Kielstau and XitaoXi catchment.

In our effort to establish a data resolution criterion in different catchments with the proposed IC ratio, it might be noted that the IC ratio only accounts for the overall basin size but not any other basin features like topography, shape or physiography. The two basins in this case have similarly elongated shapes which provide a good comparison base. For other basins it may provide an additional mode of complexity to the calculations and analysis when using IC ratio, as it would only imply an approximation of the data requirements considering the catchment area.

6.4 Conclusion

Effects of spatial input data resolutions on daily discharge simulations using the KIDS models in PCRaster are investigated for the small (51.5 km²) lowland Kielstau catchment and the medium sized (2271 km²) mountainous XitaoXi basin. The initial resolution data (50×50 m^2 for Kielstau, 200×200 m^2 for XitaoXi) are used as the base-line data (1x) and to prepare the experimental input data at various resolutions of 2x, 4x, 8x, 12x, and 20x. Then, a multi-resolution (MR), multi-calibration (MC) and multi-site (MS) methodology is employed to facilitate the grid-scale issues investigation. The following conclusions can be drawn from this study:

(1) Models with the base-line resolution data can provide satisfying simulation results – 0.8 NS value for 50 m Kielstau model (K50) and 0.75 for 200 m XitaoXi model (X200). The MR and MC tests reveal that, parameters calibrated at the finest resolutions cannot be directly applied to coarser resolutions. This is consistent with the statements in Beven (2001), Liang et

al. (2004), and Bormann et al. (2009) , that recalibration should be necessary when the input data resolution is altered. The importance of an appropriate calibration process is more distinctive for the larger XitaoXi basin, because of the higher parameter sensitivity and the greater information losses as the aggregation of input data. Therefore, a re-calibration is generally required when the grid resolution is changed.

(2) Six parameters for each catchment are calibrated to obtain a potentially optimal model performance at each spatial resolution. The analysis of resolution effect on parameter behaviour shows that most of the parameters inspected are scale dependent. The distribution function curves of these effective parameters are generally well-defined single modes with easily identifiable peak values for finer resolution data (e.g. K50 and X200 models). As grid size increases, the parameter distribution curve becomes smoother and more multi-mode style. The results obtained are more or less consistent in the findings for both Kielstau and XitaoXi. However, the larger deviations in parameter distribution patterns in XitaoXi models represent higher parameter sensitivity to grid resolution, which demonstrate more resolution dependency for the effective parameters.

(3) The overlapping hydrographs generated with different resolutions of input data indicate the resolution uncertainty derived in the current study range. The grid cell size selection will generally lead to predictive uncertainty. The results of two quantitative measures (with *R* factor<1 and *P* factor>50%) illustrate that representative uncertainty intervals can be obtained with a sufficient coverage of the observations for both basins. However, modelling with coarser resolution input data could produce different simulation results. This impact is particularly significant for the peak-flow simulations in the larger XitaoXi catchment. It indicates the importance of resolution selection and quality of input data at the scale of hydrological significance, meanwhile, taking both the basin geography and model framework into account.

(4) There is a choice to make regarding the required resolution of hydro-meteorological input data. The challenge is to determine a scale, above which sufficient information for accurate modelling of basin runoff can be provided, and at the same time with acceptable modelling cost. We proposed here a possible solution with a sound basis of the IC-ratio, for investigating suitable resolution in different catchments. Our results suggest that coarser resolutions with IC-ratio<0.001 may be used as an effective alternative for conducting preliminary analyses in discharge simulation for the Kielstau basin. In the contrast, it is recommended to use the current fine resolution data at the XitaoXi catchment in order to achieve sufficient accuracy of model outputs, or even finer data to improve the situation.

(5) The analysis of scaling effects in this study evaluated whether data aggregation is a useful regionalisation tool or whether it leads to an unacceptable loss of information. The results of this study indicate that aggregation procedure of input data cause changes in the simulation results for both study basins but at different extent. For the small lowland Kielstau catchment the grid aggregation till 800 m grid size (8x basic above) has slight information loss that leads to affected simulation results, while applying 400 m grid size (2x basic above) or more for the mesoscale XitaoXi basin causes significant decrease in modelling efficiency. In this case, when the accuracy of Kielstau model using coarser data, e.g. K200, is sufficient for applied uses, the time and efforts of pursuing finer data are saved as a benefit of this approach. Meanwhile in the opposite way, if XitaoXi model with finer data, like X50, would provide significantly better results than the X200 simulation, the costs of obtaining input data and spending additional computation time at that scale should be weighed against the benefit of a more accurate result. In this context, the aggregation approach in some watersheds (such as the Kielstau catchment) is adequate to capture the essential basin variability, but for XitaoXi catchment, the scale of hydrological significance is of critical importance to improve model efficiency. The test of different grid size in hydrological modelling could be a meaningful tool for practical model applications, especially in data scarce regions.

Finally, we should caution that some of the results obtained in this study, in particular about the comparison of resolution issues between the two study sites, might be model structure, spatial data resolution, model performance criteria, and catchment specific. And the uncertainties associated with model structures are not explicitly considered. Therefore, it is critically needed to test the validity of the results obtained here with other models or in other watersheds in the future.

Acknowledgments

The authors thank the Kiel University for financial support of this program. We appreciate help from our colleagues of the Ecology Center, Kiel University for access to their research data. We thank Nanjing Institute of Geography and Limnology, Chinese Academy of Sciences for the provision of XitaoXi data. Part of this work is sponsored by the National Research Program (No.: 2008CB418106) from Chinese Ministry of Science and Technology; and by the Key project (No.: KZCX1-YW-14-6) from Chinese Academy of Sciences.

References

Abbaspour, K.C., Johnson, C.A. & van Genuchten, M.T. 2004 Estimating uncertain flow and transport parameters using a sequential uncertainty fitting procedure, *Vadose Zone J.* 3, 1340–1352.

Beven, K. 2001 How far can we go in distributed hydrological modelling? *Hydrol. Earth Syst. Sci.* 5 (1), 1–12.

Beven, K. 2002 Towards an alternative blueprint for a physically based digitally simulated hydrologic response modelling system. *Hydrol. Process.* 16, 189–206.

Bogena, H., Kunkel, R., Montzka, C. & Wendland, F. 2005 Uncertainties in the simulation of groundwater recharge at different scales. *Adv. Geosci.* 5, 25–30.

Bormann, H. 2006 Impact of spatial data resolution on simulated catchment water balances and model performance of the multi-scale TOPLATS model. *Hydr. Earth Syst. Sci.* 10, 165–179.

Bormann, H., Breuer, L., Croke, B., Gräff, T. & Huisman, J. 2009 Assessing the impact of land use change on hydrology by ensemble modelling (LUCHEM) IV: Model sensitivity on data aggregation and spatial (re-) distribution. *Adv. Water Resour.* 32, 171-192.

Bruneau, P., Gascuel-Odoux, C., Robin, P., Merot, P. & Beven, K. 1995 Sensitivity to space and time resolution of a hydrological model using digital elevation data. *Hydrol. Process.* 9, 69–81.

Chow, V.T., Maidment, D.R. & Mays, L.W. 1988 Applied Hydrology. McGraw-Hill, New York, USA.

Cullmann. J., Mishra, V. & Peters, R. 2006 Flow analysis with WaSiM-ETH – model parameter sensitivity at different scales. *Adv. Geosci.* 9, 73–77.

DHI. 1998 In MIKE-SHE v.5.3 User Guide and Technical Reference Manual. *Danish Hydraulic Institute,* Denmark, p50.

Eggemann, G., Sterr, H. & Kuhnt, G. 2001 Geomorphologie Schleswig-Holsteins. (unpublished), Kiel, p140.

Famiglietti, J.S. & Wood, E.F. 1994 Multiscale modelling of spatially variable water and energy balance processes. *Water Resour. Res.* 30 (11), 3061–3078.

Gao, J., Lu, G., Zhao, G. & Li, J. 2006 Watershed data model: a case study of Xitiaoxi sub-waterhed, Taihu Basin (in Chinese, with English abstract). *J. Lake Science.* 18 (3), 312-318.

Glugla, G. 1969 Berechnungsverfahren zur Ermittlung des aktuellen Wassergehalts und Gravitationswasserabflusses im Boden. *Albrecht-Thaer-Archiv,* 13 (4), 371-376.

Gupta, H.V. & Sorooshian, S. 1998 Toward improved calibration of hydrologic models: multiple and noncommensurable measures of information. *Water Resour. Res.* 34 (4), 751-763.

Hebeler, F. & Purves, R.S. 2008 The influence of resolution and topographic uncertainty on melt modelling using hypsometric sub-grid parameterization. *Hydrol. Process.* 22 (19), 3965-3979.

Hörmann, G., Zhang, X.Y. & Fohrer, N. 2007 Comparison of a simple and a spatially distributed hydrologic model for the simulation of a lowland catchment in Northern Germany. *Ecolog. Model.* 209 (1), 21-28.

Kuo, W., Steenhuis, T., McCulloch, C., Mohler, C., Weinstein, D., DeGloria, S. & Swaney, D. 1999 Effect of grid size on runoff and soil moisture for a variable-source-area hydrology model. *Water Resour. Res.* 35 (11), 3419–3428.

Liang, X., Guo, J. & Leung, L.R. 2004 Assessment of the effects of spatial resolutions on daily water flux simulations. *J. Hydrol.* 298, 287–310.

Lindenschmidt, K.E., Fleischbein, K., Petrow, T., Vorogushyn, S., Theobald, S. & Merz, B. 2005 Model system development and uncertainty for the provisionary management of extreme floods in large river basins. *Adv. Geosci.* 5, 99–104.

Liu, H.H., Hörmann, G., Kiesel, J. & Fohrer, N. 2009 Suitability of S factor algorithms for soil loss estimation at gently sloped landscapes. *Catena*. 77 (3), 248-255.

Moriasi, D., Arnold, J., Van Liew, M., Bingner, R., Harmel, R. & Veith, T. 2007 Model evaluation guidelines for systematic quantification of accuracy in watershed simulations. *Transactions of the American Society of Agricultural and Biological Engineers*, 50 (3), 885−900.

Moore, I.D., Lewis, A. & Gallant, J.C. 1993 Terrain attributes: Estimation methods and scale effects, in: Modelling change in environmental systems, edited by: Jakeman AJ, Beck MB, and McAleer M, Wiley, New York, 189–214.

Nash, J.E. & Sutcliffe, J.V. 1970 River flow forecasting through conceptual models. Part I: A discussion on principles. *J. Hydrol.* 10, 282-290.

Omer, R.C., Nelson, E.J. & Zundel, A.K. 2003 Impact of varied data resolution on hydraulic modelling and floodplain delineation, *J. Am. Water Resour. Assoc.* 39(2), 467–475.

Quinn, P., Beven, K., Chevallier, P. & Planchon, O. 1991 The prediction of hillslope flow paths for distributed hydrological modelling using digital terrain models. *Hydrol. Process.* 5, 59–79.

Refsgaard, J.C. & Storm, B. 1996 Construction, calibration and validation of hydrological models. In Distributed Hydrological Modelling, Abbott MB, Refsgaard JC (eds). *Kluwer Academic: The Netherlands*, 41–54.

Schmidtke, K.D. 1999 Land im Wind, Wetter und Klima inSchleswig-Holstein. *Wachholtz Verlag*, 119p.

Schmitz, O., Karssenberg, D., van Deursen, W.P.A. & Wesseling, C.G. 2009 Linking external components to a spatio-temporal modelling framework: Coupling MODFLOW and PCRaster. *Environ. Modell. Softw.* 24, 1088-1099.

Schuol, J. & Abbaspour, K.C. 2006 Calibration and uncertainty issues of a hydrological model (SWAT) applied to West Africa. *Adv. Geosci.* 9, 137–143.

Shrestha, R., Tachikawa, Y. & Takara, K. 2002 Effect of forcing data resolution in river discharge simulation. *Annual Journal of Hydraulic Engineering*, JSCE 46, 139–144.

Shrestha, R., Tachikawa, Y. & Takara, K. 2006 Input data resolution analysis for distributed hydrological modelling. *J. Hydrol.* 319, 36–50.

Springer, P. 2006 Analyse der Interaktion zwischen Oberflächenwasser und Grundwasser am Beispiel einer Flussniederung im Norddeutschen Tiefland. *Diplomarbeit im Fach Geographie*, der Christian-Albrechts-Universit¨at zu Kiel, 191p.

Sponagel, H. 2005 Bodenkundliche Kartieranleitung. ADHOCARBEITSGRUPPE BODEN der Staatlichen Geologischen Dienste und der Bundesanstalt für Geowissenschaften und Rohstoffe. 5.verbesserte und erweiterte Auflage, Hannover, 438p.

Trepel, M. 2004 Development and application of a GISbased peatland inventory for SchleswigHolstein (Germany). In: Päivänen, J. (ed.) Proceedings of the 12th International Peat Congress Wise Use of Peatlands, Vol. 2, 931-936.

Van Deursen, W.P.A. 1995 Geographical Information Systems and Dynamic Models: development and application of a prototype spatial modelling language. *Netherlands Geographic Studies*, Issue 190, 198p

Vazquez, R.F., Feyen, L., Feyen, J. & Refsgaard, J.C. 2002 Effect of grid size on effective parameters and model performance of the MIKE-SHE code. *Hydrol. Process.* 16, 355–372.

Vazquez, R.F. & Feyen, J. 2003 Effect of potential evapotranspiration estimates on effective parameters and performance of the MIKE SHE-code applied to a medium-size catchment. *J. Hydrol.* 270 (4), 309–327.

Vazquez, R.F. & Feyen, J. 2007 Assessment of the effects of DEM gridding on the predictions of basin runoff using MIKE SHE and a modelling resolution of 600 m. *J. Hydrol.* 334, 73– 87.

Wan, R., Yang, G.， Li, H. & Yang, L. 2007 Simulating flood event in mesoscale watershed ：a case study from River Xitiaoxi Watershed in the upper region of Taihu Basin. J. Lake Science. 19 (2), 170-176.

Wesseling, C.G., Karssenberg, D.J., Burrough, P.A. & Van Deursen, W.P.A. 1996 Integrated dynamic environmental models in GIS: The development of a Dynamic Modelling language. *Transactions in GIS*, 1-1, 40–48.

Wolock, D.M. & Price, C.V. 1994 Effects of digital elevation model map scale and data resolution on topography-based watershed model. *Water Resour. Res.* 30, 3041–3052.

Xu, L., Zhang, Q., Li, H., Viney, N.R., Xu, J. & Liu, J. 2007 Modelling of Surface Runoff in Xitiaoxi Catchment, China. *Water Resour. Manag.* 21, 1313–1323.

Zhang, Q., Li, H. & Xu, L. 2006 Surface runof modelling for Xitiaoxi catchment, Taihu Basin. *J. Lake Science.* 18 (4), 401-406.

Zhang, W. & Montgomery, D.R. 1994 Digital elevation model grid size, landscape representation, and hydrologic simulations. *Water Resour. Res.* 30, 1019–1028.

Zhang, X.Y., Hörmann, G. & Fohrer, N. 2007 The Effects of Different Model Complexity on the Quality of Discharge Simulation for a Lowland Catchment in Northern Germany. Heft 20.07 ‘Einfluss von Bewirtschaftung und Klima auf Wasser- und Stoffhaushalt von Gewässern’ (2007), Band 2, *Forum für Hydrologie und Wasserbewirtschaftung*, 111-114.

Zhang, X.Y., Hörmann, G. & Fohrer, N. 2008 An investigation of the effects of model structure on model performance to reduce discharge simulation uncertainty in two catchments. *Adv. Geosci.* 18, 31–35.

Zhang, X.Y., Hörmann, G. & Fohrer, N. 2009 Hydrologic comparison between a lowland catchment (Kielstau, Germany) and a mountainous catchment (XitaoXi, China) using KIDS model in PCRaster. *Adv. Geosci.* 21, 125–130.

Zhang, X.Y., Hörmann, G., Gao, J.F. & Fohrer, N. 2011 Structural uncertainty assessment in a discharge simulation model. *Hydrol. Sci. J.* 56 (5), 854-869.

Zhao, G., Hörmann, G., Fohrer, N., & Gao, J. 2009 Impacts of spatial data resolution on simulated discharge, a case study of Xitiaoxi catchment in South China. *Adv. Geosci.* 21, 131–137.

Chapter 7

Conclusion: how reliable is our model?

7.1 Introduction

Modelling has become a valuable tool to understand and analyse the water resource system. To be able to simulate or predict the "hydrological" behaviour of any basin with perfect accuracy is the "Holy Grail" of hydrology (Beven 2001). It seems probable that this mission cannot be accomplished. That is, we may never be able to precisely predict discharge at a given location. The model outputs are based on model structure, hydrological and other time-series inputs, and a host of parameters whose values describe the system being simulated. Even if these assumptions and input data reflect conditions believed to be true, we know they will be inaccurate. The treatment of uncertainty is, therefore, critical to the problem of understanding how reliable is the modelling result. Beven (2006, 2008) suggested that all hydrological modelling investigations should include an uncertainty analysis. It is a major goal in hydrological modelling to identify and quantify sources of uncertainty in the modelling process.

This PhD thesis attempts to answer the questions raised above. The main concept is to use the KIDS modelling approach for streamflow simulation in two different basins as a starting point, and develop methodology for an overall uncertainty analysis.

7.2 Discussion of the main results

7.2.1 Case study specificity

In the present study, KIDS model has been applied to two different gauged catchments: the Kielstau in Northern Germany and the XitaoXi in Southern China. These two catchments have been chosen because they represent different catchment sizes, climatic conditions and have different geohydrologic features (Table 7.1). They are located in different geographic regions; the soil properties, landuse types, and meteorological conditions vary considerably. The specific hydrological regimes at the selected location provided important information to guide the model structure adjustment, parameter estimation and selection of an appropriate resolution level.

Table 7.1 Main physiographic characteristics of the two case study catchments (reference year for hydro-meteorological data 1990 – 1999 in Kielstau and 1979-1988 in XitaoXi).

Characteristic	Kielstau Basin	XitaoXi Basin
Area (km^2)	51.5	2271
River length	11	139
Max. altitude difference (m)	50	1572
Mean annual precipitation (mm)	860	1466
Daily runoff rate ($l/s/km^2$)	8.8	23
Runoff efficiency	0.28	0.39

The developed uncertainty assessment framework enables a full analysis and quantification of modelling uncertainty for streamflow simulation. Each step that induces its specific modelling uncertainty involves a critical calibration procedure. Parameter calibration has been applied to each individual model for both catchments system. We used an automated calibration procedure with Monte Carlo sampling methods. This approach has several advantages, including the explicit use of an appropriate statistical objective function (here we defined it as Nash-Sutcliffe efficiency), identification of those parameters that best reproduce the calibration data set with the given objective function, and the estimations of the statistical precision of the estimated parameters.

These, coupled with a probabilistically based uncertainty analysis method, can help quantify the uncertainty in key output variables of the streamflow simulation, and the selected system performance indices of Nash-Sutcliffe values. The result may differ depending upon which

output variables and indices are of interest. On the other hand, the major limitation of the applied method to estimate uncertainty is the computing time required, in order to obtain a statistical description of system performance variability. Therefore, only with low dimensional parameterized and relatively simple model structure, it may be an attractive undertaking for uncertainty analyses.

7.2.2 Modelling uncertainties – which one contributes the most?

Based on the above considerations, the modelling uncertainty associated with the streamflow simulation has been analyzed and quantified under the statistical and multi-site comparison concepts. The modelling uncertainty from different sources was estimated through the dispersion range of flow simulation ensembles around the observed data. Table 7.2 summarised the results of two statistical uncertainty measures (*P* factor and *R* factor) for both basins.

Table 7.2 List of performance indicator names, signification and measurement method.

Uncertainty source	Indicator (target value)	Kielstau Basin		XitaoXi Basin	
		Calibration 01.07.1990-01.07.1991	Validation 01.07.1998-01.07.1999	Calibration 01.01.1981-01.01.1982	Validation 01.01.1986-01.01.1987
Model structure	*R* factor (0)	0.84	0.82	0.80	0.85
	P factor (100%)	69%	75%	78%	72%
Parameter	*R* factor (0)	0.65	0.53	0.66	0.73
	P factor (100%)	53%	60%	66%	58%
Resolution	*R* factor (0)	0.45	0.41	0.50	0.55
	P factor (100%)	57%	54%	53%	55%

The different sources of uncertainty and their quantification indices are presented separately for each simulation period. Similar results are observed in the two case studies: the values of *R* factor decreases in the sequence of uncertainty from model structure, parameter estimation and resolution selection; and so does the *P* factor value, since the higher the *R* factor the wider of the uncertainty bound to cover observations. Evidences from the hydrograph comparison also show a substantially wider modelling uncertainty band from the ensemble model structures, and a relatively narrow simulation uncertainty band from parameter calibration and input data resolution. This difference indicates a high fraction of uncertainty due to model structure, as the hydrological model plays a key role in the runoff production system. The structure of a conceptual model is generally arbitrarily fixed based on some a priori knowledge. During the model structure testing, we optimised several slightly different model structures in parallel and they lead however to quite different model performance for the observed discharge simulation. This suggests that the inter-model variability of the discharge

simulations is potentially higher than the modelling uncertainty inherent in each of them – even if sometimes the different model structures correspond to only slight variations of the basic model structure.

With the result of uncertainty estimates associated with those sources, it is reasonable to ask which way is the best to improve system performance or to reduce modelling uncertainty. This can be answered by propagating all the concerned uncertainty ranges.

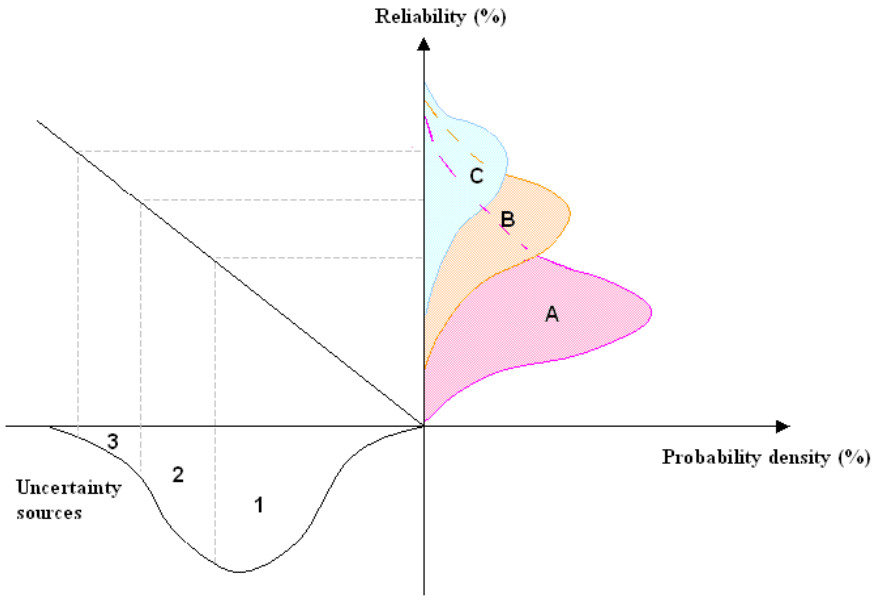

Figure 7.1 Schematic diagram showing relationship among different uncertainty sources, probability levels of system output, and the simulation reliability. The uncertainty sources considered include: 1-model structure errors, 2-parameter estimation, 3-input data resolution; uncertainty analysis at three steps: A-model structure uncertainty; B-parameter uncertainty; C- (input data) resolution uncertainty.

A complete uncertainty analysis would involve a comprehensive identification of all sources of uncertainty that contribute to the joint probability distributions of the output variable. Owing to limited data and imperfect knowledge, it would be feasible to perform uncertainty analysis step by step based on the information we have. As illustrated in Figure 7.1, the uncertainty assessment has been conducted in this study by taking into account three uncertainty sources: model structure errors, parameter estimation, and input data resolution. The area of each source describes its relative impact on the output variable uncertainty by considering the calculated values of R-factor. Here it indicates that model structure is the most important factor for the model performance.

The figure also identifies the resulting probability density distributions of modelling uncertainty from each specified source, namely, A-model structure uncertainty; B-parameter uncertainty; C- (input data) resolution uncertainty. The uncertainties deduced from each

analysis steps are overall modelling uncertainty due to the inherent interrelations of all sources, but they are mainly referred to the specified source by minimizing the influences from other factors. Figure 7.1 illustrates the shift and the flattening of the probability density function of the system output when successively presenting the three uncertainties. When more sources of uncertainty have been accounted for, it could enhance the simulation reliability level with reducing modelling uncertainties. It has been shown that, the uncertainties introduced by the model structure errors contribute the most to the total prediction uncertainty. The uncertainty analysis of different sources helps determine the best way to reduce potential uncertainty, and therefore to improve the modelling precision.

7.2.3 Model performance – Is our simulation target achieved?

The value of uncertainty assessment information will be the increase in model performance, or the reduction in its variance. Figure 7.2 describes the improvement curves of the resulting NS values at each analysis steps. It shows that the possible model structure adjustment contributes significantly to the overall improvement in the accuracy of streamflow simulations. Parameter calibration within a defined model and resolution can optimize the model performance only in a limited range. With the major sources of uncertainty have been accounted for, the model provided satisfactory agreement between observed and simulated discharge. The final validated simulation reaches a NS value of 0.83 for Kielstau and 0.75 for XitaoXi.

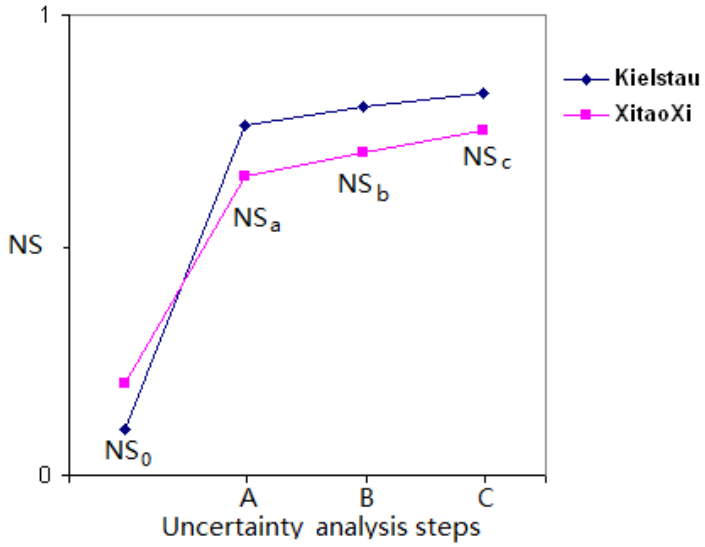

Figure 7.2 Improvement of model performance in NS index through uncertainty assessment procedures. NSo - NS value at starting point; NS_a - NS value with model structure adjustment; NS_b - NS value with parameter calibration in a given model; NS_c - NS value with parameter calibration at selected resolution level.

7.2.4 Two case studies – More in common or more differences?

The uncertainty investigation was carried out in two case studies. The results of KIDS model simulation, effective parameter behaviour and uncertainty assessment were compared between the small lowland Kielstau basin and the mesoscale mountainous XitaoXi basin. The conceptual KIDS model has been developed for the Kielstau catchment. Its application to the XitaoXi basin can help to test its transferability to other case studies, and to examine the feasibility of the developed methodology for uncertainty analysis.

Both case studies demonstrated that the uncertainty induced by the hydrological model structure errors contributes much more to the total modelling uncertainty than the uncertainties inherent in parameter estimation and input data resolution. The differences that can be observed in the results comparison all lie in the issues relating to the specific features of the respective study area. For example, the adaptation of model structure to the local hydrological system, the distribution patterns of key parameters, and the different decision on selecting an appropriate resolution level.

Therefore, the results obtained here are highly case study specific. And it also suggests the possibility to use the methodology for uncertainty assessment in other basins.

7.3 Overall summary and future work

The methods developed here for the identification and quantification of the different sources of modelling uncertainty enable a consistent estimation of the contribution at each analysis step to the overall simulation uncertainty. We have shown that the hydrological model plays a key role in streamflow simulation and in modelling uncertainty reduction. It is however important to emphasize that the obtained results are conditioned on the applied models, on the used data, and especially on the case study specificity.

The main conclusions from this PhD study are summarized as the following:

1) The model structure is an important factor affecting model performance. For the Kielstau basin, influences from drainage and wetland are critical for the local runoff generation; while for the XitaoXi basin, accurate distributions of precipitation and evapotranspiration are two of the determining factors for the success of the river flow simulations.

2) Both case studies indicate that the simulation uncertainty for low-flow period contributes more to the overall uncertainty than for peak-flow period.

3) The parameter behaviour analysis exhibited high equifinality, which implies the magnitude of uncertainty from parameter estimations.

4) Two parameters – 'I*m*' (maximum interception amount) and 'K_g' (groundwater discharge rate) - have a relatively low sensitivity and therefore not so well identifiable for a good model performance. But a moderate normal distribution 'K_g' in Kielstau indicates that groundwater plays a more important role in river runoff producing processes.

5) The value of parameter 'S_{fk}' (soil water storage capacity) is well defined but its optimal value range differs in the two basins owing to the very different soil types in two basins. The higher 'ρ' optimal values (soil groundwater flux parameter) in Kielstau reveals a more interactive relationship between soil and groundwater layers.

6) Model performances would deteriorate with coarser input data resolutions. But the modelling outputs are more sensitive to the spatial distribution of input data at the XitaoXi watershed.

7) Altering grid sizes would have various impacts on effective parameter estimation. Larger deviations in parameter distribution patterns are observed for the effective parameters in XitaoXi models.

8) Coarser resolutions with IC-ratio<0.001 may be used as an effective alternative for conducting preliminary analyses in discharge simulation for the Kielstau basin. While it is recommended to use the current fine or even finer resolution data at the XitaoXi catchment in order to achieve sufficient accuracy of model outputs.

9) As shown by the uncertainty quantification measures of *R* factor and *P* factor, uncertainty induced by model structure errors are much higher than the one induced by parameter estimation, and the influence from the changing input data resolutions on the overall uncertainty is considerably smaller.

All of these results together represent efforts for a systematic investigation of modelling process, although it is hard to cover all the possibilities that will induce model uncertainty from many other sources. However, no matter how much attention is given to quantifying and reducing uncertainties in model outputs, uncertainties will remain due to imperfect knowledge. Any uncertainty assessment will be conditional on the possibilities considered and the assumptions made. And the uncertainty studies should focus on providing information that guide research and assist model development efforts.

The present research contributes to a better understanding of the relationships between model assumptions, parameters, data and model simulations. It could help to determine, in which way we should put efforts to improve the precision of applied models. The large prediction intervals that result from each uncertainty analysis step somehow suggest that, the uncertainty inherent in the hydrological discharge simulations could be reduced by different means.

Additional data could help to optimize the hydrological model and therefore increase model accuracy. Evidence indicates additional abstractions such as evapotranspiration in the wetland area of Kielstau basin, and more detailed spatial and climatic data in the XitaoXi catchment will contribute to improvement of model performance. These efforts need to be considered for future researches at the selected location. We believe that uncertainty estimation has to be continued not as a goal in itself but as a mean to identify problems of current modelling approaches and additional needs of process knowledge and data.

References

Beven, K.J. 2001 How far can we go in distributed hydrological modelling? *Hydrol. Earth Syst. Sci.* 5(1), 1-12.

Beven, K.J. 2006 On not undermining the science: coherence, validation and expertise. *Hydrol. Process.* 20, 3141–3146.

Beven, K.J. 2008 On doing better hydrological science. *Hydrol. Process.* 22 (17), 3549–3553.

Erklärung

Hiermit erkläre ich, dass ich die vorliegende Dissertation, abgesehen von der Beratung durch meine akademischen Lehrer, selbstständig verfasst habe und keine weiteren Quellen und Hilfsmittel als die hier angegebenen verwendet habe. Diese Arbeit hat weder ganz, noch in Teilen, bereits an anderer Stelle einer Prüfungskommission zur Erlangung des Doktorgrades vorgelegen, und ist nicht veröffentlicht worden oder wurde zur Veröffentlichung eingereicht. Ich erkläre, dass die vorliegende Arbeit gemäß der Grundsätze zur Sicherung guter wissenschaftlicher Praxis der Deutschen Forschungsgemeinschaft erstellt wurde.

Xiaoyong Zhang
Kiel, 02 March 2012